uOttawa

L'Université canadienne
Canada's university

FACULTÉ DES ÉTUDES SUPÉRIEURES ET POSTOCTORALES

uOttawa

L'Université canadienne
Canada's university

FACULTY OF GRADUATE AND POSDOCTORAL STUDIES

Melissa St. Denis

AUTEUR DE LA THÈSE / AUTHOR OF THESIS

M.Sc. (Microbiology and Immunology)

GRADE / DEGREE

Department of Biochemistry, Microbiology and Immunology

FACULTÉ, ÉCOLE, DÉPARTEMENT / FACULTY, SCHOOL, DEPARTMENT

Identification and Characterization of a Heme-dedicated Periplasmic Binding Protein in *Haemophilus ducreyi*

TITRE DE LA THÈSE / TITLE OF THESIS

Dr. Craig Lee

DIRECTEUR (DIRECTRICE) DE LA THÈSE / THESIS SUPERVISOR

CO-DIRECTEUR (CO-DIRECTRICE) DE LA THÈSE / THESIS CO-SUPERVISOR

EXAMINATEURS (EXAMINATRICES) DE LA THÈSE / THESIS EXAMINERS

Dr. J. Farber

Dr. A. Stintzi

Gary W. Slater

Le Doyen de la Faculté des études supérieures et postdoctorales / Dean of the Faculty of Graduate and Postdoctoral Studies

Identification and Characterization of a Heme-dedicated Periplasmic Binding Protein in *Haemophilus ducreyi*

A thesis submitted to the School of Graduate Studies
University of Ottawa

In partial fulfillment of the requirements for the degree of
Master of Science

Department of Biochemistry, Microbiology & Immunology
Faculty of Medicine

By
Melissa St. Denis

Your file Votre référence
ISBN: 978-0-494-32480-6
Our file Notre référence
ISBN: 978-0-494-32480-6

ABSTRACT

In *Haemophilus ducreyi*, heme uptake likely proceeds via a receptor-mediated process. The initial event involves binding to either of two outer membrane receptors, TdhA and HgbA. Once heme is deposited into the periplasmic space, we hypothesize that a heme-dedicated periplasmic binding protein (hHBP) is responsible for transporting heme across the periplasmic space to the inner membrane.

To identify the hHBP, periplasmic extracts were generated from *H. ducreyi* 35000 grown under high and low heme conditions and subjected to proteome mapping. Peptide sequences of upregulated proteins grown under heme-restrictive conditions were determined by mass spectroscopy. A candidate hHBP was identified as a periplasmic binding protein homologous to YfeA of *Yersinia pestis*. The gene encoding this protein appears to be in a typical ABC transporter operon. Under iron-limiting conditions, no upregulation of the hHBP expression was observed; however, the purified hHBP was shown to specifically bind heme in a concentration-dependent manner.

Dedication

To those who endured my constant discussions on heme and to those who encouraged and supported me throughout this endeavor and always.

Acknowledgments

I would like to express my sincerest thanks and appreciation to my supervisor, Dr. Craig Lee, for his encouragement, support, and guidance and also for his sheer enthusiasm for the scientific process. I wish to convey a very special thanks to Dr. Fraser Scott (OHRI, Ottawa, ON, Canada), Dr. Marc Desjardins (Ottawa Hospital, Ottawa, ON, Canada), and Dr. Thien-Fah Mah (University of Ottawa, ON, Canada), my thesis advisory committee members.

I would also like to thank Dr. Fraser Scott for the usage of his laboratory for the 2D gel electrophoresis work; Brigitte Sonier for her patience and kindness while teaching me this technique; and Linru Wang (Canadian Food Inspection Agency, Ottawa, ON, Canada) for supplying purified rLipL32 used for supportive heme agarose binding studies.

I am also indebted to my support system in Bacteriology and Special Microbiology at the Children's Hospital of Eastern Ontario for their continued support and guidance – without you, this venture would not have been possible. Thank-you!

Table of Contents

List Of Abbreviations

1D	One-dimensional
2D	Two-dimensional
ABC	ATP-binding Cassette
AMP	Ampicillin
Anti-hHBP	Rabbit Polyclonal Antibody Against *H. ducreyi* 35 000 Heme Binding Protein
Anti-OMP	Rabbit Polyclonal Antibody Against *H. ducreyi* 35 000 Outer Membrane Proteins
Anti-SodC	Rabbit Polyclonal Antibody Against *H. ducreyi* 35 000 SodC Protein
Anti-V5-HRP	Mouse Monoclonal Antibody Against the V5 Epitope Cross-linked to Horseradish Peroxidase
CAP	Chocolate Agar Plate
CFU	Colony Forming Unit
Cu,Zn-SodC	Copper, Zinc Superoxide Dismutase
ddH_20	Double Distilled Water
DGS	Desulfoviridin Gamma Subunit
EtBr	Ethidium Bromide
FBS	Fetal Bovine Serum
Fur	Ferric Uptake Regulator
Ga-PPIX	Gallium-substituted Protoporphyrin IX
GC	Gonococcal
GUD	Genital Ulcer Disease
HgbA	Hemoglobin Outer Membrane Receptor of *H. ducreyi*
hHBP	*H. ducreyi* Heme-dedicated Periplasmic Binding Protein
His	Histidine
HIV	Human Immunodeficiency Virus
HP	Human Passaged
HSV	Herpes Simplex Virus
IEF	Isoelectric Focusing
IPTG	Isopropyl-βD-1-thiogalactopyranoside
kDa	Kilodalton
LB	Luria Bertani
LOS	Lipooligosaccharide
MALDI	Matrix-assisted Laser Desorption/Ionization
MGA	Modified Gonococcus Agar
MOMP	Major Outer Membrane Protein
MP	Metalloporphyrins
M-PCR	Multiplex Polymerase Chain Reaction
MW	Molecular Weight
OGIC	Ontario Genomics Innovation Center
OMP	Outer Membrane Protein

ORF	Open Reading Frame
PAGE	Polyacrylamide Gel Electrophoresis
PBS	Phosphate Buffered Saline
PCR	Polymerase Chain Reaction
PMSF	Phenylmethylsulphonyl Fluoride
PPIX	Protoporphyrin IX
rhHBP	Recombinant *H. ducreyi* Heme-dedicated Periplasmic Binding Protein
SDS	Sodium Dodecyl Sulfate
SEB	Sequential Extraction Reagent 3
SodC	Superoxide Dismutase Protein
STI	Sexually Transmitted Infection
TBP	Tributyl Phosphine
TdhA	Heme Outer Membrane Receptor of *H. ducreyi*
Zn-PPIX	Zinc-substituted Protoporphyrin IX
ZnuA	Periplasmic Zinc Transport Protein of *H. ducreyi*

List of Figures

List of Tables

List of Appendices

CHAPTER ONE

INTRODUCTION

1.1 *Haemophilus ducreyi*

Haemophilus ducreyi is a Gram-negative pathogenic bacillus. This bacterium is fastidious with optimal growth at 33°C in a water-saturated environment under 5% CO_2 or microaerophilic conditions [1,2]. *H. ducreyi* tends to autoagglutinate in liquid media or form cohesive colonies that can be pushed intact across an agar plate [1]. Intercellular adhesion properties can also be seen on Gram stain where *H. ducreyi* has been described to resemble schools of fish, railroad tracks, or fingerprints of coccobacilli [1]. Although *H. ducreyi* was originally classified as part of the *Haemophilus* genus due to its absolute requirement for heme and similar biochemical and antigenic properties, more recent rRNA analysis indicate it is only remotely related to other *Haemophilus* species. Due to this evidence, *H. ducreyi* has been placed in the *Actinobacillus* genus within the *Pasteurellaceae* family [3,4]. The complete genome sequence of 35 000HP (human-passaged strain) is now available and consists of a single chromosome 1.7Mb in length encoding 1693 putative open reading frames (ORF) [5].

1.2 Chancroid

H. ducreyi is the etiological agent responsible for the sexually transmitted infection (STI) known as chancroid. Chancroid gets its name from the soft chancres produced by the infection on the genital area of men and women. These ulcers are usually present on the prepuce and frenulum in men and on the vulva, cervix and perianal area in women [1,6]. Although chancroid is a genital ulcer disease (GUD), there have been occasional reported cases of lesions present on inner-thighs, breasts, and fingers thought to be caused by

autoinoculation [1,7]. There have also been cases of laboratory-acquired infection [8]. Lack of systemic spread is thought to be, in part, due to the constricted temperature range shown *in vitro* by *H. ducreyi* limiting its ability to spread. This property also probably accounts for its preference for the skin [9]. It is speculated that the infective process of *H. ducreyi* begins with small abrasions in the skin that occur during sexual intercourse [1,10]. Erythematous papules appear four to seven days after initial infection and progress to pustules [11]. Two to three days thereafter, pustules often burst producing very painful ulcers. These shallow ulcers with granulomatous bases typically have ragged and undermined edges and purulent exudates. In 50% of cases, inguinal lymphadenopathy occurs with involved lymph nodes developing buboes in some cases [12]. Buboes can unexpectedly rupture if not drained or aspirated. Other complications that can arise are phimosis in men or additional ulceration caused by secondary bacterial infection [11].

1.2.1 Natural History

Leon Bassereau first identified chancroid to be separate from the chancres of syphilis in 1852. However, Augusto Ducrey was the pioneer in *H. ducreyi* research and in recognition, the bacterium was named after him [13]. Ducrey was unable to culture *H. ducreyi* on laboratory media so he used innovative forearm autoinoculation techniques using pus taken from soft genital ulcers. After repeated passage, Ducrey was able to microscopically demonstrate a microorganism 1.48 microns in length and 0.5 microns in width with rounded ends [13]. Although there is still controversy as to how *H. ducreyi* was first cultured on blood agar, Bezancon was the first to fulfill Koch's postulates in 1900. He was able to re-culture the organism from humans re-inoculated with *H. ducreyi* cultured from genital ulcers [13]. Tomasczewski later confirmed this work [13]. Of late, *H. ducreyi* has exhibited plasmid-mediated antimicrobial resistance to β-lactams, penicillins, tetracyclines,

chloramphenicol, sulphonamides, and aminoglycosides [1]. There have also been reported cases of chromosomally-mediated resistance to penicillin, ciprofloxacin, ofloxacin, and trimethoprim [1].

1.2.2 Epidemiology

The epidemiology of chancroid is still poorly understood due to the continued lack of diagnostic tests available [14]. Under reporting of chancroid likely derives from the fastidious growth requirements of *H. ducreyi* that lead to difficulty in culturing the organism from clinical specimens. In addition, culture media is expensive for resource-poor endemic areas. Therefore, using the surveillance of syphilis as a guide, the World Health Organization approximates that there are annually about 6 million cases of chancroid worldwide [15].

Chancroid continues to play a causative leading role in GUD in resource poor countries such as Asia, Latin America, and Africa and has been linked to high morbidity rates [11,16-21]. There have been reports that chancroid is responsible for up to 56% of GUDs in these countries [14,17-20]. Conversely, chancroid is uncommon in developed countries such as the United States [7,22], Canada [23], and Europe [24] where chancroid is restricted to only sporadic outbreaks. Individuals infected with chancroid have been epidemiologically linked to low socioeconomic status and/or to having sex with commercial sex workers [25-28]. Interventional therapy targeting sex workers in many countries have resulted in a sharp decline in chancroid cases. For instance, Kenya implemented programs that increased condom usage by sex workers by 80% resulting in a decline in the proportion of GUDs caused by chancroid to less than 10% [27]. Similar results were also seen in Thailand where there was a 95% decline in chancroid within five years of initiating a 100% condom policy for commercial sex establishments [27,29]. Chancroid once was the most

prominent GUD in Kenya [27]. Legalization of prostitution, offering regular examinations and treatment options to sex workers in Senegal resulted in only infrequent reports of chancroid [27]. A dramatic drop in chancroid rates can also be achieved by presumptive antibiotic treatment of female sex workers in areas where the rates of male circumcision are low without changing condom usage. Such a strategy has resulted in a 46% decrease in clients reporting *H. ducreyi* infection over a one-year period [30].

Chancroid is more common in men than in women with a ratio as low as 3:1 and as high as 25:1, respectively. Uncircumcised men [23] and persons using crack cocaine or engaged in sex with crack cocaine users are at particular risk for acquiring chancroid [22,31].

1.3 Methods of Diagnosis

1.3.1 Clinical and Culture Detection

The clinical presentation of chancroid is difficult to differentiate from other GUDs such as infections caused by *Treponema pallidum* and herpes simplex virus (HSV) [22]. Also, pre-existing human immunodeficiency virus (HIV) infection alters the clinical presentation and clinical course of chancroid making it harder for clinicians to identify [32-35]. As a result, chancroid has a clinical diagnostic accuracy ranging from 33% to 80% [36,37] with the best accuracy in clinical areas where chancroid is endemic as clinicians were more clinically experienced in the diagnosis [7]. There have been many studies performed to determine the best media to support the growth of all *H. ducreyi* strains [38-41]. No single media has been shown to be superior due to differences in nutrient requirements, mainly nitrogen source, required by various strains of *H. ducreyi* [10]. The combination of using two agar-based media, gonococcal agar base medium supplemented with hemoglobin, fetal bovine serum, IsoVitalex, and vancomycin, and Mueller-Hinton agar supplemented with chocolatized horse blood, IsoVitalex, and vancomycin, is optimal for *H. ducreyi* isolation

[38,39]. Together, these two media possess a 71% positive detection rate from clinical samples [38,39]. The replacement of fetal bovine serum with either activated charcoal [7,42,43] or bovine albumin [44] lessens the cost of the media without affecting the isolation rates. More recently, Mueller Hinton agar base with chocolate horse blood and Isovitalex added in tandem with Columbia agar base with bovine hemoglobin, activated charcoal, fetal calf serum and Isovitalex have been advocated as the primary isolation media [45]. This approach would allow for the identification of vancomycin-sensitive strains previously reported in the United States [46] at the expense of not inhibiting the growth of Gram-positive normal flora [47]. Despite these limitations, laboratory culture remains the "gold standard" in diagnosis of chancroid due, in part, to its cost-effectiveness and availability [1].

1.3.2 Non-culture Techniques

The diagnostic tools described in this section are only used as research tools at the present time. These techniques would be too expensive to implement in resource-poor areas where *H. ducreyi* remains endemic [1]. *H. ducreyi* can be identified by polymerase chain reaction (PCR) using primers to amplify a variety of different genes: *groE*L gene [48], 16S rRNA gene [49-51], *rrl* (23S) and *rrs* (16S) ribosomal intergenic spacer region [52], and an anonymous 1.1kb fragment [1,53]. A multiplex PCR (M-PCR) able to identify several pathogens responsible for GUDs – *H. ducreyi*, *T. pallidum*, HSV 1 and 2 – has demonstrated an increasing trend of multiple GUD infections in the same patient at the time of specimen collection [54]. Thus far, M-PCR is not available commercially or for clinical use and still has some unresolved problems. M-PCR has proven to be successful for *in vitro* cultured *H. ducreyi*; however, identification of *H. ducreyi* from genital ulcer specimens by M-PCR has been a challenge because of the presence of *Taq* polymerase inhibitors in the transport media resulting in a 75% sensitivity rate as compared to culture [16,53,54]. This diagnostic

accuracy is a significant improvement over culture techniques that exhibit a 35-75% sensitivity rate [1].

Antigen detection methods, including an indirect immunofluorescence assay using a monoclonal antibody against either an outer membrane protein [55] or lipooligosaccharide [56], have shown a greater sensitivity (>90%) for chancroid detection as compared to culturing methods [55]. DNA-DNA hybridization techniques using ^{32}P-labelled probes has proven successful for the detection of *H. ducreyi* from pure or mixed bacterial suspensions or from material sampled from rabbit lesions [57]. Finally, enzyme immunoassays using sonicated whole-cells [58,59], outer membrane proteins [60], or purified lipooligosaccharide [60] as antigen have all been problematic for serological detection due to the cross-reactivity of human sera with other *Haemophilus* species [59,61].

1.4 Links to HIV Transmission

Several epidemiological prospective and cross-sectional African studies have unequivocally demonstrated that *H. ducreyi* infections are a risk factor for the spread of heterosexually acquired HIV infection [22,62-64]. In countries where HIV is prevalent, chancroid is the most common GUD with a strong synergy between the two [65-67]; conversely, chancroid is uncommon in countries with low HIV infection rates [27]. There are many mechanisms that facilitate HIV transmission in individuals with chancroid. Firstly, GUDs, including chancroid, disrupt the epithelial and mucosal barriers as opposed to non-ulcerative STIs [68-72]. Secondly, chancroid ulcers have been shown to contain $CD4^+$ T lymphocytes – the primary cellular target of HIV [32,33]. HIV has also been isolated from chancroid ulcers [70-71]. Macrophages present in the ulcers have significant upregulation of both CCR5 and CXCR4 expression with CD4 T cells having significantly increased expression of CCR5. Therefore, this significant increase in HIV-1 co-receptor expression

could facilitate the acquisition of certain HIV strains – i.e. R5 (CCR5), X4 (CXCR4), and dual-tropic strains [73]. Thirdly, semen from HIV seropositive patients co-infected with chancroid has a higher quantity of HIV as compared to those HIV-seropositive persons not infected by *H. ducreyi* [74]. HIV-chancroid co-infected patients have an increased number of chancroid ulcers that require more prolonged antibiotic therapy for microbiological and clinical cure compared to HIV-seronegative chancroid infected patients [74]. GUDs also increase the vaginal shedding of the HIV [75]. The risk of both HIV infection and chancroid is increased in uncircumcised men [68,76].

1.5 Treatment and Prevention

The recommended antibiotic treatment for chancroid issued by the World Health Organization includes either 500mg oral erythromycin three times daily for one week, a single intramuscular dose of 250mg ceftriaxone, a single oral dose of 500mg ciprofloxacin, or a single intramuscular dose of 2g spectinomycin [11]. The single dose antibiotic treatments are advantageous because of patient compliance as compared to treatments lasting several days [27,77]. Uncircumcised men [32,78,79], individuals co-infected with HIV [32, 80], or undiagnosed HSV infection [11] all have an increased risk of treatment failure. The World Health Organization has also implemented a syndromic management approach in which patients presenting with presumptive STIs are treated with antimicrobial agents active against all probable STIs endemic for that local area. This management system eliminates expensive laboratory culture tests, problematic culturing of this fastidious organism, and requires minimal clinical diagnostics [81].

Proper hygiene has been shown in the pre-antibiotic era to reduce the spread of chancroid. During World Wars I and II, washing the genital area with soap and water after

sexual intercourse decreased the risk of acquiring chancroid [26,82]. Male circumcision reduces the risk of acquiring both *H. ducreyi* and HIV infections [78,83,84].

Evidence exists to support the possibility for the total eradication of chancroid. There are three important factors that determine if eradication is possible and *H. ducreyi* infection meets all three [85]. Firstly, chancroid can be diagnosed clinically and microbiologically thus aiding in treatment and surveillance of the infection. Secondly, chancroid is easily treated with antibiotics. Lastly, chancroid cannot be maintained outside of active human sexual networks because there are no other known biological reservoirs [27].

1.6 Host Immune Response

Results from the human model of chancroid infection indicate that at the pustular stage of infection 48 hours after inoculation, *H. ducreyi* is observed both in epithelial micropustules as well as in the dermis. The bacterium has been shown to co-localize with polymorphonuclear leukocytes, collagen, fibrin, and macrophages [86]. As the infection progresses, an abscess is formed by polymorphonuclear leukocytes with a ring of macrophages at the base of the pustule [5,86]. In the human challenge model of chancroid, there is also recruitment of both CD4 and CD8 cells to the dermis [87]. Little association with the following cells is seen: keratinocytes, fibroblasts, T cells, Langehans cells, laminin or bironectin [86]. *H. ducreyi* is maintained extracellularly and evades phagocytosis by poorly understood mechanisms [14]. This latter observation remains to be confirmed during natural infection. In both natural and human experimental infection, the production of a delayed-type hypersensitivity reaction occurs [87-90]. A humoral immune response is mounted as demonstrated by anti-*H. ducreyi* antibodies present in the serum [58,60,91]. However, the immune response is non-protective as re-infection is common [6,92-96]. The immune response also does not seem to be effective in clearing the bacterial infection with

lesions lasting for a lengthy period of time and most often unresolved without antibiotic treatment [1]. However, a higher anti-*H. ducreyi* antibody level is detected in patients with longer lasting ulcers (>4weeks) as opposed to ulcers lasting only 14 days. This suggests that the humoral immune response occurs late in the ulcerative stage of chancroid infection [97].

Recent investigations suggest that immunizing pigs with the *H. ducreyi* hemoglobin receptor, HgbA, protects the animals against experimental chancroid infection. Additional studies are being pursued to determine if an HgbA subunit vaccine can prevent chancroid [98]. This outer membrane protein appears to be an excellent vaccine candidate because a *H. ducreyi* HgbA mutant cannot initiate infection as seen in the human model [14].

1.7 Potential Virulence Factors

Several potential virulence factors are thought to contribute to the pathogenicity of *H. ducreyi*. The *H. ducreyi* lipooligosaccharide (LOS) with a molecular mass of 3.5 to 6kDa [99] is physiologically similar to that of other Gram-negative pathogens exhibiting mucosal surfaces adherence characteristics and displays an epitope similar to a precursor of a major blood group antigen [100,101]. This property allows for possible evasion of host immune responses. The LOS can be sialyated resulting in a serum-resistant phenotype [102,103] but with reduced ability to attach and invade human karotocytes [104].

The surface of *H. ducreyi* is covered with pili that mediate host cell adhesion [105] and have a molecular mass of 24kDa [105]. A mutant lacking pili was not attenuated in virulence in the temperature-dependent rabbit model of chancroid infection [1]. The host receptor for pili has not yet been identified [7].

H. ducreyi secretes both a cytolethal distending toxin and a hemolysin that cause destruction of tissue and aid in evasion of the immune system [14]. The cytolethal distending toxin is comprised of three soluble proteins – 22, 33, and 26kDa – and is

transported to the Golgi apparatus of epithelial cells, arresting the cells in G2 phase of growth [106,107]. Cytolethal distending toxin also induces apoptosis in both T and B cells. The hemolysin, responsible for ß-hemolysis [108], damages human foreskin fibroblasts in cell culture [109] and lyses a variety of cell types including keratinocytes, fibroblasts, macrophages, T, and B cells [110,111]. Hemolysin is comprised of two proteins that are 15 and 16kDa in size [112].

The outer membrane receptors for hemoglobin (HgbA; 100kDa) and heme (TdhA; 82kDa) allow *H. ducreyi* to acquire iron and heme [113,114]. An HgbA isogenic mutant is attenuated in virulence both in the rabbit [1,115] and in the human challenge models of chancroid infection [1]. The importance of TdhA as a virulence determinant is unknown as a TdhA mutant is yet to be tested in the human challenge model.

Also, a major outer membrane protein (MOMP) ranging from 39 to 42kDa has been found in many strains *H. ducreyi* and exhibits no properties typical of a porin [116]. There is some evidence to support a role of this protein in serum resistance [117,118].

A Cu-Zn containing superoxide dismutase (Cu,Zn-SOD), termed SodC, catalyzes the conversion of superoxide ions to oxygen and hydrogen peroxide. As the 21kDa SodC protein resides in the periplasmic space and endogenously produced superoxide cannot permeate the cytoplasmic membrane [119], *H. ducreyi* SodC has been proposed to protect the organisms from exogenous superoxide anions generated by polymorphonuclear neutrophils [120]. In support of this proposal, a SodC isogenic mutant was more susceptible to extracellular superoxide killing compared to the parental strain [120].

Finally, a periplasmic zinc transport protein (ZnuA) is responsible for shuttling this essential nutrient required for protein structural stability and protein catalytic activity across the periplasmic space [121,122]. The *znuA* gene encodes a mature protein of 32kDa [123].

The *in vitro* growth rate of an isogenic ZnuA mutant was decreased and produced fewer lesions in the rabbit model as compared to the wild-type isolate [123].

1.8 Animal Models of Chancroid Infection

1.8.1 Human Challenge Model

In the human challenge model of chancroid infection, human volunteers are inoculated using a Multi-Test Applicator (similar to the device used in allergy testing) with 10^1 to 10^2 colony forming units (CFUs) of viable *H. ducreyi* on the upper arm for lesion development [5]. The experimental endpoint is fourteen days post-infection and no adverse systemic symptoms are incurred [90]. This model provides information on the first few weeks of infection since patients with naturally occurring chancroid tend not to visit a clinic until three to four weeks after becoming infected [90]. This model is limited to the study of the early stages of chancroid infection as lesions are not allowed, for ethical and safety reasons, to proceed to ulceration. In addition, only antibiotic sensitive strains are tested [124].

1.8.2 Swine Model

The skin of pigs is structurally and physiological similar to human skin. Lesions occurring seventeen days post-inoculation of pig ears resemble that of natural infection with *H. ducreyi* [124]. Using an extremity (ears) is advantageous because the optimal temperature for the growth of *H. ducreyi* is 33°C to 35°C. Inoculation of *H. ducreyi* is performed with the same device used in the human model with about 10^4 CFU per dose. This model has been used to study both the pathogenicity and immunology of *H. ducreyi* infection [124].

1.8.3 Rabbit Model

In the temperature-dependent rabbit model of chancroid infection, rabbits are intradermally injected with 10^5 CFUs of viable *H. ducreyi* [125]. The entire clinical

expression of disease is recapitulated in this model from the formation of necrotic lesions to ulcer development. Live organisms are recovered from the ulcers. This model does have a drawback as the rabbits must be housed at 15-17°C for necrotic lesion formation. *H. ducreyi* grows optimally at 33°C which is achieved by dropping the body temperature of the rabbit [125].

1.8.4 Primate Model

In the primate model of chancroid infection, adult macaques are injected with 10^7 to 10^8 CFUs of viable *H. ducreyi* into the male foreskin or female vaginal labia [126]. Similar to natural infection, ulcers develop after six to twelve days post-inoculation. The changes in lesion and histopathological appearance during the course of infection mirror the abnormalities seen during natural chancroid, although the ulcers are less prominent in the female macaques. *H. ducreyi* is recovered from lesions up to twenty days post-inoculation. Inguinal lymphadenopathy is noted in male macaques. The expense of maintaining primates is a significant limitation of this model [124].

1.9 Heme and Iron Assimilation in Gram-negative Bacteria

To survive in the low iron and heme environment of the human host, high affinity pathways for iron and heme acquisition are required by pathogenic bacteria to obtain iron, an essential molecule in many metabolic pathways [127]. Iron is limited in the human host due to the low abundance of extracellular free iron and due to binding to the glycoproteins transferrin and lactoferrin [128]. Host iron restriction serves as a defense against microbial invaders and protects host cells from ferric iron toxicity [129]. Also, the vast majority of total body iron (99%) is found intracellularly in the form of heme and hemoproteins [130]. Therefore, pathogenic bacteria with an intracellular lifestyle can utilize heme directly

whereas extracellular bacteria require the release of cellular heme and iron sources by means of hemolysins, cytotoxins, or permeases [131].

Bacteria overcome the iron and heme restriction imposed by the human host by several mechanisms (Figure 1). Firstly, some bacteria secrete small molecules termed siderophores or hemophores that capture iron or heme and heme-hemoplexin complexes, respectively. Examples of pathogenic bacteria using siderophores to scavenge free iron are as follows: *Neisseria gonorrheae* [132], *Escherichia coli* [133], and *Salmonella* spp. [134] using the siderophore enterobactin; *Yersinia pestis* using the siderophore yersiniabactin [135-139]; and mycobacteria using the siderophore carboxymycobactin [140]. The ability of siderophores to chelate iron is due in part to the high affinity these molecules display for iron. For example, the affinity of enterochelin (10^{-49}M) for iron exceeds that of transferrin (10^{-20}M) by several orders of magnitude [141]. Following binding to a specific outer membrane receptor, the siderophore-iron complex is transported into the periplasmic space [142]. Bacteria shown to produce hemophores include: *H. influenzae* (HxuA), *Serratia marcescens*, *Y. pestis* (HasA), and *Pseudomonas* spp. (HasAp) [143,144]. Once bound to their respective heme source, the hemophore then shuttles the complex to an outer membrane receptor.

The expression of outer membrane receptors that specifically recognize host iron-containing proteins and hemoproteins represents another significant mechanism for iron and heme acquisition (Figure 1). These high affinity outer membrane receptors bind free heme, hemoproteins, hemophore-bound proteins, transferrin, and lactoferrin [145,146]. The iron and heme are then extracted from the ligand-receptor complex by a poorly understood mechanism and transported across the outer membrane using a TonB-mediated process.

Figure 1: Proposed heme acquisition pathways in Gram-negative bacteria (adapted from reference 127).

In both cases, energy for transport across the outer membrane is supplied by the TonB complex. This complex includes the TonB protein anchored to the cytoplasmic membrane and two accessory proteins, ExbB and ExbD. Once deposited into the periplasmic space, iron and heme are conveyed to the cytoplasm via an ABC transporter. This system is composed of a periplasmic binding protein to shuttle heme through the periplasmic space, a membrane-associated permease, and an ATPase to supply the necessary energy. These mechanisms for heme transport are also demonstrated in iron transport.

A: Direct binding of ligand to its specific TonB-dependent outer membrane receptor.
B: Hemophore capture of heme or hemoproteins.

Hb = hemoglobin; HbR = hemoglobin receptor; Hm = heme; HmR = heme receptor; OM = outer membrane; P = periplasm; CM = cytoplasmic membrane.

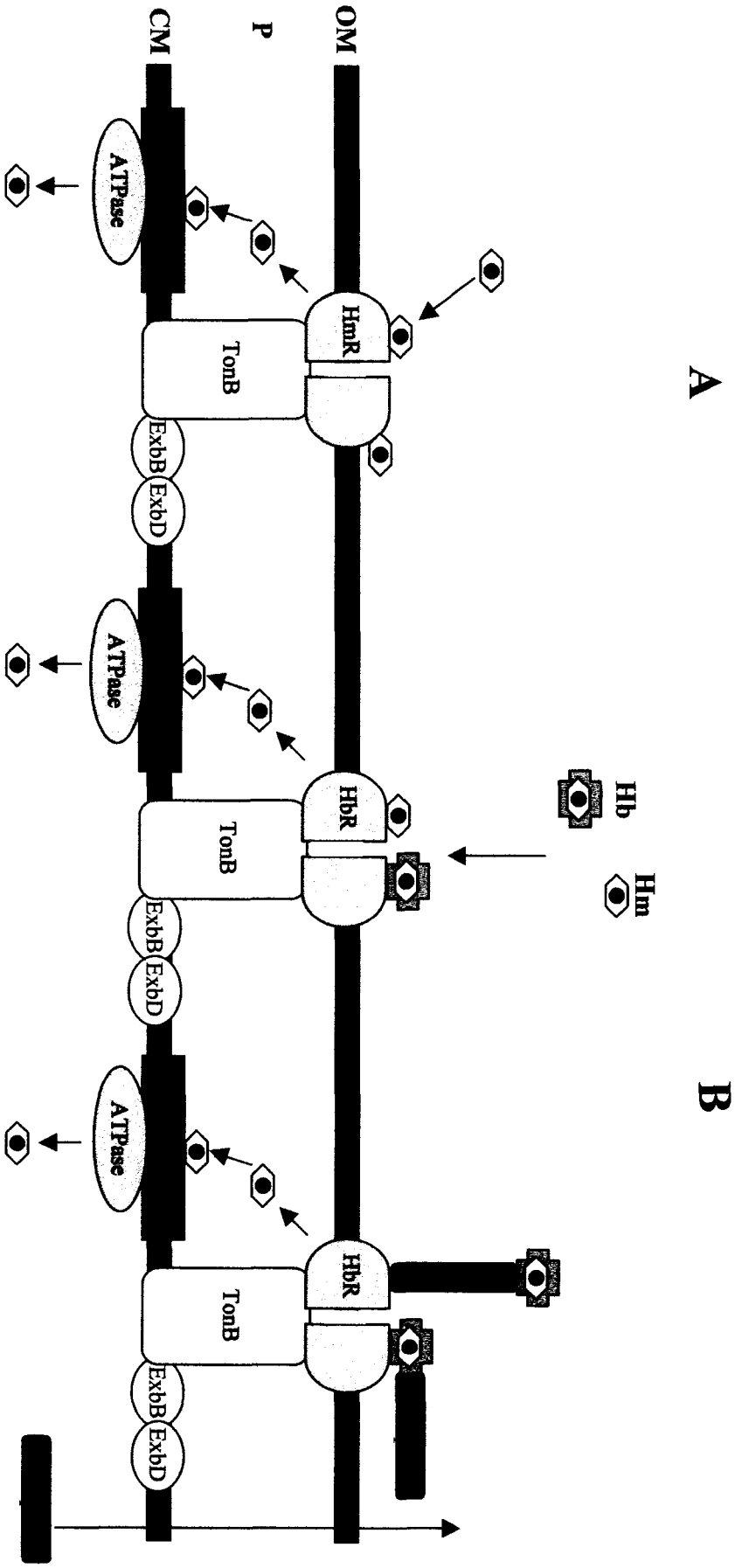

Several such outer membrane proteins have been identified in this receptor-mediated process and include the following: HmbR, the hemoglobin receptor, HpuAB, the hemoglobin-haptoglobin receptor, LbpAB, the lactoferrin receptor, TbpAB, the transferrin receptor for both *N. gonorrheae* and *N. meningitidis* [147-150]; HmuR, the heme receptor for *Y. pestis* [151]; ShuA, the heme receptor for *Shigella dysenteriae* [152]; and PhuR and HasR, the heme receptors for *P. aeruginosa* [153].

1.9.1 TonB System

Once captured by the ligand-specific outer membrane receptors, iron and heme are transported into the periplasm of Gram-negative bacteria by an energy-mediated TonB-dependent process (Figure 1)[154]. It has been experimentally shown that many outer membrane receptors require a functional TonB system for successful iron and heme transport [113,114,151,152,154-158]. The proton motive force responsible for this displacement arises from the TonB complex comprised of the TonB protein anchored to the cytoplasmic membrane and two accessory proteins, ExbB and ExbD. Receptors requiring energy supplied by the TonB system are therefore deemed TonB-dependent and possess similarities in amino acid sequences referred to as TonB boxes [154]. TonB boxes in the receptor sequences are areas that interact directly with the TonB protein.

1.9.2 ATP-Binding Cassette (ABC) Transporters

Once deposited in the periplasmic space, iron and heme are conveyed to the cytoplasm via an ABC transporter (Figure 1) [159]. Thus, the ABC transporter represents a point of convergence for both the iron and heme uptake pathways as each system uses this mechanism to transport its respective ligand into the cytoplasm [160]. A typical ABC transporter in Gram-negative bacteria consists of a periplasmic binding protein that shuttles its ligand across the periplasmic space, a specific cytoplasmic permease, and an ATPase

which supplies the energy necessary to transport the ligand across the cytoplasmic membrane [161]. HitABC is used for iron transport in *H. influenzae* [162], SfuABC for iron transport in *S. marcescens* [163], FbpABC for iron transport in pathogenic *Neisseria* species [164], YfeABCD for acquisition of inorganic iron and HmuTUV for heme and hemoprotein transport in *Y. pestis* [165], HutWXZ for heme acquisition in *Vibrio cholerae* [166], PhuUVW for heme transport in *P. aeruginosa* [153], and ShuTUV for heme transport in *S. dysenteriae* [151]. Despite the lack of homology among these proteins, their existence in several pathogenic bacteria suggests that these systems are required for pathogenicity [164 167,168].

1.9.3 Ferric Uptake Regulation

Iron acquisition and therefore virulence are often regulated in bacteria by a ferric uptake regulated (Fur) protein [169-174]. When ferrous iron is present, the Fur protein binds as a homodimer to DNA regulatory sequences known as Fur boxes. This binding action represses gene transcription and therefore suppresses genes involved in iron transport [175].

1.10 Heme and Iron Acquisition in *H. ducreyi*

H. ducreyi has an absolute requirement for heme due to the absence of several enzymes in the heme biosynthesis pathway. Circumstantial biochemical evidence suggests that the organism lacks ferrochetalase [176,177], the enzyme that catalyzes the insertion of ferrous iron into the porphyrin ring. The bacterium exhibits a high heme requirement (77μM) that is in excess of that needed by other heme-obligate organisms [7,44,113]. *H. ducreyi* produces no siderophores [176]. Various compounds can satisfy the high heme demands of *H. ducreyi* including hemoglobin, hemoglobin-haptoglobin, catalase, free heme, and heme-albumin [176]. Access to many of these intracellular compounds is likely by cell lysis via the *H. ducreyi* produced hemolysin and cytotoxins [178,179]. As the heme moiety

is comprised of a porphyrin ring and a chelated iron molecule, the acquisition of heme by *H. ducreyi* fulfills both the heme and iron requirements of the organism. Size considerations suggest that heme entry into the periplasmic space does not involve passage through outer membrane porins. The 600 Daltons (Da) size exclusion limit of these channels poses a barrier to heme [128] which is usually complexed to chloride or hydroxide or forms a homodimer in solution [127]. Heme uptake in *H. ducreyi* proceeds by a receptor-mediated process. Two TonB-dependent receptors have been identified, HgbA which binds hemoglobin [114] and TdhA which binds heme [113]. Once heme is in the periplasmic space of *H. ducreyi*, nothing is known about its fate. It is reasonable to assume that a heme-dedicated ABC transporter shuttles heme across the periplasmic space into the cytoplasm similar to other Gram-negative bacteria (Figure 1).

A Fur protein has been identified in *H. ducreyi*; however, the genes that it regulates have not been identified [74]. Evidence linking Fur regulation of *tdhA* and *hgbA* include upregulation of TdhA and HgbA expression under heme-limiting conditions; putative Fur box promoters present in *tdhA* and *hgbA*; and upregulation of TdhA and HgbA when expressed in TonB mutants [113].

1.11 Proteomics

Proteomics is defined as a large-scale study of proteins with particular attention to structure and function. The approach encompasses protein separation, identification, quantification, and cellular interactions [180]. The most commonly used method involves two-dimensional (2D) gel analysis [181,182]. In this process, a protein sample is first separated by pI via isoelectric focusing (1^{st} dimension) followed by separation based on mass via SDS-PAGE (2^{nd} dimension). The second dimension allows for protein spot visualization using various gel staining methods and the peptide signature of the protein spot is determined

by mass spectroscopy [183]. Two-dimensional gel electrophoresis is both quantitative and highly reproducible and is mainly used to identify the entire protein complement within a protein sample, to determine differences in protein expression between different protein samples, and to identify post-translational protein modifications [182,184].

2D gel electrophoresis has been successfully used in a variety of medical disciplines such as in neuropathology research to compare differences in protein expression in abnormal brain and normal brain tissue [185], in cardiology to compare diseased and normal myocyte protein expression [186], and in oncology to identify new tumor markers in various cancerous cells [183]. The most extensive use of this technology has been in microbiology linking genomic and proteomics in pathogens such as *S. typhimurium* [187], *E. coli* [188], and *H. influenzae* [189]. Proteomics is also an important tool to identify alterations in protein expression influenced by environmental changes that are difficult to discern using a genomics approach. Such analysis has identified many bacterial virulence determinants as well as chemical and temporal resistance to many biochemical effects [190-193].

In the *Haemophilus* genus, 2D gel electrophoresis has been performed on *H. ducreyi* and *H. influenzae*. For *H. ducreyi*, the 35 000HP proteome was subjected to 2D gel analysis followed by mass spectrometry identifying a total of 122 soluble and insoluble proteins [194]. There was only minimal protein diversity when compared to protein profiles from other clinical *H. ducreyi* strains with most of the proteins having homology to *H. influenzae* proteins. The *H. influenzae* proteome comprises one of the largest 2D proteome databases available to date [189].

There are several limitations to using 2D gel electrophoresis as a proteomics tool. Hydrophobic proteins are difficult to both solubilize and separate. Very basic proteins, high-mass proteins, and protein complexes are also difficult to separate. Lastly, proteins

expressed in low amounts are not well visualized because of the low sensitivity of available staining methods [190].

1.12 Metalloporphyrins

As mentioned previously, a large number of bacterial pathogens possess a heme uptake pathway for iron acquisition. Iron is an essential nutrient not only for these pathogens but also for the host. Therefore, this uptake system is a virulence mechanism for the bacterium and can, in turn, be exploited as a potential target for drug delivery. New drug strategies are warranted with increasing emergence of antibiotic resistance not only in *H. ducreyi* isolates, but also in many other pathogenic bacteria.

Metalloporphyrins (MPs) are compounds formed from a porphyrin ring and a metal ion. Several non-iron metalloporphyrins possess antibacterial activity against many pathogenic bacteria [195,196]. These compounds enter the bacteria by using the heme uptake pathway. However, the precise molecular components co-opted are unclear. In *Y. entercolitica*, the presence of both the outer membrane heme receptor, HemR, and TonB were necessary for entry of the non-iron substituted MP. However, transport across the inner membrane was not necessary for its antibacterial action [196]. In contrast, in *N. gonorrheae*, the outer membrane hemoglobin receptor was not required for the anti-gonococcal activity of the MP [195].

Gallium protoporphyrin IX (Ga-PPIX) shows the most potent antibacterial action against Gram-negative and Gram-positive bacteria and against *Mycobacterium* spp. [195]. The antibacterial activity of Ga-PPIX is a function of the entire molecule as free gallium possesses no deleterious effects on pathogenic bacteria. Ga-PPIX exerted the most antibacterial activity when bacteria were grown under iron-limiting conditions where the expression of the components of the heme uptake pathway is maximal [195]. Zinc

protoporphyrin IX (Zn-PPIX) is highly active against several clinical strains of *H. ducreyi*. Zn-PPIX and Ga-PPIX are the most active MPs tested against *N. gonorrheae* strain FA-19 [196]. These MPs do not inhibit the residential vaginal microflora of which *Lactobacillus* spp. comprises the most populous component [196]. Maintenance of the normal vaginal flora is important as these organisms are thought to naturally aid in the prevention of colonization by pathogenic bacteria [197]. Ga-PPIX is non-toxic to primary human fibroblasts (in concentrations up to 100μg/ml) and produces no visible adverse affects in mice intraperitoneally injected with 25-20mg/kg followed by four daily injections of 10-12mg/kg [196]. The addition of 2μg of Ga-PPIX to mouse vaginal mucosa significantly protected against *N. gonorrheae* infection [195]. These observations suggest that substituted non-iron MPs may lead to the development of novel topical microbicides in preventing STIs.

1.13 Hypothesis

We propose that once heme is deposited into the periplasmic space of *H. ducreyi*, a heme-dedicated periplasmic binding protein, a component of an ABC transporter, shuttles heme across the periplasmic space to the cytoplasmic membrane.

1.13.1 Objectives

To confirm the hypothesis, we pursued the following objectives:

1. Identification of a periplasmic protein in *H. ducreyi* upregulated under heme-limiting conditions.
2. Cloning the gene encoding the *H. ducreyi* periplasmic heme binding protein.
3. Production of polyclonal antisera against the *H. ducreyi* periplasmic heme binding protein.
4. Affinity purification of the *H. ducreyi* periplasmic heme binding protein.
5. Functional characterization of the *H. ducreyi* periplasmic heme binding protein.
6. Determination of the ubiquity of the *H. ducreyi* periplasmic heme binding protein.

CHAPTER TWO

MATERIAL AND METHODS

2.1 Bacterial Strains and Growth Conditions

All *H. ducreyi* strains were kindly provided by Dr. D.W. Cameron (University of Ottawa, Ottawa, ON, Canada)(Table 1). *H. ducreyi* 35 000 strain was isolated in the 1975 Winnipeg chancroid outbreak; this strain was used for hHBP (*H. ducreyi* heme-dedicated periplasmic binding protein) identification, expression, and purification experiments. *H. ducreyi* was grown at 35°C with 5% CO_2 and saturated humidity. *E. coli* TOP10 cells and BL21 Star™ (DE3) cells were purchased from Invitrogen (Carlsbad, CA, USA) and were used for cloning and expression of the *hhbp* gene (Table 1). *E. coli* strains were grown at 35°C in ambient air. *H. influenzae* and *Y. entercolitica* clinical isolates were kindly provided by Dr. F. Chan (Children's Hospital of Eastern Ontario, Ottawa, ON, Canada)(Table 1). *H. influenzae* strains were grown at 35°C in an atmosphere containing 5% CO_2 and saturated humidity; *Y. entercolitica* strains were grown at 35°C in ambient air.

2.2 Media and Culture Conditions

2.2.1 Chocolate Agar Plates (CAP)

All bacterial strains were subcultured from stock cultures frozen at –80°C onto supplemented chocolate agar plates [CAP; GC Medium Base (Difco/Becton Dickinson, Sparks, MD, USA), 1% (w/v) bovine hemoglobin (BBL/Becton Dickinson, Cockeysville, MD, USA), 5% (v/v) heat inactivated fetal bovine serum (FBS; Gibco/Invitrogen, Carlsbad, CA, USA), 1% (v/v) Isovitalex (BBL/Becton Dickinson, Cockeysville, MD, USA)] for 24 hours prior to growth on selective media. For protein and DNA extraction, bacteria were grown on CAP for 24 hours.

Table 1. Bacterial strains used in the current study

Bacterial Strains	Relevant Strain Information	Reference
H. ducreyi		
35 000	Clinical isolate; Winnipeg, Canada	Dr. D.W. Cameron
J1159	Clinical isolate; Nairobi, Kenya (1986-87); Serotype E; LOS Class 6	Dr. D.W. Cameron
G29677	Clinical isolate; Nairobi, Kenya (1986-87); LOS Class 4	Dr. D.W. Cameron
C148	Clinical isolate; Nairobi, Kenya (1981); Serotype A; LOS Class 1	Dr. D.W. Cameron
PPC 263/1293	Clinical isolate; Nairobi, Kenya (1986-87); Serotype E; LOS Class 3	Dr. D.W. Cameron
V1157	Clinical isolate; Seattle, USA; Serotype C; LOS Class 5	Dr. D.W. Cameron
RO-27	Clinical isolate; Nairobi, Kenya (1986-87); LOS Class 2	Dr. D.W. Cameron
K10159	Clinical isolate; Nairobi, Kenya (1986-87); LOS Class 1	Dr. D.W. Cameron
R0-12	Clinical isolate; Nairobi, Kenya (1986-87); LOS Class 2	Dr. D.W. Cameron
36-F-2	Pasteur Institute, Paris, France; LOS Class 3	Dr. D.W. Cameron
PPC358/1315	Nairobi, Kenya (1986-87); Serotype D; LOS Class 7	Dr. D.W. Cameron
H. influenzae		
70824	Non-typeable; Biotype III; Blood culture clinical isolate	Dr. F. Chan
15631	Non-typeable; Otitis media clinical isolate	Dr. F. Chan
HI-38	Non-typeable; Otitis media clinical isolate	Dr. F. Chan
51944	Non-typeable; Biotype III; Blood culture clinical isolate	Dr. F. Chan
Y. entercolitica		
731918	Biotype IV; Serotype 0:3; Stool culture clinical isolate	Dr. F. Chan
M58850	Biotype IV; Serotype 0:3; Stool culture clinical isolate	Dr. F. Chan
E. coli		
One Shot® TOP10	F^- mcrA Δ(mrr-hsdRMS-mcrBC) Φ80lacZΔM15 ΔlacX74 recA1 araD139 Δ (ara-leu)7697 galU galK rpsL (str^R) endA1 nupG	Invitrogen; Burlington, ON, Canada
BL21 Star™ (DE3)	F^- ompT $hsdS_B$ ($r_B^-M_B^-$) gal dcm rne131 (DE3)	Invitrogen; Burlington, ON, Canada

2.2.2 Modified Gonococcal Agar Plates

H. ducreyi 35 000 was grown on gonococcal agar plates [GC; GC Medium Base and 1% (v/v) Isovitalex] supplemented with determined concentrations (15-100 μg/ml) of heme and (10-200μM) of desferoxamine. Heme stock solutions were made by dissolving bovine hemin chloride (Sigma, St. Louis, MO, USA) in 0.1N NaOH and were used without further sterilization. Desferoxamine (desferal; Ciba Pharmaceutical Co., Summit, NJ) stocks (10mM) were made by dissolving the compound in double-distilled H_20 (ddH_20) followed by filter-sterilizing using 0.75mm filters (Nalge Nunc International, Rochester, NY, USA). For cell fractionation, bacteria were grown on modified gonococcal agar plates (MGA) for 24 hours. For periplasmic protein extraction samples to be used for 2D gel analysis, bacteria were subcultured three subsequent times on GC agar plates supplemented with the same concentration of heme and desferoxamine to deplete intracellular heme stores.

2.2.3 Luria Bertani Agar Plates or Broth plus Ampicillin

E. coli strains were grown on Luria Bertani (LB) agar plates [LB broth (Difco/Becton Dickinson, Sparks, MD, USA), 1.5% (w/v) Bacto Agar (Difo/Becton Dickinson, Sparks, MD, USA)] or in LB broth with vigorous shaking at 200rpm using the appropriate growth conditions. To induce expression of the *hhbp* gene in BL21 Star™ (DE3) *E. coli* cells, isopropylthio-B-galactoside (IPTG; Invitrogen, Carlsbad, CA, USA) was added to a final concentration of 1mM at the mid-log phase (OD_{600} 0.5-0.8) of growth. For positive transformant selection, ampicillin (AMP; Sigma, St. Louis, MO, USA) was also added to the media to a final concentration of 100 μg/ml.

2.3 Cell Fractionation Procedures

2.3.1 Periplasmic Extraction

2.3.1.1 Osmotic Shock Method

Osmotic periplasmic extractions were performed as previously described [123]. Briefly, bacteria were grown on MGA under the appropriate growth conditions. After 24 hours of incubation, bacterial lawns were harvested by scraping cells with a sterile loop. Cells were suspended in sterile phosphate buffered saline [PBS; 0.14M NaCl (Sigma, St. Louis, MO, USA), 2.7mM KCl (BDH, Toronto, ON, Canada), Na_2PO_4 (Fisher, Fair Lawn, NJ, USA), KH_2PO_4 (Sigma, St. Louis, MO, USA), pH 7.4] and pelleted by centrifugation (CR3*i* centrifuge, Jouan, Winchester, VA, USA) at 8000 x g for 10 minutes at room temperature. The wet weight of the pellet was determined and 25% (w/v) 20mM Tris-HCl (BDH, Toronto, ON, Canada), pH 8.0, containing 20% (w/v) sucrose (BDH, Toronto, ON, Canada), 0.1M EDTA (Sigma, St. Louis, MO, USA), pH 8.0 (200µl per gram of pellet), lysozyme (Sigma, St. Louis, MO, USA)(600µl per gram of pellet), and 1mM phenyl-methyl-sulfonyl floride (PMSF; Boehringer, Germany) were added. Following incubation of the cell suspension on ice for 40 minutes, 0.5M $MgCl_2$ (Sigma, St. Louis, MO, USA)(160µl per gram of pellet) was added and mixed gently. Spheroplasts were pelleted by centrifugation for 20 minutes at 23 000 x g (Beckman TLA-100.3 rotor, Mississauga, Ontario) at 4°C. The supernatant was centrifuged again for 90 minutes at 100 000 x g at 4°C. The resultant supernatant was collected and frozen at –20°C.

2.3.1.2 Chloroform Method

The chloroform method of protein extraction was adapted from a previously described technique [198]. Bacteria were grown on MGA for 24 hours with the appropriate growth conditions. After 24 hours of incubation, bacterial lawns were harvested by scraping

cells with a sterile loop. Cells were suspended in sterile PBS and pelleted by centrifugation at 4000 x g for 10 minutes at room temperature. The pellet was washed twice with sterile PBS prior to suspension in an equal volume of sonication buffer (10mM Tris-HCl, 5mM EDTA) and chloroform (EMD, Gibbstown, NJ, USA) with the addition of PMSF to a final concentration of 1mM. Following an incubation for 20 minutes at room temperature, the mixture was centrifuged for 60 minutes at 100 000 x g at 4°C. The supernatant above the supernatant-chloroform interface was collected and frozen at –20°C. The pellet was used for the extraction of the cytoplasmic fraction as described below.

2.3.2 Cytoplasmic Extraction

After removal of the periplasmic protein fraction contained in the supernatant, the chloroform interface was discarded to avoid periplasmic protein contamination during the cytoplasmic protein extraction. The pellet was resuspended in sonication buffer (1mL per gram wet weight) followed by four short bursts of sonication using the sonifier/disrupter at 15-20W output (Branson Sonic Power Co., Danbury, CT, USA)(4 rounds: 15 seconds sonication followed by 10 seconds interruption on ice). The sonicated mixture was then centrifuged at 100 000 x g for 60 minutes at 4°C. The supernatant was collected and frozen at -20°C.

2.3.3 Outer Membrane Protein Extraction

The outer membranes were harvested as previously described with a few modifications [199]. In brief, bacteria were grown on MGA containing 50μg/ml (77μM) heme and 50μM desferoxamine at the appropriate growth conditions. After 24 hours of incubation, bacterial lawns were scraped from the agar plates and suspended in 0.01M Tris-HCl, pH 7.0. Following centrifugation at 3000 x g for 10 minutes, the pellet was suspended in 10mM HEPES buffer (Sigma, St. Louis, MO, USA) and sonicated six times on ice using

the sonifier/disrupter at 15-20W output (6 rounds: 30 seconds sonication followed by 15 seconds interruption on ice). After centrifugation for 20 minutes at 10 000 x g at 4°C, the supernatant was removed and centrifuged again for 60 minutes at 100 000 x g at 4°C. The pellet was suspended in 10mM HEPES containing 1% (w/v) N-lauroyl-sarcosine (Sigma, St. Louis, MO, USA). After incubation for 45 minutes at room temperature, the mixture was centrifuged for 60 minutes at 100 000 x g at 4°C. The pellet was then resuspended into 100µl sterile PBS and frozen at –20°C.

2.3.4 Whole Cell Lysates

Bacteria were grown on CAP or MGA at the appropriate growth conditions. After 24 hours of incubation, the bacterial lawns were harvested and suspended in sterile PBS. This suspension was pelleted by centrifugation at 4000 x g for 10 minutes at room temperature. The pellet was then washed twice with sterile PBS and subsequently suspended in an equal volume of sonication buffer. Sonication was performed four times using the sonifier/disrupter at 15-20W output (4 rounds: 15 seconds sonication followed by 10 seconds interruption on ice). The mixture was centrifuged for 60 minutes at 100 000 x g at 4°C. The supernatant was collected and stored at –20°C.

2.4 Two-dimensional Gel Electrophoresis

The procedure used for two-dimensional (2D) gel electrophoresis is a modified version of the ReadyStrip IPG strip protocol (BioRad, Hercules, CA, USA) and was performed in the laboratory of Dr. Fraser Scott (Ottawa Health Research Institute, Ottawa, ON, Canada).

2.4.1 Periplasmic Protein Desalting

Protein desalting spin columns (Pierce, Rockfort, IL, USA) were used to desalt the periplasmic extracts according to the manufacturer's instructions prior to the rehydration step below. The desalted periplasmic extracts were quantified and stored at –20°C.

2.4.2 Step One - Rehydration

Ten micrograms of desalted *H. ducreyi* 35 000 periplasmic proteins were suspended in reconstituted ReadyPrep Sequential Extraction Reagent 3 (SEB; BioRad, Hercules, CA, USA), 1% tributyl phosphine (TBP; BioRad, Hercules, CA, USA), and a few crystals of orange G (Sigma, St. Louis, MO, USA). After mixing by inversion and briefly vortexing, the 125µl of rehydration buffer containing the periplasmic proteins was carefully loaded into the rehydration tray. A 7cm ReadyStrip™ IPG strip, pH 3-10 (BioRad, Hercules, CA, USA) was placed on this solution gel side down. After removing any trapped air bubbles, an overlay of 3ml mineral oil was added. The IPG strip was rehydrated at room temperature for 12-16 hours.

2.4.3 Step Two - Isoelectric Focusing (IEF)

Paper wicks (BioRad, Hercules, CA, USA) were moistened with ddH_20, blotted with tissue and placed to cover each wire electrode in the IEF focusing tray. After draining the mineral oil from the rehydrated IPG strip, the strip was placed gel side down in the focusing tray with the ends of the strip covering the moistened electrode wicks in the correct polarity. The IPG strip was then covered with 2ml mineral oil and trapped air bubbles were eliminated. The strips were focused at 20°C with a maximum current of 50µA per IPG strip using the Protean IEF cell (BioRad, Hercules, CA, USA) with the following run parameters: (250V for 15 minutes; 5 000V until approximately 28 000Volt-hours). After completion of

the run, the focused IPG strips were drained of excess mineral oil, wrapped in plastic wrap, flash frozen in liquid nitrogen and stored at –80°C.

2.4.4 Step Three - IPG Strip Equilibration

After complete thawing, the focused IPG strip was placed gel side up in the reduction tray to which reduction buffer [0.05M Tris-HCl, pH 6.8, 8M Urea (BioRad, Hercules, CA, USA), 35% glycerol, 2% (w/v) DTT (Sigma, St. Louis, MO, USA), 0.3% (w/v) SDS] was added. The strip was incubated for 15 minutes with gentle shaking at 37°C. The strip was then removed and placed gel side up into the alkylation tray to which alkylation buffer [0.05M Tris, HCl, pH 6.8, 8M Urea, 35% glycerol, 2.5% (w/v) iodoacetamide (Sigma, St. Louis, MO, USA), 0.3% (w/v) SDS] was added. The strip was incubated for 15 minutes with gentle shaking at 37°C.

2.5 Polyacrylamide Gel Electrophoresis

2.5.1 Two-dimensional Gel Electrophoresis

Proteins were separated in the second dimension by sodium dodecyl sulfate polyacrylamide gel electrophoresis (SDS-PAGE) with a 10% acrylamide gel [0.375M Tris-HCl, pH 8.8, 0.1% (w/v) SDS, 10% (w/v) acrylamide-Bis (acrylamide/Bis 37.5:1; BioRad, Hercules, CA, USA)]. Before the strip was loaded into the gel, excess alkylation buffer was washed off of the strip by rinsing with a small volume of electrophoresis running buffer [25mM Tris, 192mM glycine, 0.1% (w/v) SDS]. The strip was then carefully pushed into the well of the gel and covered with overlay agarose (BioRad, Hercules, CA, USA). Electrophoresis was carried out using the miniVE system (GE Healthcare Bio-Sciences Corp., Piscataway, NJ, USA) in electrophoresis running buffer with constant amperage of 40mA per gel.

2.5.2 One-dimensional Gel Electrophoresis

All one-dimensional (1D) SDS-PAGE gels were performed with a 12% resolving gel [0.375M Tris-HCl, pH 8.8, 0.1% (w/v) SDS, 12% (w/v) acrylamide (Protogel; 30% (w/v) acrylamide, 0.8% (w/v) bisacrylamide, National Diagnostics, Altlanta, GA, USA)] and a 4.5% stacking gel [0.125M Tris-HCl, pH 6.8, 0.1% (w/v) SDS, 4.5% (w/v) acrylamide] using a discontinuous buffer system [200]. Protein samples were diluted to the desired concentration in ddH_20 in an equal volume of SDS-PAGE 2x sample buffer [125mM Tris, 20% (v/v) glycerol, 4% (w/v) SDS, 10% (v/v) 2-mercaptoethanol (BDH, Toronto, ON, Canada), 0.002% (w/v) bromophenol blue (Fisher, Fair Lawn, NJ, USA)]. Samples were heated at 100°C for 5 minutes prior to electrophoresis at 100-200V in the Mini-Protean II electrophoresis cell system (BioRad, Richmond, CA, USA).

2.6 Staining Methods for SDS-PAGE

2.6.1 SYPRO Ruby Staining

2D gels were washed twice for 30 minutes each in fixer solution (50% ethanol, 5% acetic acid). 1D gels were washed twice in fixer solution for 10 minutes each. The gels were placed in Ziploc containers with 25mL SYPRO Ruby Stain (Sigma, St. Louis, MO, USA) and covered with tin foil. After gels were stained overnight with gentle shaking at room temperature, 2D gels were washed twice for 15 minutes in ddH_20; 1D gels were washed twice for 10 minutes in ddH_20. The gels were visualized and photographed with UV light using the MultiImage Light Cabinet. 2D gels were also analyzed for changes in net intensities using two-dimensional analysis software (PDQuest; Bio-Rad, Hercules, CA, USA).

2.6.2 Coomassie Staining

1D SDS-PAGE gels were stained with Coomassie [0.1% (w/v) Coomassie Brilliant Blue R-250 (EM Science, Darmstadt, Germany), Bismark brown R (Sigma, St. Louis, MO, USA), 40% (v/v) ethanol (Commercial Alcohols Inc., Brampton, ON, Canada), 7% (v/v) glacial acetic acid] followed by destaining with 40% (v/v) ethanol and 7% (v/v) glacial acetic acid until protein bands were visible and the background was clear. Alternatively, 1D SDS-PAGE gels were stained with RapidStain (G Bioscience, St. Louis, MO, USA) for 1 hour followed by several washes in ddH_20 until the protein bands became visible and the background was clear.

2.6.3 Silver Staining

SDS-PAGE gels were washed three times for 5 minutes each in ddH_20. The gels were incubated in fixer solution for 30 minutes at room temperature followed by a 10-minute wash in 50% (v/v) ethanol and a 10-minute wash in ddH_20. The gels were then placed in a sensitizer solution [0.02% (w/v) sodium thiosuphate (Sigma, St. Louis, MO, USA)] for 5 minutes. Two washes in ddH_20 of 5 minutes each were then followed by incubation in silver nitrate solution [0.1% (w/v) silver nitrate (BDH, Toronto, ON, Canada)] for 30 minutes. The gels were washed for 1 minute in ddH_20. To remove excess silver nitrate solution, the gels were rinsed twice briefly with a small amount of developer solution [0.04% (v/v) formalin (BDH, Toronto, ON, Canada), 2% (w/v) sodium carbonate (BDH, Toronto, ON, Canada)]. To develop the protein spots, the gels were incubated in developer solution at room temperature until protein spots appeared. The reaction was terminated by rinsing briefly in ddH_20 followed by the addition of a 5% (v/v) acetic acid solution. For long-term storage, gels were placed in 1% (v/v) acetic acid and kept at 4°C.

2.7 Western Immunoblotting

When performing western blots, samples underwent SDS-PAGE in duplicate in order to transfer one gel onto a Nitrocellose-1 membrane (Gibco Life Technologies, Gaithersburg, MD, USA) or Immobilon-FL (Millipore, Billerica, MA, USA). The second gel was stained with Coomassie or SYPRO Ruby as described above to ensure correct loading. The transfer gel was first equilibrated in fresh Towbin transfer buffer [25mM Tris, 192mM glycine, 20% (v/v) methanol (Fisher, Fair Lawn, NJ, USA)] for approximately 30 minutes. The semi-dry Mini-Protean II blotting apparatus (BioRad, Richmond, CA, USA) was then assembled according to the manufacturer's instructions. The transfer conditions were as follows: 30 minutes at 20V with a constant amperage of 0.5A. After the transfer was complete, the blot was stained with 10% (v/v) Ponceau S (Sigma, St. Louis, MO, USA) to identify the molecular weight markers. The stain was removed by washing the blot several times in ddH_20 followed by overnight incubation in a 2% skim milk blocking solution [2% (w/v) skim milk (EM Science, Gibbstown, NJ, USA) in PBS]. The blot was rinsed with ddH_20 followed by incubation for 30 minutes in a 1% skim milk solution [1% (w/v) skim milk, 0.1% (v/v) Tween 20 (Sigma, St. Louis, MO, USA) in PBS]. After rinsing with ddH_20, the blot was probed for 30 minutes at room temperature with the primary antibody solution [0.1% (v/v) Tween 20 in PBS]. After three washes of 5 minutes each in PBS, the blot was incubated with a 1:10 000 dilution of goat anti-rabbit immunoglobulin horse radish peroxidase conjugated secondary antibody (BioSource, Camarillo, CA, USA) solution [0.1% (v/v) Tween 20 in PBS] for 30 minutes at room temperature. After three washes of 5 minutes each in PBS, the membrane was developed with TMB peroxidase substrate (KPL, Gaithersburg, Maryland, USA) for 1-5 minutes. The reaction was stopped by rinsing the blot with ddH_20.

2.7.1 Primary Antibodies for Western Immunoblotting

The rabbit polyclonal antibody raised against the *H. ducreyi* 35 000 SodC protein (anti-SodC) was produced by a Master's student, Shahin Negari (University of Ottawa, Ottawa, ON, Canada), in our laboratory. Anti-SodC was used in a dilution of 1:1 000.

The rabbit polyclonal antibody raised against *H. ducreyi* outer membrane proteins (anti-OMP) was produced by a previous PhD student, Isabelle Leduc (University of Ottawa, Ottawa, ON, Canada), in our laboratory. Anti-OMP was used in a dilution of 1:1 000.

The anti-V5-HRP antibody (Invitrogen, Carlsbad, CA, USA) was used in a dilution of 1:5 000 in immunoblot experiments to detect recombinant protein containing the V5 epitope. The procedure supplied by the manufacturer was followed for membrane incubation steps. The membrane was developed with TMB membrane peroxidase substrate as indicated above.

The rabbit polyclonal antibody raised against the *H. ducreyi* 35 000 heme-dedicated periplasmic binding protein (anti-hHBP) was produced in the present study (see below) using Ni-NTA affinity-purified fusion hHBP expressed in BL21 Star™ (DE3) *E. coli* cells. Serum obtained from rabbits 10 weeks after the first immunization was used in a dilution of 1:8 000.

2.7.2 Western Blot Stripping

In order to probe the same membrane with two different primary antibodies, the blot was stripped by incubation in 100mM Glycine-HCl, pH 2.5 (Sigma, St. Louis, MO, USA) at 53°C with gentle shaking. The solution was changed every hour for approximately 3-4 hours until the immunoreactive bands were not visible. The membrane was washed three times with PBS for 5 minutes each. The blot was then incubated with TMB peroxidase substrate for 10 minutes at room temperature to ensure the absence of immunoreactive bands due to incomplete stripping of the primary antibody. The membrane was then washed thoroughly

with ddH_20 and blocked in a 2% skim milk solution for 2 hours at room temperature. The blot was reacted with a different primary antibody as detailed above in section 2.7.

2.8 Champion™ pET Directional TOPO® Expression System

The pET151/D-TOPO® kit (Invitrogen, Carlsbad, CA, USA) was used to express the recombinant hHBP protein with a N-terminal fusion tag containing the V5 epitope and 6xHis region (Figure 2) using the manufacturer's instructions with the modifications described below.

2.8.1 Genomic DNA Extraction and PCR Amplification

H. ducreyi 35 000 genomic DNA was extracted using the QiAmp DNA minikit (Qiagen, Mississauga, ON, Canada) according to the instructions supplied by the manufacturer and was used as template for PCR amplification of the *hhbp* gene. The following primers were designed using Whitehead Institute for Biomedical Research's web-based primer picking interface (http://frodo.wi.mit.edu/cgi-bin/primer3/primer3_www.cgi). An additional pET151 recognition sequence was added to the 5' end of the forward primer: pET151-hHBPFOR: 5'-CACCATGAATCTTTCCTTTCTAA; pET151-hHBPREV: 5'-GGATGCTGTAGCTTGTGTTATATTG (Invitrogen, San Diego, CA, USA). In order to achieve a blunt-end PCR product, the *PfxUltima*™ (Invitrogen, Carlsbad, CA, USA) proofreading DNA polymerase was used in the following PCR reaction: 0.625U *PfxUltima*™ , 1x *PfxUltima*™ PCR buffer, 1.0mM dNTPs, pH 8.0 at 0.25mM each, 0.4μM primers at 0.2μM each, and 2μl *H. ducreyi* genomic DNA as template. The 940bp PCR product was amplified using the Touchgene Gradient Thermocycler (Techne; Cambridge, UK) with the following conditions: an initial denaturation of 94°C for 2 minutes; 30 cycles of 94°C for 15 seconds, 42.5°C for 30 seconds, and 68°C for 45 seconds; and a final extension of 68°C for 5 minutes.

Figure 2: Vector map and polylinker DNA sequence for pET151/D-TOPO®[1]

The expression vector pET151/D-TOPO® uses directional cloning for the insertion of the blunt-ended hHBP PCR amplification product. The hHBP protein is expressed in both *E.coli* TOP10 cells and *E. coli* BL21 Star™ (DE3) cells under the control of the T7 promoter. This expression vector has a N-terminal fusion tag consisting of V5 and 6xHis; there is also a TEV (Tobacco etch virus) protease recognition site for removal of the N-terminal peptide tag. Positive transformants are selected for by an ampicillin resistance marker.

[1]Obtained directly from www.invitrogen.com/content/sfs/vectors/pet151dtopo_map.pdf and www.invitrogen.com/content/sfs/vectors/pet151dtopo_mcs.pdf

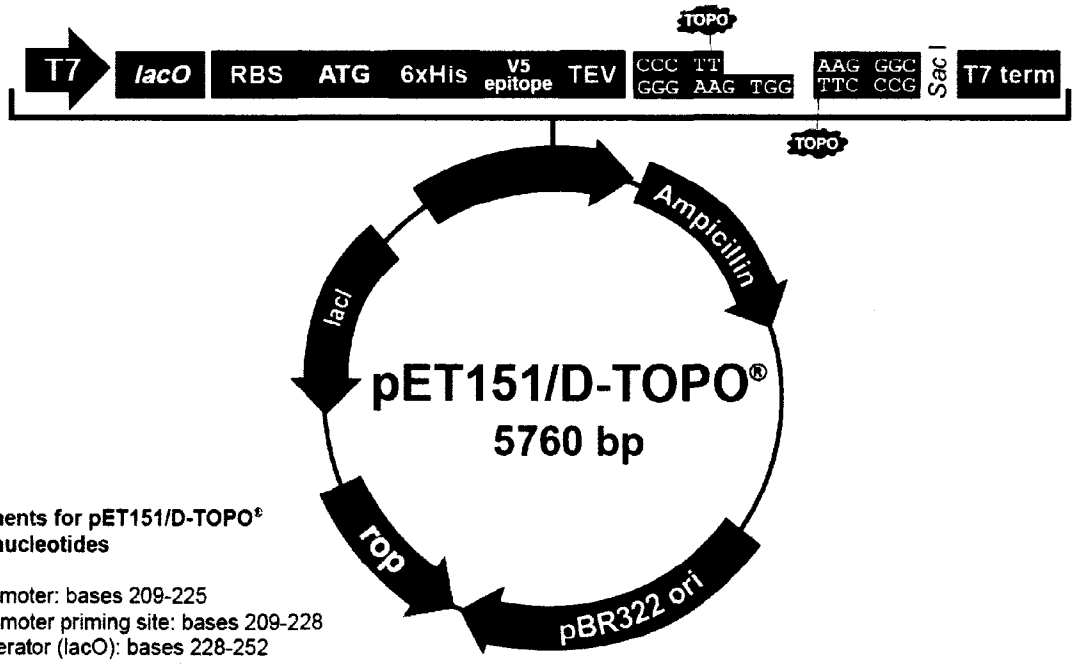

Comments for pET151/D-TOPO®
5760 nucleotides

T7 promoter: bases 209-225
T7 promoter priming site: bases 209-228
lac operator (lacO): bases 228-252
Ribosome binding site (RBS): bases 282-289
Initiation ATG: bases 297-299
Polyhistidine (6xHis) region: bases 300-317
V5 epitope: bases 318-359
TEV recognition site: bases 360-380
TOPO® cloning site (directional): bases 387-400
T7 reverse priming site: bases 455-474
T7 transcription termination region: bases 416-544
bla promoter: bases 849-947
Ampicillin (*bla*) resistance gene: bases 948-1808
pBR322 origin: bases 1953-2626
ROP ORF: bases 2997-3188 (complementary strand)
lacI ORF: bases 4500-5612 (complementary strand)

2.8.2 TOPO® Cloning Reaction and Transformation

The TOPO® cloning reaction was comprised of a PCR product at a molar ratio of 1:4 to TOPO® vector. The cloning reaction mixture was used to transform chemically competent OneShot® TOP10 *E. coli* cells for 30 minutes on ice according to the manufacturer's instructions. Two different volumes of transformation mixture (100µl and 150µl) were plated onto pre-warmed LB agar plates containing AMP. After overnight incubation at 37°C, several transformants were selected for further analysis.

2.8.3 Analysis of Positive TOP10 Transformants

Colonies picked from LB agar plates containing AMP were analyzed by colony PCR using the PCR amplification conditions listed above for the pET151hHBPFOR/pET151hHBPREV primers with the exception that the initial denaturation time was increased to 10 minutes. Vector size was determined by agarose gel electrophoresis of plasmid extracted using the PureLink™ HiPure Mini Plasmid DNA Purification kit (Invitrogen, Carlsbad, CA, USA). Transformants exhibiting the appropriate size amplicon were frozen in LB broth containing AMP with 15% (v/v) glycerol and stored at –80°C.

2.8.4 Expression of Recombinant Fusion Protein

To express the recombinant hHBP (rhHBP), plasmid isolated from a TOP10 transformant was used to transform BL21 Star™ (DE3) One Shot® *E. coli* cells according to the manufacturer's instructions. Expression of the recombinant fusion protein was achieved by induction with IPTG at a final concentration of 1mM added at mid-log (OD_{600}: 0.5-0.8) of growth.

2.9 Ni-NTA Protein Purification

The Ni-NTA purification system (Invitrogen, Carlsbad, CA, USA) was used to purify the polyhistidine-containing recombinant protein from IPTG induced BL21 Star™(DE3) *E. coli* cells containing the pET151-hHBP vector. Briefly, bacterial cell lysates were prepared under denaturing conditions according to the manufacturer's instructions. rhHBP was purified with Ni-NTA agarose under hybrid conditions. In the final elution step, the bound rhHBP was eluted in native elution buffer with sequentially increasing imidazole concentrations (50mM to 250mM). The rhHBP eluted optimally in the 100mM and 150mM imidazole fractions as verified by SDS-PAGE. These fractions were then buffer exchanged with 1x purification buffer [50mM NaH_2PO_4, pH8.0, 0.5M NaCl] and concentrated using Amcon Ultra centrifugal filter devices (Millipore, Carrigtwohill, Cork, Ireland). Five percent (v/v) glycerol was added to the buffer exchanged and concentrated affinity-purified rhHBP and stored at –80°C.

2.9.1 AcTEV™ Cleavage Trials

The AcTEV™ protease (Invitrogen, Calsbad, CA, USA), an enhanced version of the Tobacco Etch Virus, was used to cleave the fusion tag from the affinity-purified rhHBP. The recommended conditions for fusion protein cleavage provided by the manufacturer were followed. Six-hour time course trials as well as overnight incubations were performed with the following reaction mixture: 1X TEV buffer, 1mM DTT, and 0.5U AcTEV™ protease per microgram of affinity-purified rhHBP. These time course trials and overnight incubations were performed at 4°C, room temperature, and 30°C.

2.10 Agarose Gel Electrophoresis

Gels composed of either 0.8% or 1.0% (w/v) agarose were electrophoresed using the Hoefer HE 33 Mini Submarine (Amersham Biosciences, Piscataway, NJ, USA) or the Wide Mini-Sub Cell GT (BioRad, Hercules, CA, USA) as per the manufacturers' instructions. Briefly, UltraPure™ agarose (Invitrogen, Carlsbad, CA, USA) was diluted in 1x Tris-Borate-EDTA buffer [TBE; 0.55% (w/v) boric acid (BioShop, Burlington, ON, Canada), 1.1% (w/v) Tris base, 0.4% (v/v) 0.5M EDTA, pH 8.0)]. Prior to gel loading, 2µl of 10x DNA gel loading buffer (Eppendorf, Westbury, NY, USA) was added to each sample. Gels were electrophoresed at 80-150V and DNA bands were visualized by adding 0.005% (v/v) ethidium bromide (EtBr; Invitrogen, Carlsbad, CA, USA) to the molten agarose prior to casting. Agarose gel images were observed and photographed with UV light using the MultiImage Light Cabinet (Alpha Innotech Corp., San Leandro, CA, USA).

2.11 Rabbit Immunization Protocol for hHBP Polyclonal Antibody Production

The rabbit polyclonal antibody directed against rhHBP was produced at Cedarlane laboratories (Hornby, ON, Canada). The protocol was approved by the animal care committee from the University of Ottawa. A single New Zealand white female rabbit was immunized with 1ml of antigen/adjuvant mixture comprised of 100µg of antigen (affinity-purified rhHBP fusion protein) and 20µg Gerbu adjuvant. Each injection series consisted of four 200µl subcutaneous injections in four widely separated anatomic sites and two 100µl intramuscular injections in two biceps femoris sites of the two hind limbs. Prior to the first injection, 3ml pre-immune blood was collected. Three weeks after the first injection, 3ml of blood was collected from the marginal ear vein and a booster was administered. Six weeks after the first injection, 3ml of blood was collected and a second booster was administered.

Ten weeks after the first injection, the rabbit was anaesthetized after pre-medication with parenteral analgesic followed by exsanguination by cardiac puncture for terminal bleed collection. The rabbit was then euthanized by an injection of sodium pentobarbital.

2.12 DNA and Protein Quantification

2.12.1 DNA Quantification

The quantity of genomic or plasmid DNA was estimated by running a known volume of DNA sample with a high mass or low mass DNA ladder (both from Invitrogen, Carlsbad, CA, USA) on a 1% agarose gel.

2.12.2 Protein Quantification

Protein concentrations were determined using the BCA protein assay reagent or the Coomassie Plus – The Better Bradford Assay Reagent (both from Pierce, Rockfort, IL, USA).

2.13 Protein and DNA Sequencing

2.13.1 Mass Spectrometry of Periplasmic Binding Protein Candidates Identified by 2D Gel

High urea concentrations are incompatible with the MALDI tandem mass spectroscopy process used to determine the peptide signature of candidate proteins identified by 2D gel electrophoresis. Therefore, for 2D gels used for protein spot excision, the following equilibration buffers were replaced in section 2.4.4 above: reduction buffer [26.5mM Tris-HCl, 35.25mM Tris Base, 2.7% (w/v) SDS, 2.5% (v/v) glycerol, 2% (w/v) DTT]; alkylation buffer [26.5mM Tris-HCl, 35.25mM Tris Base, 0.5% (w/v) SDS, 2.5% (v/v) glycerol, 2.5% iodoacetamide]. In addition, all silver staining solutions were filter-sterilized using 0.75mm filters (Nalge Nunc International, Rochester, NY, USA) and staining was performed in a laminar flow hood. Desired protein spots were excised from the gel and

stored in 1% (v/v) acetic acid (Fisher, Nepean, ON, Canada). Candidate protein spots were sent to the Ontario Genomics Innovation Center (OGIC; Ottawa, ON, Canada) for identification by MALDI tandem mass spectrometry.

2.13.2 Ni-NTA Affinity-purified Recombinant hHBP Analysis

SDS-PAGE gels were stained with RapidStain and washed with filter-sterilized ddH_20. All staining was done in a laminar flow hood. The protein bands were excised from the gel using a sterile scalpel and gel slices were stored in 1% (v/v) acetic acid solution. The protein bands were sent to the OGIC for identification by MALDI tandem mass spectrometry.

2.13.3 pET151-hHBP DNA Sequencing

Plasmid DNA was extracted with the PureLink™ HiPure Plasmid DNA Purification kit (Invitrogen, Carlsbad, CA, USA) according to the manufacturer's instructions. The sample was diluted with sterile ddH_20 to a final concentration of 12.5ng in 10µl and sent to the OGIC for fluorescent DNA sequencing with the Applied Biosystems 3730 DNA Analyzer using the T7 promoter standard primer (5'-TAA TAC GAC TCA CTA TAG GG).

2.14 Heme Agarose Binding

2.14.1 Direct Heme Agarose Binding

Twenty microlitres of bovine hemin-agarose suspension (≥4µmol hemin/ml; Sigma, St. Louis, MO, USA) was washed three times with 1mL binding buffer [100mM NaCl, 25mM Tris-HCl, pH 8.0] and the affinity matrix was pelleted by centrifugation at 10 300rpm for 5 minutes at room temperature. The heme agarose was suspended in 500µl of binding buffer to which 10µg of affinity-purified rhHBP was added. In the specificity assay, the affinity gel was incubated with concentrations of affinity-purified rhHBP ranging from 500ng to 10µg. The mixture was gently agitated on a Labquake Shaker Rotisserie

(Barnstead/Thermolyne, Dubuque, Iowa, USA) for 60 minutes at room temperature followed by three washes with 500µl of binding buffer. Bound proteins were eluted by the addition of 50µl 2x sample buffer and the sample was incubated at 100°C for 5 minutes. After centrifugation at 10 300rpm for 5 minutes at room temperature, 40µl of the supernatant was used for SDS-PAGE gel electrophoresis.

2.14.2 Competitive Inhibition Heme Agarose Binding

Competitive binding experiments were performed in which 10µg of the affinity-purified rhHBP was pre-incubated with increasing concentrations of the competing ligands in a final volume of 200µl in PBS. The following concentrations of competing ligands were used: bovine hemin chloride [300µM to 1mM; dissolved in 192µl 0.1N NaOH per mg bovine hemin chloride in PBS] with or without 2,2-dipyridyl [(Sigma, St. Louis, MO, USA); 1.25mM/1mM heme; dissolved in PBS], protoporphyrin IX [PPIX (Frontier Scientific, Logan, UT, USA); 25µM to 1mM; dissolved in 3µl 0.1N HCl per mg PPIX, 10% (v/v) ethanol in PBS], ferric nitrate [(Sigma, St. Louis, MO, USA); 10nM to 1mM; dissolved in PBS], ferric chloride [(Sigma, St. Louis, MO, USA); 10nM to 1mM; dissolved in PBS], or zinc protoporphyrin IX [Zn-PPIX (Frontier Scientific, Logan, UT, USA); 1mM to 10mM; dissolved in 192µl 0.1N NaOH per mg Zn-PPIX] to a final volume of 200µl in PBS. Following incubation for 60 minutes at room temperature on a Labquake Rotisserie, the samples were added to the heme affinity gel suspended in 300µl of binding buffer. Heme affinity chromatography was then conducted as described above.

A N-terminal 6xHis tagged purified recombinant outer membrane lipoprotein from *Leptospira*, rLipL32, expressed in *E. coli* BL21 Star™ (DE3) was kindly provided by Linru Wang (Canadian Food Inspection Agency, Ottawa, ON, Canada) as a positive control in heme agarose binding experiments. The purified recombinant protein was concentrated and

buffer exchanged in the same manner as indicated in Section 2.9 above. Ten micrograms of rLipL32 was pre-incubated with increasing concentrations of heme in a competition binding assay.

CHAPTER THREE

RESULTS

To identify the heme-dedicated periplasmic binding protein in *H. ducreyi* (hHBP) using a proteomics approach, we compared 2D gel periplasmic protein profiles grown under heme-limiting and heme-replete conditions. This strategy capitalizes on the observation that the expression of an ABC transporter is enhanced under ligand-restrictive conditions [201].

3.1 Determination of Heme-limiting Conditions for *H. ducreyi*

H. ducreyi 35 000 strain was grown on GC agar supplemented with defined concentrations of heme (10μg/ml to 100μg/ml) and 50μM of the iron chelator, desferoxamine. The addition of the iron chelator eliminated any excess inorganic iron present in the media allowing only supplementary heme to act as both the heme and iron source for the bacterium. *H. ducreyi* growth was supported at supplementary heme concentrations as low as 10μg/ml; however, the lawn of bacteria produced was not substantial for the large scale bacterial harvesting necessary for protein extraction. Therefore, the lower exogenous heme concentration (heme-limiting condition) was arbitrarily chosen to be 15μg/ml. The bacterial colonies grown with higher heme concentrations (≥50μg/ml) were dark brown with a progression to off-white as the concentration of heme reached 10μg/ml heme (data not shown).

3.2 Determination of the Appropriate Two-dimensional Gel Conditions

3.2.1 Osmotic Shock Versus Chloroform Method of Periplasmic Protein Extraction and Correct Protein Rehydration Concentration

Lawns of *H. ducreyi* 35 000 grown on GC agar supplemented with 50μg/ml heme and 50μM desferoxamine were collected for periplasmic protein extraction. Both the

osmotic shock method and chloroform method of periplasmic protein extraction were performed to compare 2D protein profiles. A distinct difference in periplasmic protein profile was seen with the chloroform method resulting in crisper more defined protein spots (Figure 3). In addition, two concentrations of periplasmic protein extracts, 10μg and 20μg, were compared by 2D gel protein profile to determine the optimal rehydration protein concentration. The 2D periplasmic protein profile rehydrating 10μg of protein sample produced more distinct protein spots (Figure 3B*i*). Therefore, the optimal 2D gel periplasmic protein profile was achieved by rehydrating 10μg of periplasmic proteins extracted from *H. ducreyi* 35 000 using the chloroform method.

3.2.2 *H. ducreyi* Growth Conditions Needed to Determine Upregulation of Candidate Periplasmic Heme Binding Proteins Under Heme-limiting Conditions

Initial experiments compared 2D gel periplasmic protein profiles from *H. ducreyi* grown under heme-limiting conditions (15μg/ml heme and 50μM desferoxamine) or with 50μg/ml heme and 50μM desferoxamine. Two independent periplasmic extracts were obtained for each of these two growth conditions and 2D gel protein profiles were evaluated in pairwise comparisons in duplicate. The difference in protein expression between these two growth conditions was not obvious (Figure 4A and 4B). Therefore, the concentration of heme supplementation was increased from 50μg/ml to 100μg/ml in the presence of 50μM desferoxamine. The 2D gels were stained with SYPRO Ruby, a quantitative stain as sensitive as silver staining, in order to identify changes in protein expression. There was a marked difference in protein expression when comparing these two conditions (Figure 5A and 5B). Therefore, the heme-replete condition used in further 2D gel analysis to determine candidate proteins consisted of *H. ducreyi* 35 000 grown on GC agar with 100μg/ml heme

Figure 3. Two-dimensional periplasmic protein profiles of *H. ducreyi* 35 000 prepared using either the osmotic shock or chloroform method of protein extraction.

Overnight bacterial lawns of *H. ducreyi* 35 000 grown on GC agar supplemented with 50μg/ml heme and 50μM desferoxamine were collected and subjected to periplasmic protein extraction using either the osmotic shock **(A)** or chloroform method **(B)**. Desalted periplasmic protein extracts were separated in the 1st dimension (pI) for 28 314Vhrs using 7cm IPG strips, pH 3-10 and two protein extraction concentrations: 10μg ***(i)*** and 20μg ***(ii)***. The proteins were separated in the second dimension by a 10% SDS-PAGE gel and silver stained. Molecular mass standards are indicated in kilodaltons (kDa).

Figure 4. Initial two-dimensional periplasmic protein profile analysis to determine optimal *H. ducreyi* 35 000 growth conditions for visible upregulation of candidate heme-binding proteins.

Overnight bacterial lawns of *H. ducreyi* 35 000 grown on GC agar supplemented with either 50μg/ml **(A)** or 15μg/ml **(B)** heme and 50μM desferoxamine were collected and subjected to periplasmic protein extraction using the chloroform method. Ten micrograms of desalted protein sample was separated in the 1st dimension (pI) for 28 842Vhrs using 7cm IPG strips, pH 3-10. The proteins were separated in the second dimension by a 10% SDS-PAGE gel and silver stained. Molecular mass standards are indicated in kilodaltons (kDa).

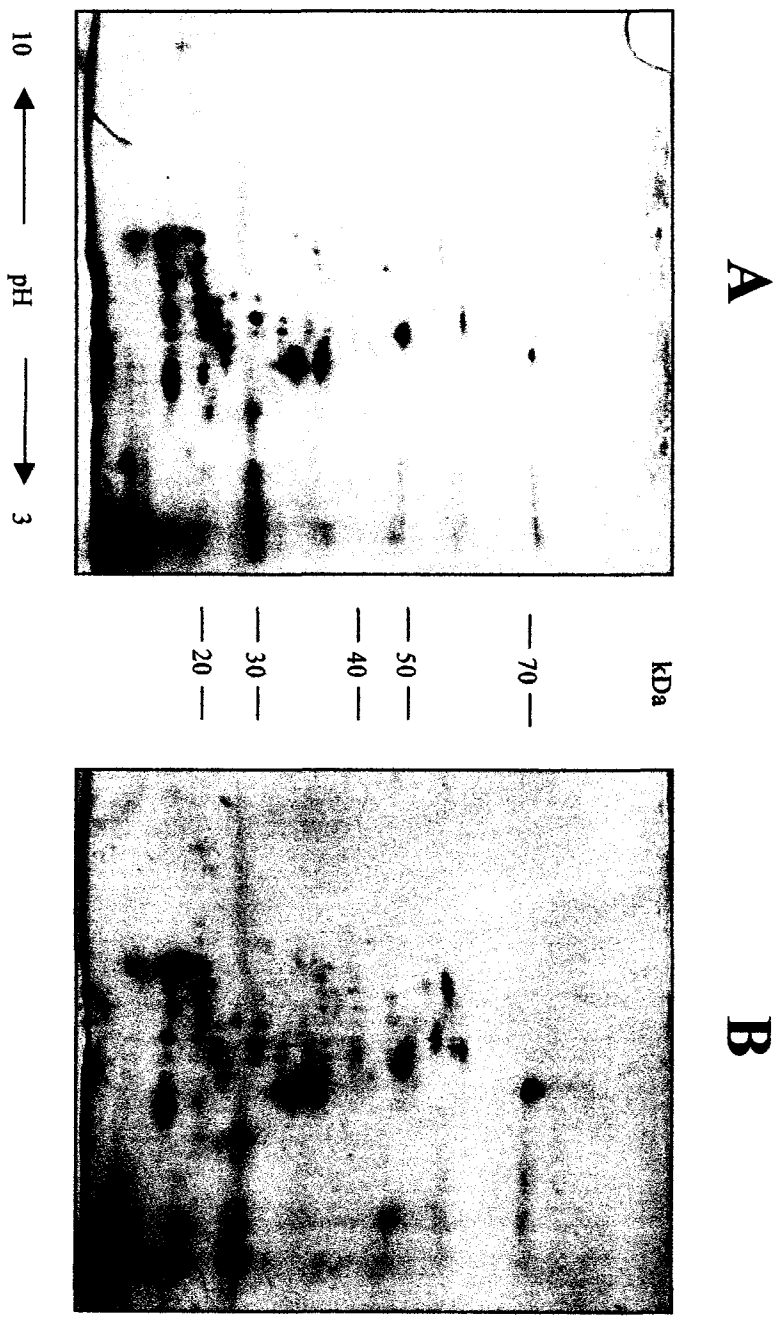

Figure 5. Optimal growth conditions of *H. ducreyi* 35 000 to visualize upregulation in protein expression under heme-limiting conditions.

Overnight bacterial lawns of *H. ducreyi* 35 000 grown on GC agar supplemented with either 100μg/ml **(A)** or 15μg/ml **(B)** heme and 50μM desferoxamine were collected and subjected to periplasmic protein extraction using the chloroform method. Ten micrograms of desalted protein sample were rehydrated in the 1st dimension (pI) for 30 000Vhrs using 7cm IPG strips, pH 3-10. The proteins were separated in the second dimension by a 10% SDS-PAGE gel and stained with SYPRO Ruby. Molecular mass standards are indicated in kilodaltons (kDa).

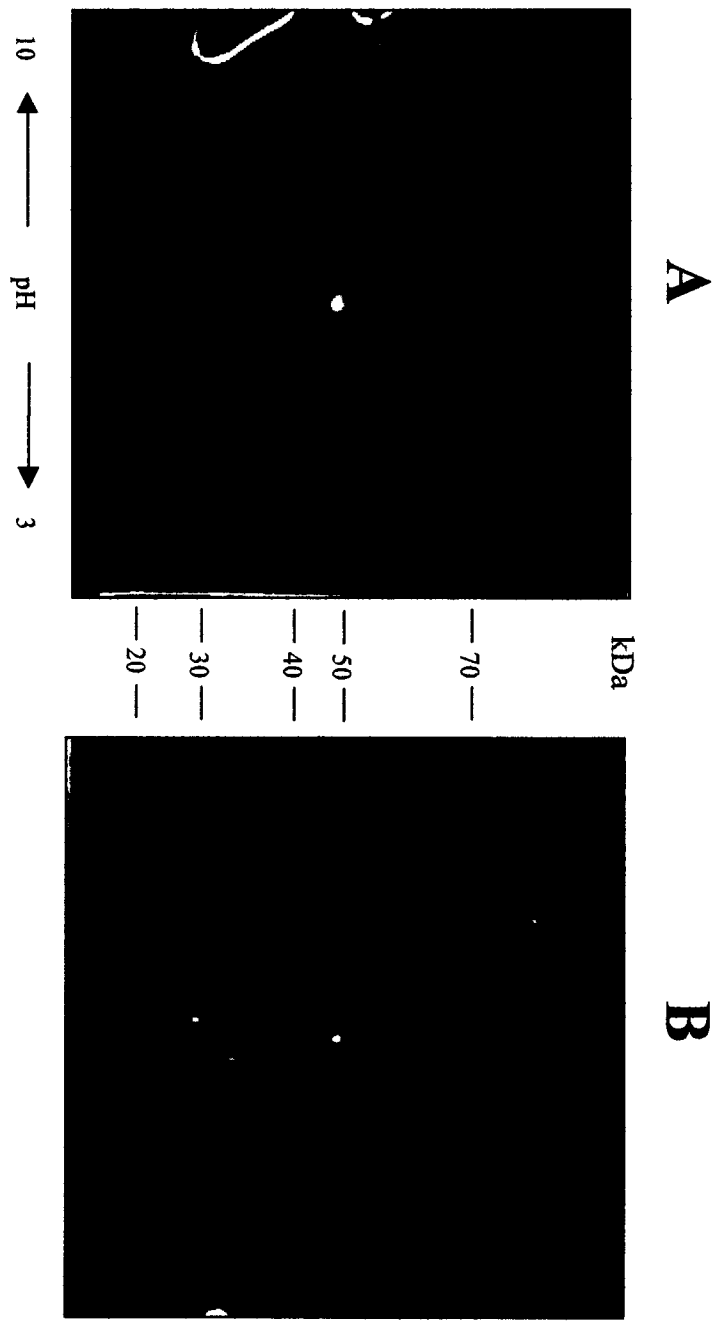

and 50μM desferoxamine and the heme-limiting condition consisted of *H. ducreyi* 35 000 grown on GC agar with 15μg/ml heme and 50μM desferoxamine.

Subsequently, three independent protein extractions to prepare periplasmic and cytoplasmic fractions were collected for each of these two heme growth conditions. Bacterial lawns were harvested for protein extraction from growth on different GC agar batches with incubation on separate occasions and protein extractions performed on different days.

3.2.3 Verification of Periplasmic Protein Extraction Preparations

Each periplasmic protein extraction and the corresponding cytoplasmic protein extraction were analyzed by 1D SDS-PAGE. Protein profiles of the periplasmic and cytoplasmic fractions were distinctly different from each other as well as from an *H. ducreyi* outer membrane preparation (Figure 6).

To ensure that each periplasmic protein extraction was enriched for periplasmic proteins, Western immunoblots were performed probing cell fractions with an antibody against *H. ducreyi* SodC, a protein localized in the periplasmic space [202,203]. An immunoreactive band was present in both periplasmic and cytoplasmic fractions. A representative experiment is depicted in Figure 6. Identical results were obtained from all the protein extractions. The presence of SodC in the cytoplasmic fraction likely arises from contamination of the cytoplasmic fraction during the isolation protocol or from identification in the cytoplasm of the newly synthesized protein prior to its export to the periplasmic space. Evidence supporting the latter explanation arises from the observation that the cytoplasmic hHBP-specific immunoreactive bands were only present if *H. ducreyi* was grown under heme-limiting conditions when hHBP expression would be maximal. Western immunoblots probed with an antibody against *H. ducreyi* OMPs indicated no outer membrane protein

Figure 6. Western immunoblot detection of SOD-C and OMPs in periplasmic, cytoplasmic, and outer membrane protein profiles of *H. ducreyi* 35 000 grown under heme-limiting and heme-replete conditions.

Overnight bacterial lawns of *H. ducreyi* 35 000 grown on GC agar supplemented with either 100μg/ml **(H-R)** or 15μg/ml **(H-L)** heme and 50μM desferoxamine were collected and subjected to periplasmic **(P)** and cytoplasmic **(C)** extraction using the chloroform method. The outer membrane **(OMP)** protein extraction was performed from *H. ducreyi* 35 000 grown on GC agar supplemented with 50μg/ml heme and 50μM desferoxamine. Two micrograms of each protein sample were separated by a 10% SDS-PAGE gel **(A)** followed by transfer to nitrocellulose **(B)**. The immunoblot was probed with antiserum against SodC (left) and OMPs (right). The immunoreactive band representative of the (~22kDa) SodC protein is indicated by a filled arrow. Molecular mass standards are indicated in kilodaltons (kDa).

contamination of the periplasmic fractions (Figure 6B). The presence of outer membrane proteins in the cytoplasmic extracts was likely the result of contamination from pelleted membrane proteins. Therefore, these results indicate that the chloroform extraction method produced preparations enriched for periplasmic proteins with no discernable contamination from outer membrane proteins.

Desalting the six periplasmic extraction samples required for 2D gel analysis did not significantly alter the 1D SDS-PAGE protein profiles (Figure 7).

3.3 Identification of Periplasmic Proteins with Upregulated Expression Under Heme-limiting Conditions by 2D Gel Analysis

Each of the three periplasmic extraction samples collected from *H. ducreyi* grown under heme-limiting conditions was analyzed in conjunction with corresponding periplasmic extraction samples collected from *H. ducreyi* grown under heme-replete conditions. For each pair, two separate 2D gel experiments were performed resulting in a total of six pairwise comparisons with a total of twelve 2D protein profiles.

By pairwise comparisons of 2D gel protein profiles, four proteins consistently exhibited differential expression under heme-limiting conditions compared to heme-replete conditions (Figure 8, Appendix I). Using MALDI tandem mass spectroscopy and MASCOT, these four protein spots were identified as elongation factors G, Tu, P and an iron (chelated) ABC transporter periplasmic binding protein. The latter had significant amino acid homology (73%) to YfeA, a periplasmic binding protein from *Y. pestis* involved in iron acquisition [204,165]. Net intensity analysis demonstrated that the expression of the elongation factors G and P was varied under heme-limiting conditions with only half the gel comparisons demonstrating upregulation (Figure 8B, Appendix IB). The expression of

Figure 7. Comparison of desalted and non-desalted periplasmic protein profiles of *H. ducreyi* 35 000 grown under heme-limiting or heme-replete conditions.

Periplasmic protein profiles from *H. ducreyi* 35 000 grown under heme-limiting **(1,3,5)** or heme-replete **(2,4,6)** conditions and extracted using the chloroform method. Periplasmic protein samples were desalted **(D)** with Pierce spin columns and 10μg of each sample was separated by a 12% SDS-PAGE gel and stained with Coomassie. Each periplasmic extraction is paired with its desalted counterpart on the SDS-PAGE gel. Molecular mass standards are indicated in kilodaltons (kDa).

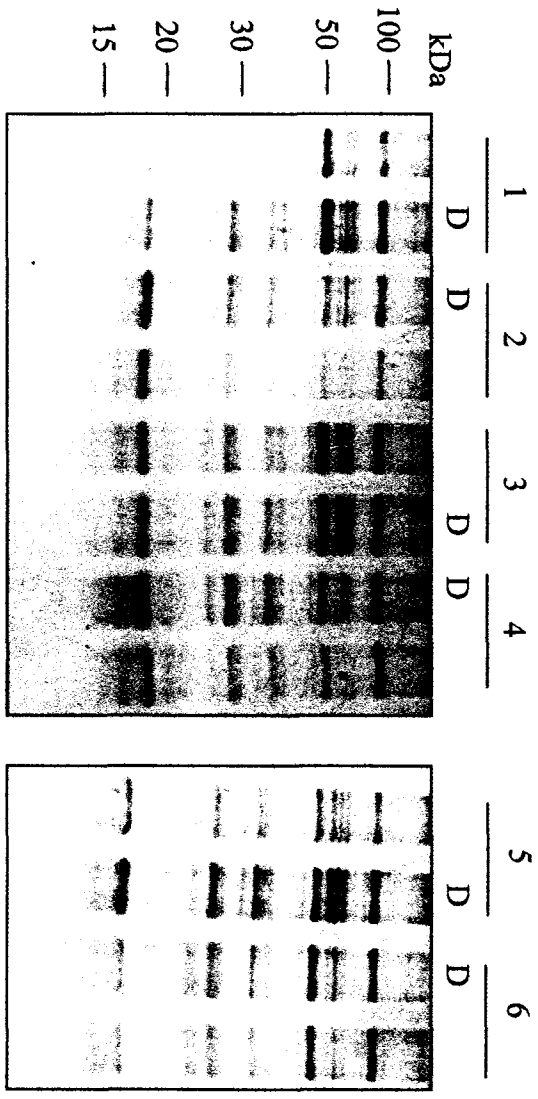

Figure 8. *H. ducreyi* 35 000 periplasmic proteins upregulated under heme-limiting conditions.

2D gel comparison of chloroform extracted periplasmic proteins of *H. ducreyi* 35 000 grown under heme-replete conditions (100μg/ml heme plus 50μM desferoxamine) **(A)** and heme-limiting conditions (15μg/ml heme plus 50μM desferoxamine) **(B)**. Ten micrograms of each protein sample was rehydrated onto 7cm IPG strips, pH 3-10 and separated in the 1st dimension (pI) for 28 903Vhrs. The 2nd dimension (kDa) was resolved by a 10% SDS-PAGE and stained with SYPRO Ruby. Circled protein spots were identified by MALDI tandem mass spectroscopy and MASCOT to be elongation factors G; MW: 77 kDa **(1)**, Tu; MW: 43.4kDa **(2)**, and P; MW: 20.7kDa **(3)** and an iron (chelated) periplasmic binding protein; MW: 33.2kDa **(4)** of *H. ducreyi* 35 000. Changes in net intensity of each protein spot circled determined by PDQuest are listed in the table with (↑) indicating an upregulation in protein expression under heme-limiting conditions. Molecular mass standards are indicated in kilodaltons (kDa). Trial 2 experiments were performed on July 7, 2005.

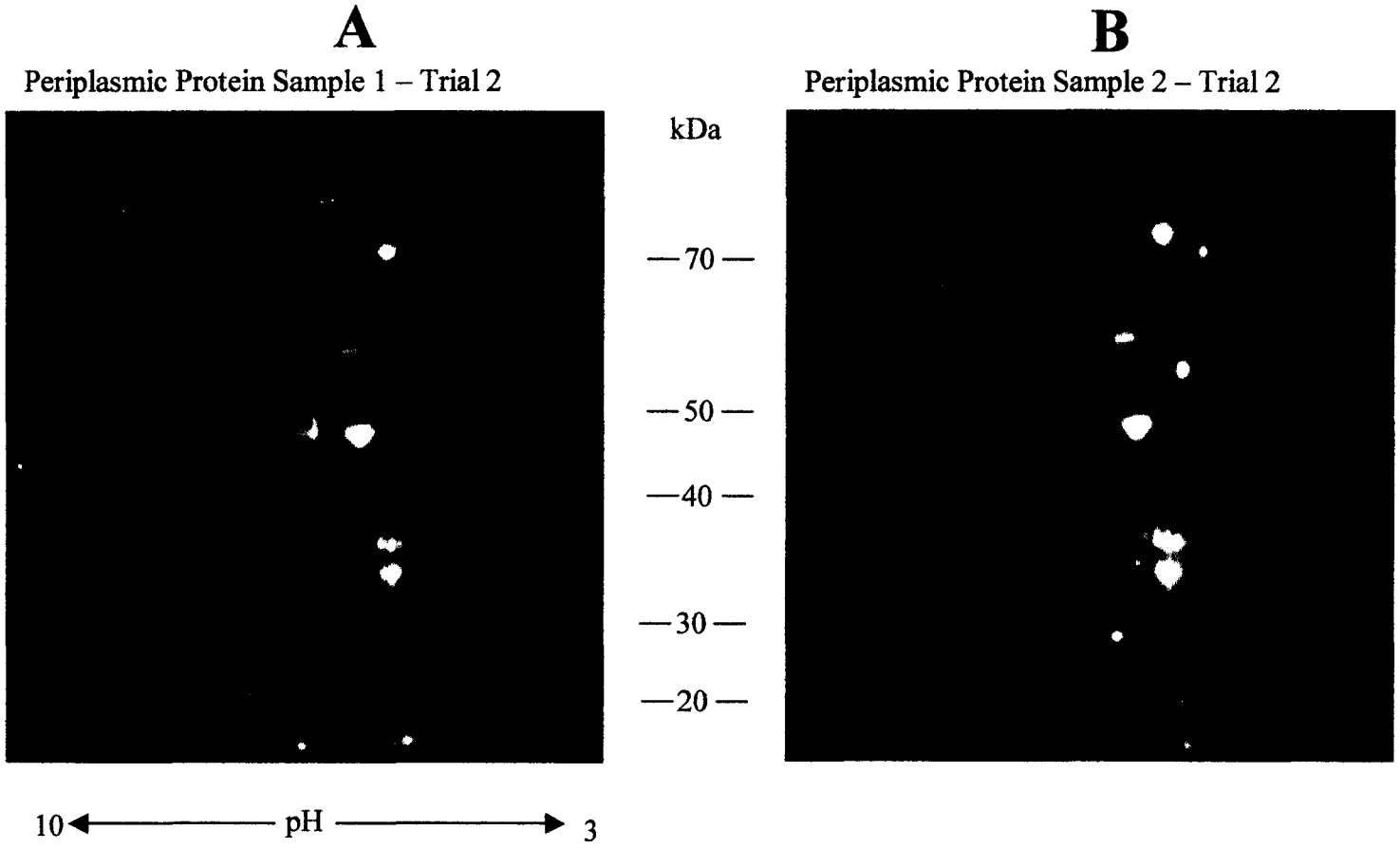

Protein Spot #	Net Intensity		Change in Net Intensity
	Gel A	Gel B	
1	709	1952	↑ 1293
2	1982	3119	↑ 1137
3	115	275	↑ 160
4	590	1073	↑ 483

elongation factor Tu and the iron (chelated) periplasmic binding protein was consistently upregulated under heme-limiting conditions (Figure 8B, Appendix IB).

3.4 Identification of an Iron (chelated) ABC Transporter Periplasmic Binding Protein

The molecular mass of the *H. ducreyi* putative iron (chelated) periplasmic binding protein calculated from 2D gels was approximately 30kDa and is similar to other characterized periplasmic binding proteins (Figure 8, Appendix I) [123,160,163,165,167,205]. This *H. ducreyi* protein was designated hHBP – *H. ducreyi* heme-dedicated periplasmic binding protein. Matching the peptide mass fingerprint of hHBP against the sequenced genome of *H. ducreyi* facilitated the identification of the responsible gene as HD1816 (Figure 9). The 906bp coding sequence predicted a protein with a molecular weight (MW) of 33 240 consisting of 302 amino acids (aa) and has been classified as a solute-binding protein [206]. hHBP was paralogous to another *H. ducreyi* gene, *ZnuA,* that encodes a periplasmic binding protein involved in zinc transport. The top fourteen Position Specific Iterated BLAST (PSI-BLAST) protein sequence alignments indicated that hHBP was 88% similar (residues 1-298) to the periplasmic adhesin component of a metal ion transport system in *Actinobacillus pleuropneumoniae* (Figure 10). Interestingly, hHBP was 75% similar (residues 10-293) to an iron (chelated) ABC transporter periplasmic binding protein in *H. influenzae* and 73% similar (residues 23-293) to YfeA, a periplasmic binding protein in *Y. pestis*. NCBI conserved domain search indicated that hHBP belongs to the TroA superfamily of periplasmic metal binding proteins (data not shown).

Using the PSORT tool, a predictor of signal sequences and cellular localization sites, the N-terminus of hHBP appeared to be a typical signal sequence, i.e., two positively charged residues followed by a hydrophobic stretch (Figure 9)[207]. The predicted cleavage site of

Figure 9. Protein sequences and characteristics of a putative heme transport operon.

H. ducreyi 35 000 *hHBP* (HD1816) is flanked by three open reading frames (ORFs) in a putative operon encoding a carrier-transport protein (ORF-1; HD1814), a desulfoviridin gamma subunit (ORF-2; HD1815), and an ATP-binding protein (ORF-3; HD1817). The portion of the hHBP protein sequence highlighted in green identifies the periplasmic signal sequence predicted to be cleaved resulting in a mature protein ~31kDa. The intergenic region located directly upstream of HD1814 contains the only putative promoter region of this operon. Both the –10 and –35 promoter regions are highlighted in blue. The gene directly downstream of hHBP encodes HD1817 with Walker A, Walker B, and signature motifs highlighted and underlined in red.

Intergenic region (IGR1339):

AGCTAGCGCGGAAAGGT
AAAAATTCAGTTTATTTA
GTGTATCACAGTACTCA
ACAATCAGCTATTGCTCG
CTAAATTTAATCCTATAC
ATTCTTTAAAAACGACTA
ATTTACACTTGATTTATG
GGATTTTGTCCATATATA
GCTTATAATTTTCGAGC
TTTATCATTAAAGAGGA
AACAAA

(HD1815):

Gene length: 112aa; Protein size: 12.8kDa

MHMIECNGKQYLTDPTGYLLNLNDWSTE
LAIAIASKEQINLTEEHWEIIW
LVRDFYQEYKTSPAIRMLVKAMTLKFGEE
KGNSRYLQRLFPEGPAKQATK
IAGLPKPIKCLStop

hHBP (HD1816):

Gene length: 302aa; Protein size: 33.24kDa
Mature Protein size: 30.86kDa

MNLSFLKKTLIIACAMGTTVAIAAPFKVVTTFTV
IQDIAQNVAGDKAIVESITKPGAEIHDYQPTPKDIV
KAQKADLILQNGMNLERWFERFFENVKNTPAVV
VTEGIQPIAILEGEYKNLPNPHAWMSSANALQYIE
NIRAALVKYDPENAVSYNQNAKAYAEKIKAISEPL
RQRLSVIPEKQRWLVTSEGAFSYLAQDYGLQELYL
WPINAEEQGSPQQVRKVIDGVKANHIPVVFSESTV
SDKPAKQVAKETGALYGGVLYVDSLSTKEGPVPT
YLDLLKVTISTIVDGFEASKKEPKStop

ORF-1 ORF-2 ORF-3

(HD1814):

Gene length: 222aa; Protein size: 23.75kDa

MENRLIANTAHNQSLLSTHKVLRNTYLLLSMTLAF
SAIVAYFAMAMNAPALPWWGLLIGFYGLLFLTNT
NANSAIGLACVFALTGFLGYTLGPILNRYVGAGLG
DAVMLALASTALVFFSCSAYILTTKKDMSFLSGM
MMALFIVLLVGVIANIFLAIPALSLAMSVLFALFST
GAILLTTSNIIHGGETNYIRATVDLYVSLYNLFLSL
LQIFGVLSKDDStop

(HD1817):

Gene length: 253aa; Protein size: 27.83kDa

MNNITQATASISVDKLTVRYNNGHLALENVSFQL
QHGTVCALIGVNGGGKSTLFKSLMGLVKPLTGQ
VLLNQMPIQKALKQNLVSYVPQSEEVDWQFPVSV
YDVVMMGRYGYMNFLRNPSALDKQKVEQAMQR
VDISHLQHRQIGELSGGQKKRVFLARALAQESQII
LLDEPFTGVDVKTENAIVALLQQLRSEGHLVLVST
HNLNSVSSFCDQVLMINRTLLASGPTATTFNHQNL
EKVFGGIVHYLQASStop

Figure 10. Amino acid sequence alignments of hHBP with homologous proteins from PSI-BLAST search analysis.

PSI-BLAST search with the protein sequence of hHBP used for alignment with the fourteen most homologous proteins. The dots represent the amino acids that are identical to the aligned residues in the query sequence; dashes are used to symbolize gapped sequences. [A.] ABC-type metal ion transport system periplasmic component/surface adhesin [B.] Iron-chelated ABC transporter periplasmic binding protein.

```
hHBP                                      1 MNLSFLKKTLIIACAM----GTTVAIA-AP----------FKVVTTFTVIQDIAQNVAG 44
Haemophilus ducreyi[A]                    1 ....................----.....-.----------..................... 44
Actinobacillus pleuropneumoniae[A]        1 .K.....QVFVV.LGL----SA.L.M.-.----------..................... 44
Pasteurella multocida[A]                 22                              .K----------..................... 42
Yersinia mollaretii ATCC 43969[A]        53                                          .....I..........  71
Yersinia intermedia ATCC 29909[A]        25        ..FTLV.F----SSVIS.S-.SAENKPSDADKK..I.....I..........  71
Yersinia frederiksenii ATCC 33641[A]     76                                          ..I.....I.........  94
Haemophilus influenzae Rd KW20[B]         7         IMT.L.L-----.LFAMQ.N.K----------..................... 42
Haemophilus influenzae R2846[A]          15                              .K----------..................... 35
Actinobacillus actinomycetemcomitans[A]   3      .LA..VSIL.L----SLSSSL.Y.K----------.....I...M.....  42
Photorhabdus luminescens - YfeA          31                        .SA.-KQ----------.....I..........  55
Haemophilus somnus 129PT[B]              15                              .K----------..................... 35
Erwinia carotovora[B]                     8   .PA.FRRVALP..LLLLAN.SAQA.-EK----------L..I....I.......I..  53
Yersinia bercovieri ATCC 43970[A]        53                                          .....I..........  71
Yersinia pseudotuberculosis - YfeA       50                             .-KK----------.....I.......I..  71
Yersinia pestis - YfeA                   51                             .-KK----------.....I.......I..  72
Yersinia pseudotuberculosis[A]           39                             .-KK----------.....I.......I..  60
```

```
hHBP                                     45 DKAIVESITKPGAEIHDYQPTPKDIVKAQKADLILQNGMNLERWFERFFENVKNTPAVVV 104
H. ducreyi                               45 ..................................................... 104
A. pleuropneumoniae                      45 ...V.....................A.........W.................GK..... 104
P. multocida                             43 .A................E.........H...V.W..L.......K......DK..... 102
Y. mollareti ATCC 43969                  72 .A.V..................R......S.....W..............I.DV.S... 131
Y. intermedi ATCC 29909                  72 .A.V..................R......S.....W..............I.DV.SA.. 131
Y. frederiksenii                         95 .A..................R......S.....W..............I.DV.SA.. 154
H. influenzae Rd KW20                    43 NA.T............E.E.........S.....W..L.........Q...DK..... 102
H. influenzae R2846                      36 NA.T............E.E.........S.....W..L.........Q...DK..... 95
A. actinomycetemcomitans                 43 .A.T............E.........S...V.W..L.......K..Q...DK..... 102
P. luminescens - YfeA                    56 .A.....................I.S.H.....W..L...........L.DV....I 115
H. somnus 129PT                          36 .A.V.....E........E...Q......S...V.W............TQ..DK..... 95
E. carotovora                            54 .A.T..................R....T.S.Q.V.W.........T........V..A.. 113
Y. bercovieri ATCC 43970                 72 .A.V..................R......S.....W..............I.DV.SA.. 131
Y. pseudotuberculosis - YfeA             72 .V.V..................R......S.....W..........K...SI.DV.SA.. 131
Y. pestis - YfeA                         73 .V.V..................R......S.....W..........K...SI.DV.SA.. 132
Y. pseudotuberculosis                    61 .V.V..................R......S.....W..........K...SI.DV.SA.. 120
```

Figure 10 cont'd.

```
hHBP                              105  TEGIQPIAILEGEYKNLPNPHAWMSSANALQYIENIRAALVKYDPENAVSYNQNAKAYAE  164
H. ducreyi                        105  ..................................................  164
A. pleuropneumoniae               105  ....T....T.....................................K..E.......I...  164
P. multocida                      103  ....T..S.Y..P..DA........TS...I.....KN.......K..DI.VK..EN..N  162
Y. mollareti ATCC 43969           132  .D..T.LP.R..P.TGI........PS...I......K...EH..AH.DT..R.......  191
Y. intermedi ATCC 29909           132  .D..T.LP.R..P..GI........PS...I......K...EH..AH.ET..R.......  191
Y. frederiksenii                  155  .D..T.LP.R..P..GI........PS...I......K...EH..AH.ET..R...T...  214
H. influenzae Rd KW20             103  ......LS.Y..P..DA........PS...I.....KN.......Q..AV.EK..AD..Q  162
H. influenzae R2846               96   ......LS.Y..P..DA........PS...I.....KN.......Q..AV.EK..AD..Q  155
A. actinomycetemcomitans          103  ....E.MS.H..P.TGN........PS...I.V...KN..I....Q.KET.EK.TAL.IQ  162
P. luminescens - YfeA             116  .D..E.LP.R..P.NGN........PT...I......Q.F.....K.TET..K.......  175
H. somnus 129PT                   96   .K..D..S.Y..P..GM........TK...V......E.......K..DT..A......D  155
E. carotovora                     114  ....T.LP.R..A.NGN........PS...I......KG..QA..A..ET..R.......  173
Y. bercovieri ATCC 43970          132  .N..T.LP.R..P.EGIA.......PS...I......K...EH..AH.ET..R.......  191
Y. pseudotuberculosis - YfeA      132  .A..T.LP.R..P.SGIA.......PS...I......K...EH..AH.ET..R..Q....  191
Y. pestis - YfeA                  133  .A..T.LP.R..P.SGIA.......PS...I......K...EH..AH.ET..R..Q....  192
Y. pseudotuberculosis             121  .A..T.LP.R..P.SGIA.......PS...I......K...EH..AH.ET..R..Q....  180

hHBP                              165  KIKAISEPLRQRLSVIPEKQRWLVTSEGAFSYLAQDYGLQELYLWPINAEEQGSPQQVRK  224
H. ducreyi                        165  ..................................................  224
A. pleuropneumoniae               165  .V...A............A.................Q.K.....A............K.  224
P. multocida                      163  ...QLDQ...EK.AK...G..............K......A...........T.....H  222
Y. mollareti ATCC 43969           192  ..A.LDA...E...R..AE..............K....K.V.......D.........R  251
Y. intermedi ATCC 29909           192  ..A.LDA...E...R..AQ..............K...FK.V.................R  251
Y. frederiksenii                  215  ..A.LDA...E...R...E..............K...FK.V.................H  274
H. influenzae Rd KW20             163  ...QLD....AK.AQ...A..............K..N.K.G........Q..T......  222
H. influenzae R2846               156  ...QLD....AK.AQ...A..............K..N.K.G........Q..T......  215
A. actinomycetemcomitans          163  ...ELDQ...EK.AQV..A..............R...FK.A........Q..T......  222
P. luminescens - YfeA             176  ..AQLDS...E...R..QD..............K..QFK.V.................H  235
H. somnus 129PT                   156  ..V.LDA...AE.EKV.AS..............H...FK.............T.K.IKN  215
E. carotovora                     174  ....LDA...E..AR...Q..............K..QFN.V.......D.........R  233
Y. bercovieri ATCC 43970          192  ..A.LDA...E...R..AEL.............K...FK.V.......D...T.....R  251
Y. pseudotuberculosis - YfeA      192  ....LDA...E...R..AE..............K...FK.V........Q..I.....H  251
Y. pestis - YfeA                  193  ....LDA...E...R..AE..............K...FK.V........Q..I.....H  252
Y. pseudotuberculosis             181  ....LDA...E...R..AE..............K...FK.V........Q..I.....H  240
```

Figure 10 cont'd.

```
hHBP                                225  VIDGVKANHIPVVFSESTVSDKPAKQVAKETGALYGGVLYVDSLSTKEGPVPTYLDLLKV  284
H. ducreyi                          225  ............................................................  284
A. pleuropneumoniae                 225  ........N.....................................D.A.........  284
P. multocida                        223  ..ET.RK.N.........I.............K............AK......I...NT  282
Y. mollareti ATCC 43969             252  ...TIR..K...I.....I........S................NEK......I..INT  311
Y. intermedi ATCC 29909             252  ...TMR..K...I.....I........S.....Q..........NEK......I..INT  311
Y. frederiksenii                    275  ...TMR..K...I.....I........S.....Q..........NEK......I..INT  334
H. influenzae Rd KW20               223  ...L.RK.N.........I.A...Q.....S..K..........A.N......I...N.  282
H. influenzae R2846                 216  ...L.RK.N.........I.A...Q.....S..K..........A.N......I...N.  275
A. actinomycetemcomitans            223  ..ET....N.........I.P..........K...........GAK......I.....  282
P. luminescens - YfeA               236  ...T.R..K.........I........S...D.R..........GSS......I...NK  295
H. somnus 129PT                     216  ..KK.REHK.........I............N.K............D.K....I...N.  275
E. carotovora                       234  ...T.REKA.........I........S.....K............EK......I...Q.  293
Y. bercovieri ATCC 43970            252  ...TMR..K...I.....I........S.....Q..........NEK......I..INT  311
Y. pseudotuberculosis - YfeA        252  ...IIRE.K.........I........S.....Q..........GEK......IS.INM  311
Y. pestis - YfeA                    253  ...IIRE.K.........I........S.....Q..........GEK......IS.INM  312
Y. pseudotuberculosis               241  ...IIRE.K.........I........S.....Q..........GEK......IS.INM  300

hHBP                                285  TISTIVDGFEASKKEPK  301
H. ducreyi                          285  ................  301
A. pleuropneumoniae                 285  ..........K...     298
P. multocida                        283  .V....K...         292
Y. mollareti ATCC 43969             312  .VQ..AK..          320
Y. intermedi ATCC 29909             312  .VQ..AK..          320
Y. frederiksenii                    335  .VQ..AK..          343
H. influenzae Rd KW20               283  .V....K..          291
H. influenzae R2846                 276  .V....K..          284
A. actinomycetemcomitans            283  .V...AK...         292
P. luminescens - YfeA               296  .VD..AK..          304
H. somnus 129PT                     276  .V....N..K         285
E. carotovora                       294  .VE..AK..          302
Y. bercovieri ATCC 43970            312  .VQ..AK..          320
Y. pseudotuberculosis - YfeA        312  .VD..AK..          320
Y. pestis - YfeA                    313  .VD..AK..          321
Y. pseudotuberculosis               301  .VD..AK..          309
```

the signal sequence between residues 23 and 24 would result in a mature protein ~31 000 MW and 278aa in length that localized to the periplasmic space. The predicted MW of the mature protein corresponded to the size of hHBP determined from 2D gel analysis (Figure 8, Appendix I). PSORT results were confirmed experimentally with periplasmic, cytoplasmic, and outer membrane preparations from *H. ducreyi* 35 000 run on 1D SDS-PAGE followed by Western immunoblots probed with anti-hHBP polyclonal antiserum (Figure 11B). An immunoreactive band of ~31 000 MW was present in all periplasmic samples with only weak immunoreactive bands present in cytoplasmic samples from *H. ducreyi* 35 000 grown under heme-limiting conditions. Of note, the expression of hHBP was upregulated in periplasmic protein samples collected from *H. ducreyi* grown under heme-limiting conditions compared to those grown under heme-replete conditions.

Three open reading frames flanked the hHBP gene indicated by ORF-1, 2, and 3 (Figure 9). A potential promoter region was located immediately upstream of ORF-1 preceded by a well conserved Shine-Dalgarno sequence appropriately spaced from the initiation codon. No associated Fur binding site, typical of iron-regulated genes, was detected. The translational start codon of hHBP and ORF-3 overlap indicating that these proteins are translationally coupled. An inverted repeat, indicating a possible site for transcriptional termination, was found 45bp downstream of the ORF-3 stop codon [208]. The predicted ORF-1 product revealed that this protein contains six possible membrane-spanning segments and is classified as an inner-membrane protein as predicted by the PHDhtm algorithm and PSORT [208,209]. ORF-1 had the highest homology to other membrane carrier or transport proteins including *Erwinia carotovora* (65%; residues 3-220), *S. flexneri* (61%; residues 2-220), *E. coli* (61%; residues 3-220), *H. somnus* (64%; residues 3-220), and *Pasteurella multocida* (63%; residues 1-221). Little is known about the role of

Figure 11. Cellular localization and mature protein size of hHBP in *H. ducreyi* 35 000.

All six periplasmic and corresponding cytoplasmic extractions from *H. ducreyi* 35 000 grown under heme-limiting **(1,3,5)** and heme-replete **(2,4,6)** conditions used for 2D gel identification of upregulated periplasmic proteins along with an outer membrane protein extraction (OMP) collected from *H. ducreyi* 35 000 grown on GC agar supplemented with 50μg/ml heme and 50μM desferoxamine were separated by a 12% SDS-PAGE gel and stained with Coomassie **(A)**. Affinity-purified rhHBP was loaded as a positive control for the immunoblot detection. A Western immunoblot **(B)** was performed probing with rabbit polyclonal antiserum against rhHBP. The arrow indicates the ~31kDa mature hHBP protein band. Molecular mass standards are indicated in kilodaltons (kDa).

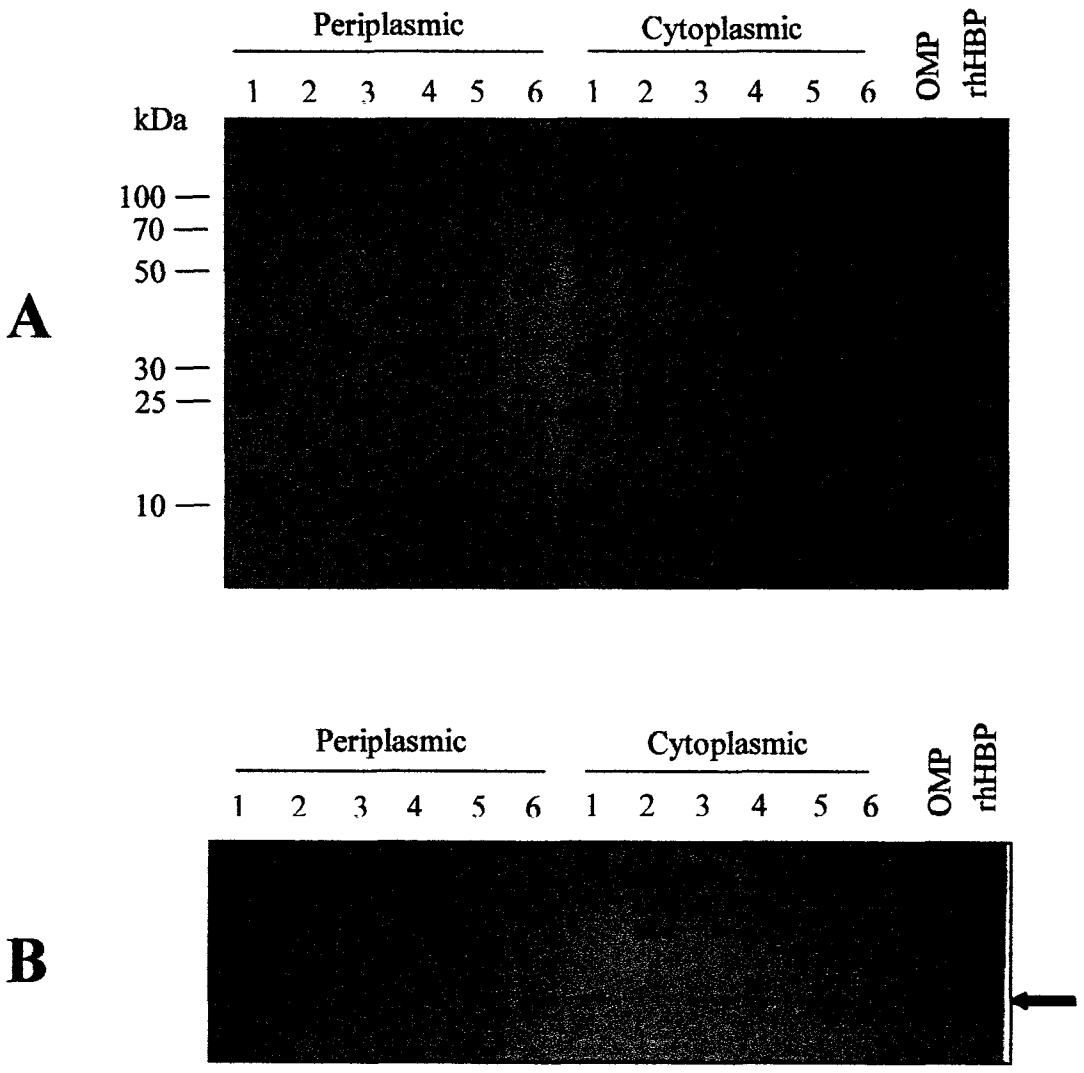

the putative membrane carrier or transport proteins homologous to ORF-1. When interrogating the genomes of the organisms listed above, the gene immediately downstream of the homologous membrane carrier or transport proteins encoded a predicted desulfoviridin gamma subunit (DGS). This was also observed in *H. ducreyi* 35 000 strain with the ORF-2 proposed to encode a putative DGS showing high homology to the DGS of *Actinobacillus pleuropneumoniae* (80%) and of *H. influenzae* (67%). The DGS protein encoded by ORF-2 is a member of the dissimilatory sulphite reductase family, DsrC [210]. Typically, this protein is found in sulfate-reducing bacteria possessing dissimilatory sulfite reductases comprised of three subunits: alpha, beta, and gamma. In these bacteria, the gene encoding DGS, *dsvC*, is not transcriptionally coupled with the other two subunits and is found downstream [211]. Desulfoviridin-type sulfite reductases were originally described to consist of a heterodimer of alpha and beta subunits; however, recent studies have indicated that the third gamma or DGS subunit forms a multimer with the alpha and beta subunits [212]. In addition, the DGS is only loosely associated with the sulfite reductase enzyme complex and is thought to possibly be involved in the assembly, folding or stabilization of sirohaem proteins in sulfite reductase lacking bacteria such as *E. coli*, and *H. influenzae* [211, 213]. The predicted ORF-3 product encodes a protein exhibiting homology to the ATP-binding component of an ABC transporter system and contains the two Walker motifs (Walker A 13-GVNGGKST- 22 and Walker B 163-DEPF-166) that have been identified in all nucleotide-binding proteins [214]. A third linker motif (139-LSGGQ-143) that typically precedes the Walker B motif is also present and is thought to be essential for transmembrane solute transport; although, the exact role of this sequence remains unclear [146].

3.5 Cloning of hHBP into a pET Vector and Protein Purification

3.5.1 Cloning of hHBP Gene into the pET151/D-TOPO® Vector

The gene encoding the hHBP protein was cloned into the pET151/D-TOPO® vector and maintained in *E. coli* TOP10 cells. Positive transformants were analyzed for recombinant plasmids by colony PCR amplification and sequencing of the plasmid inserts to confirm that the hHBP gene was in-frame and in the correct orientation (data not shown). The size of the recombinant plasmids was determined by agarose gel electrophoresis. Plasmids carrying a 6700bp insert (pET151 vector: 5760bp; hHBP insert: 940bp)(Figure 12, lane 3) were designated pET151-hHBP and were introduced into BL21 Star™ (DE3) *E. coli* cells for recombinant protein expression. Upon IPTG induction, the recombinant protein (rhHBP) was expressed predominantly in the remaining pellet fraction of *E. coli* (Figure 13A). The remaining pellet fraction included all proteins in the pellet following either periplasmic and cytoplasmic extraction or removal of the soluble protein fraction. The calculated mass of the recombinant fusion protein was 37.24kDa (N-terminal fusion tag: 4kDa; hHBP: 33.24kDa) as demonstrated on SDS-PAGE gel with a protein band ~37kDa. Little difference was seen between the IPTG-induced and un-induced remaining pellet fractions (Figure 13A). Sample loading of this gel was based on volume (10μl) and not on protein concentration in the fraction. However, a six-hour IPTG induction time-course experiment demonstrated an increase in rhHBP protein expression in the presence of IPTG as compared to the absence of IPTG induction (data not shown).

As hHBP is proposed to reside in the periplasmic space, the protein would be expected to appear predominantly in the soluble fraction of *E. coli*. However, as hHBP is a heterologously expressed protein in *E. coli*, the proper export of hHBP to the periplasm may be dependent on the presence of a native signal sequence. As seen from periplasmic and

Figure 12. Positive transformants were analyzed for the correct recombinant pET151-hHBP by plasmid size determination.

Plasmid DNA was extracted from TOP10 *E. coli* cells of positive transformants, resolved by a 0.8% agarose gel, and stained with ethidium bromide. The positive TOPO® cloning control plasmid **(1)** had an expected size of 6510bp (pET151 vector: 5760bp; control insert: 750bp); the pET vector alone **(2)** was represented by a 5760bp band; the pET151 vector plus hHBP insert plasmid **(3)** had an expected size of 6700bp (pET151 vector: 5760bp; hHBP insert: 940bp). Molecular mass standards are indicated in basepairs (bp).

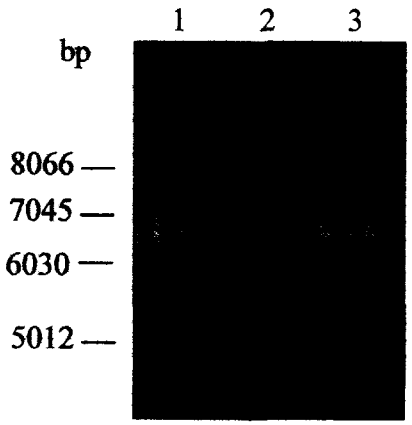

Figure 13. Expression of rhHBP in BL21 Star™ (DE3) *E. coli* cells.

A: Crude soluble protein extractions and remaining pellet samples were prepared from BL21 Star™ (DE3) *E. coli* cells containing recombinant plasmid pET151-hHBP in the presence **(I)** or absence **(U)** of IPTG induction. Ten µl of each extract was separated by a 12% SDS-PAGE gel and stained with Coomassie. Positions of protein markers in kilodaltons are shown on the left.
B: Twenty micrograms of periplasmic **(P)**, cytoplasmic **(C)**, and remaining pellet **(Rp)** fractions from IPTG induced Bl21 Star™ (DE3) *E. coli* cells containing the pET151-β-Gal control construct (expected fusion protein size: ~120kDa) or the pET151-hHBP construct were separated by a 12% SDS-PAGE gel and stained with Coomassie. Positions of protein markers in kilodaltons are shown on the left. The filled arrow indicates the rhHBP protein bands and the hollow arrow indicates the recombinant fusion β-Gal protein bands.
C: Various protein extracts from induced BL21 Star™ (DE3) *E. coli* were separated by a 12% SDS-PAGE gel and stained with Coomassie (left). The following samples were applied to the gel: two micrograms of periplasmic **(P)** and remaining pellet **(Rp)** extracts from *E. coli* cells containing pET151-hHBP; one microgram of crude soluble **(S)** and the remaining pellet fractions from *E. coli* cells with no plasmid **(BL21)**, with pET151 vector only **(BL21-pET151)**, and with the recombinant plasmid pET151-hHBP **(BL21-pET151-hHBP)**; two micrograms of affinity-purified rhHBP was loaded as a positive control for Western immunoblotting. Positions of protein markers in kilodaltons are shown to the left of the SDS-PAGE gel. The corresponding Western immunoblot was probed with rabbit polyclonal antiserum against rhHBP (right). The filled arrows represent the uncleaved rhHBP immunoreactive band (~37kDa) and the mature hHBP immunoreactive band (~31kDa). Positions of protein markers in kilodaltons are shown on the left. The (*) indicates the ~33kDa immunoreactive band.

A

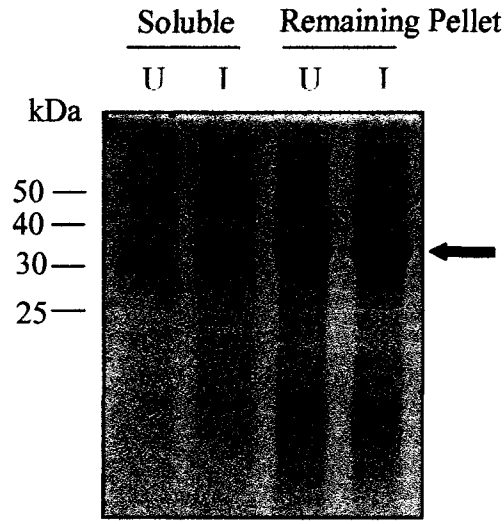

B

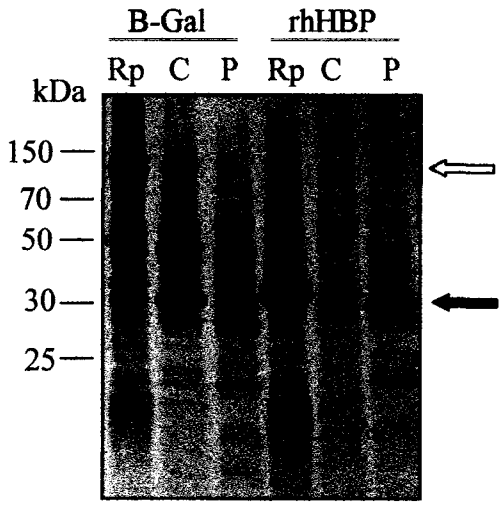

C

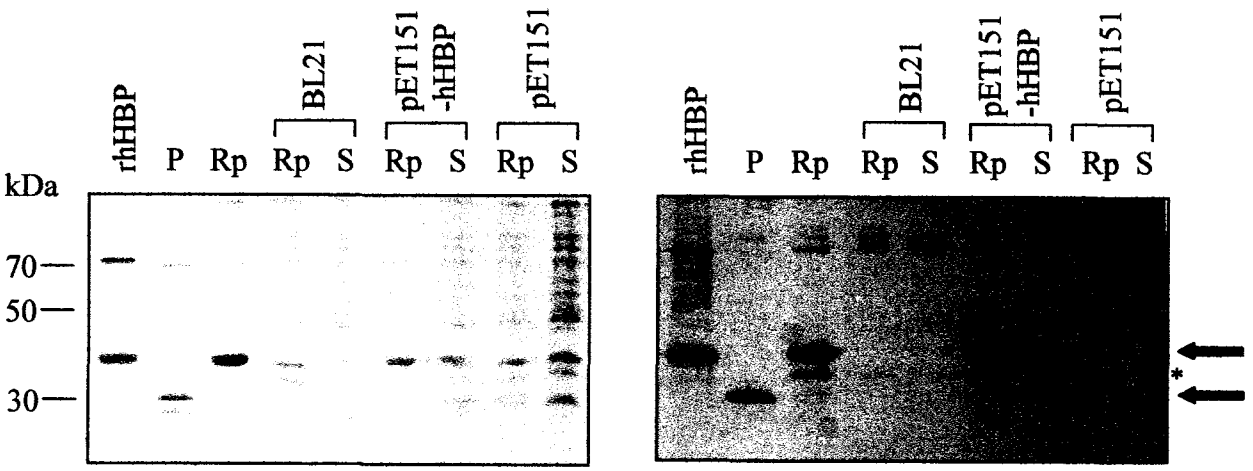

remaining pellet protein extractions of BL21 Star™ (DE3) *E. coli* cells containing the pET151-hHBP construct, expression of rhHBP was seen in all three cellular locations (Figure 13B). However, the majority of the expression was present in the remaining pellet fraction. The protein band representing hHBP in the periplasmic fraction was the expected size of the mature protein (~31kDa); rhHBP expressed in the remaining pellet and cytoplasmic fractions was the expected size of the uncleaved fusion protein (~37kDa). This was reiterated in Western blots probing cellular fractions with the anti-hHBP polyclonal antiserum (Figure 13C). The pET151/D-TOPO® vector expression control expressed the recombinant fusion cytoplasmic protein β-Galactosidase (rβ-Gal). rβ-Gal was mainly expressed in the cytoplasmic fraction as expected with no expression in the periplasmic space (Figure 13B). However, like rhHBP, the control rβ-Gal also was present in the remaining pellet fraction.

In addition, the expression of rhHBP was specific for only BL21 Star™ (DE3) *E. coli* cells containing the pET151-hHBP construct as seen from Western immunoblots probing with anti-hHBP polyclonal antiserum (Figure 13C). There was an immunoreactive band ~37kDa present in the remaining pellet protein fraction representative of the uncleaved rhHBP protein and a band representative of the mature hHBP (~31kDa) in the soluble fraction (Figure 13C). Both BL21 Star™ (DE3) cells with or without the pET151 vector produced a faint immunoreactive band ~33kDa in the remaining pellet fractions. Recalling that the antibody against hHBP was produced with affinity-purified rhHBP with an intact fusion tag, the presence of this faint band was possibly due to the recognition of a protein sequence in the uncleaved fusion tag. However, a much more intense same-size band was present in the remaining pellet fraction from BL21 Star™ (DE3) *E. coli* cells expressing the

pET151-hHBP construct which could indicate that this immunoreactive band represents the uncleaved hHBP lacking the 4kDa fusion tag.

3.5.2 Purification of the Recombinant Fusion Protein

Metal affinity chromatography was used to purify the recombinant fusion protein, rhHBP. rhHBP was expressed predominantly in the insoluble fraction of *E. coli* with the mature form of hHBP, following cleavage of the signal sequence, expressed in the soluble fraction. The fusion tag is located upstream of the signal sequence of the protein; therefore, hHBP in the soluble fraction would also lack a fusion tag making metal affinity chromatography purification impossible. Therefore, the Ni-NTA purification hybrid method of protein purification was used to maintain protein activity for functional characterization of the protein. Cell lysates of the remaining pellet protein fractions were prepared under denaturing conditions. However, elution was then performed using native buffers to re-fold the proteins in order to restore function. An excess of imidazole was added to fusion-tagged proteins bound to the Ni ions of the chromatography column to free the fusion-tagged proteins. rhHBP eluted mainly in the fractions containing 150, 200, and 250mM imidazole (Figure 14A). When elutions were applied to 1D SDS-PAGE gel, two protein bands representative of the rhHBP monomer (37.24kDa) and of the rhHBP homodimer (~75kDa) were visualized. A Western immunoblot of rhHBP eluted from the Ni-NTA column probed with an antibody against the fusion tag, anti-V5-HRP, demonstrated two immunoreactive bands representative of the monomer and homodimer (Figure 14B). The additional immunoreactive bands present between the monomer and dimer are most likely higher order derivatives of the rhHBP monomer with the proper V5 epitope present in the N-terminal fusion tag for antibody recognition.

Figure 14. Recombinant hHBP was purified by metal immobilized affinity chromatography using several concentrations of imidazole in the elution buffer.

IPTG induced BL21 Star™ (DE3) *E. coli* cells containing the pET151-hHBP construct were utilized to purify rhHBP. Proteins were extracted using Ni-NTA purification system's hybrid method and eluted with native buffers containing increasing concentrations of imidazole. Aliquots of elutions containing 150mM **(1)**, 200mM **(2)**, and 250mM **(3)** imidazole were separated by a 12% SDS-PAGE gel and stained with SYPRO Ruby **(A)**. The corresponding Western immunoblot **(B)** was probed with the anti-V5-HRP antibody. The rhHBP monomer (~37kDa) and homodimer (~75kDa) are indicated by filled arrows. Molecular mass standards are indicated in kilodaltons (kDa).

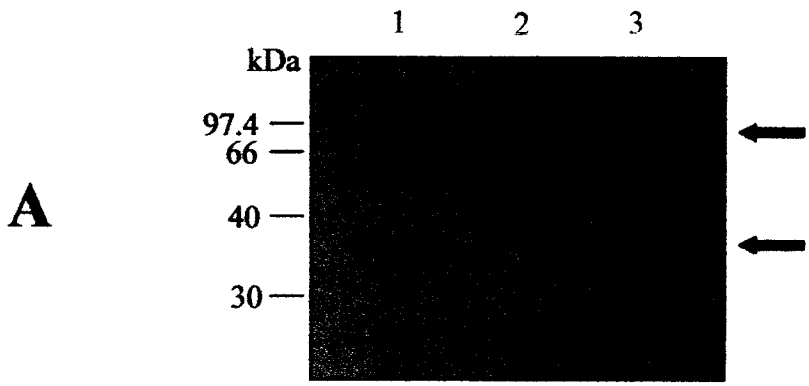

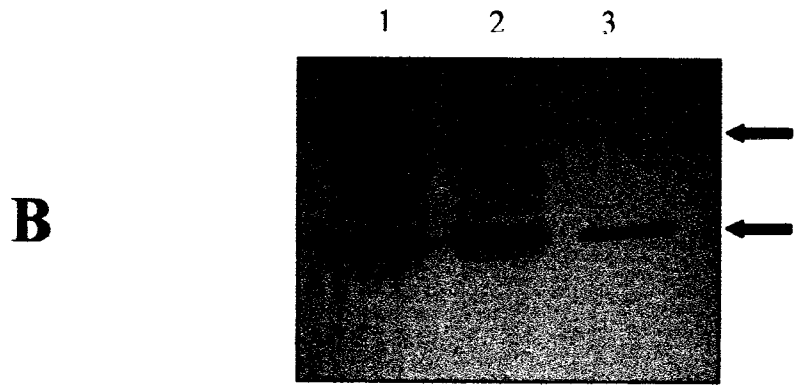

Furthermore, the identity of the ~37kDa protein band visualized by SDS-PAGE was confirmed by MALDI tandem mass spectroscopy to be the iron (chelated) ABC transporter periplasmic binding protein of *H. ducreyi* 35 000 identified previously by 2D gel analysis (data not shown).

3.5.3 Cleavage of the N-terminal Fusion Tag of rhHBP

The N-terminal fusion tag on the affinity-purified rhHBP would be expected to be cleaved at the TEV recognition site recognized by the AcTEV™ enzyme (Figure 2). However, the fusion tag could not be completely removed despite exhaustive trials in which the incubation time, incubation temperature, and ratio of rhHBP to enzyme were varied (Figure 15). At 4°C incubation with 0.5U AcTEV™/μg protein, no obvious cleavage was demonstrated by 1D SDS-PAGE gel (Figure 15A). Incubation at room temperature with 0.5U AcTEV™/μg protein produced a small amount of cleavage product; however, a Western blot probing with anti-V5-HRP antibody demonstrated no decrease in the amount of either the rhHBP monomer or dimer with increasing incubation time (Figure 15B). Although enzymatic removal of the N-terminal fusion tag was enhanced during incubation at 30°C with 4U AcTEV™/μg protein, the amount of protein product remained insufficient for the subsequent experiments designed for functional characterization of the protein (Figure 15C). Overnight incubation with 4U AcTEV™/μg protein at room temperature or 30°C resulted in degradation of the protein with little increase in the quantity of cleaved protein (data not shown). Therefore, the affinity-purified rhHBP used for functional characterization and antibody production possessed the N-terminal fusion tag.

3.6 Specificity of the Polyclonal Antibody Against rhHBP

A polyclonal antibody directed against rhHBP was produced by immunization of a rabbit with rhHBP possessing the N-terminal fusion tag. Affinity-purified rhHBP was

Figure 15. Fusion tag cleavage trials of rhHBP with the AcTEV™ enzyme.

Affinity-purified rhHBP was incubated with the AcTEV™ enzyme over a time course of 6 hours (as indicated above each lane). An aliquot from each timepoint was separated by a 12% SDS-PAGE gel and SYPRO Ruby stained. Western blots were probed with the anti-V5-HRP antibody. Filled arrows indicate the monomer (~37kDa) and homodimer (~75kDa) of rhHBP. Open arrows indicate the AcTEV™ protease protein band (~27kDa). Protein bands highlighted with a (*) represent cleaved rhHBP (~33kDa). Molecular mass standards are indicated in kilodaltons (kDa).
A: 0.5U AcTEV™/μg rhHBP was incubated at 4°C.
B: 0.5U AcTEV™/μg rhHBP was incubated at room temperature.
C: 4U AcTEV™/μg rhHBP was incubated at 30°C. rhHBP represents an aliquot of affinity-purified rhHBP prior to the addition of AcTEV™ enzyme.

A

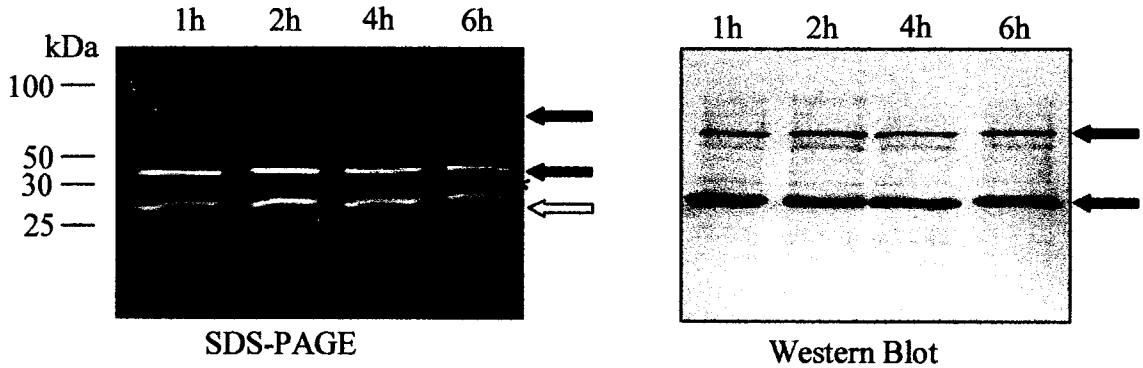

B

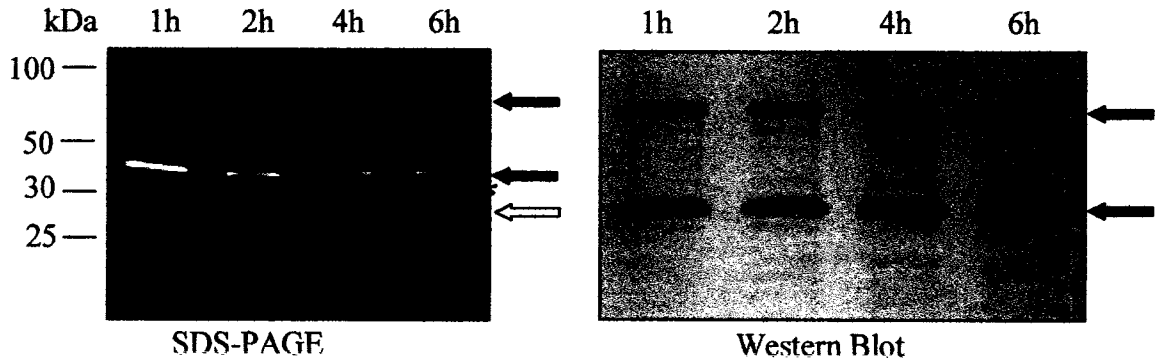

C

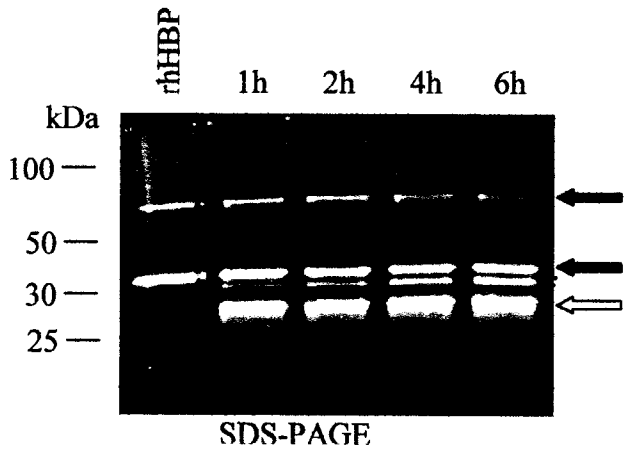

separated by 1D SDS-PAGE and probed with several dilutions of serum obtained from the terminal bleed. The appropriate dilution of the antibody for Western immunoblotting was determined to be 1/8 000 (data not shown).

Serum was collected prior to the first immunization and prior to both booster injections. Western immunoblots probing affinity-purified rhHBP with serum collected at these timepoints demonstrated increasing antibody response to rhHBP after each immunization as reflected by increasing size and intensity of the immunoreactive bands (Figure 16A). The presence of the faint immunoreactive bands between the rhHBP monomer and dimer were similar to those immunoreactive bands present in preparations of affinity-purified rhHBP used to inoculate the rabbit as detected with the anti-V5-HRP antibody (Figure 14B).

No hHBP-specific immunoreactive bands were present when rhHBP was reacted either with pre-immune sera or with secondary antibody alone (Figure 16B). These results confirmed the specificity of the polyclonal antiserum against rhHBP. The immunoblot probed with pre-immune serum illustrated a lower molecular weight immunoreactive band ranging from 10 to 15 kDa in each whole cell lysate tested and was most likely representative of an antibody in the rabbit prior to first immunization. When probing Western immunoblots of cellular protein fractions of *H. ducreyi* 35 000 (Figure 11 and 26), *E. coli* (Figure 13C), and clinical isolates of *H. ducreyi*, *H. influenzae*, and *Y. entercolitica* (Figure 27) with the anti-hHBP polyclonal antiserum, immunoreactive bands >70kDa were present. As the affinity-purified rhHBP sample used to inoculate the rabbit for anti-hHBP polyclonal antiserum production contained the fusion tag, these immunoreactive bands likely represent proteins containing a sequence similar to that present in the fusion tag of rhHBP. Further evidence supporting this conclusion is derived by the presence of similar immunoreactive

Figure 16. Specificity of a polyclonal antibody against *H. ducreyi* hHBP.

A: One microgram of affinity-purified rhHBP was separated by a 12% 1D SDS-PAGE gel followed by transfer to nitrocellulose. The blots were probed with serum collected prior to immunization **(1)**, prior to the administrations of the first **(2)** and the second **(3)** boosters, and at the terminal bleed **(4)**. **MM** represents the molecular mass standards in kilodaltons.
B: Five micrograms whole cell lysate derived from *H. ducreyi* J1159, *H. influenzae* 70824, *Y. entercolitica* 73918, and BL21 Star™ (DE3) *E. coli* cells containing the pET151-hHBP construct were separated by a 12% SDS-PAGE gel followed by transfer to nitrocellulose. Blots were either probed with secondary antibody only (left) or with rabbit pre-immune serum (right). Molecular mass standards are indicated in kilodaltons (kDa). The rhHBP monomer (~37kDa) and homodimer (~75kDa) are indicated by filled arrows.

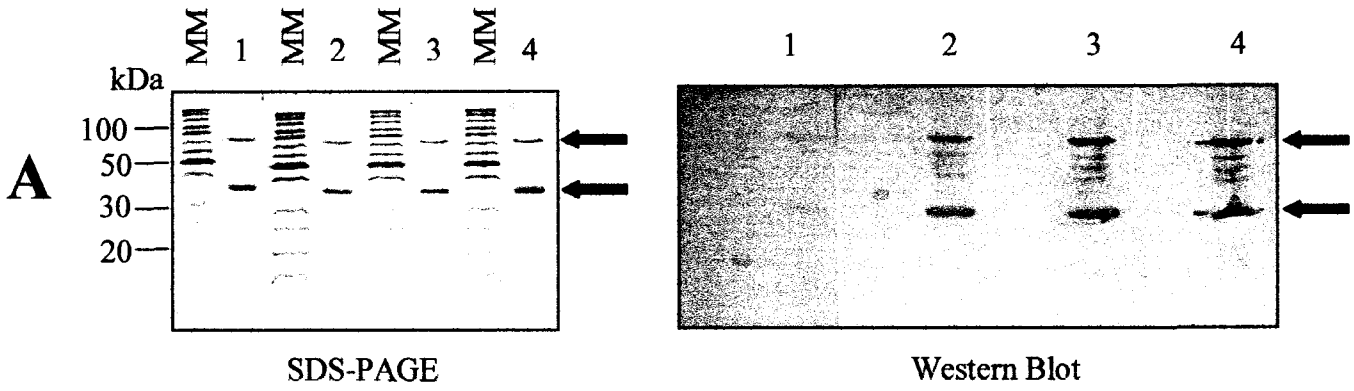

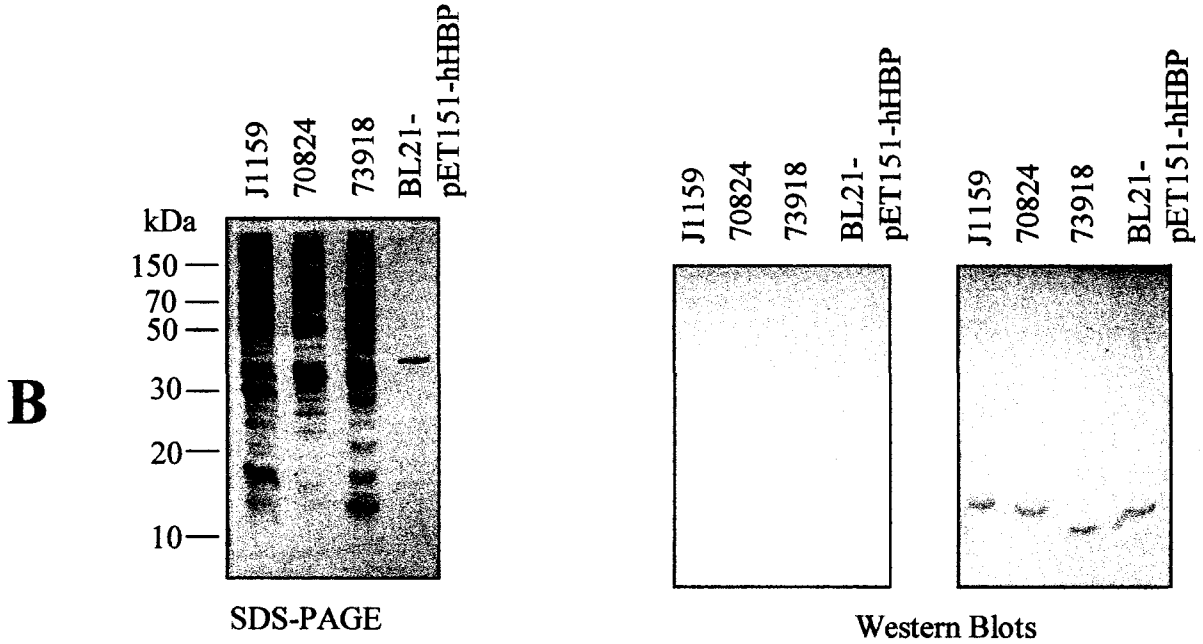

bands >70kDa on Western blots of *E. coli* cellular fractions probed with the anti-V5-HRP (data not shown).

3.7 Functional Characterization of hHBP by Heme Agarose Binding

Prior to elution of heme agarose bound protein, wash fractions were collected, concentrated, and separated by SDS-PAGE. No proteins were seen in these fractions indicating that the rhHBP remained absorbed onto the heme-bound polysaccharide matrix until its elution (data not shown). These proteins were absent when the affinity resin alone was subjected to the affinity protocol indicating that the bound proteins were not degradation products or derivatives from the sepharose matrix (denoted as the negative control sample, NC, in subsequent experiments).

3.7.1 Specificity of hHBP

Concentrations ranging from 500ng to 10μg of affinity-purified rhHBP were incubated with a fixed amount (20μl) of heme agarose. Proteins bound to the heme agarose were eluted and separated by SDS-PAGE. Experiments were performed in triplicate. The affinity-purified rhHBP bound to heme agarose in a concentration dependent manner (Figure 17).

3.7.2 Competitive Binding Assays

In the competition binding assays, a fixed concentration (10μg) of affinity-purified rhHBP was pre-incubated with increasing concentrations of ligand prior to heme affinity chromatography. In the presence of a ligand that specifically bound the affinity-purified rhHBP, retention of the rhHBP to the immobilized heme would be abolished in a concentration dependent manner. In contrast, no such binding inhibition would be expected when rhHBP was pre-incubated with a non-interacting ligand (Figure 18).

Figure 17. Specificity of hHBP determined by heme agarose binding assay.

Affinity-purified rhHBP at the indicated concentrations was incubated with heme agarose for one hour. Bound protein was eluted with 2x sample loading buffer and 40μl of each boiled sample was separated by a 12% SDS-PAGE gel and SYPRO Ruby stained. The arrows indicate the rhHBP monomer (~37 kDa) and the homodimer (~75kDa). NC represents the negative control in which no protein was incubated with the heme agarose.

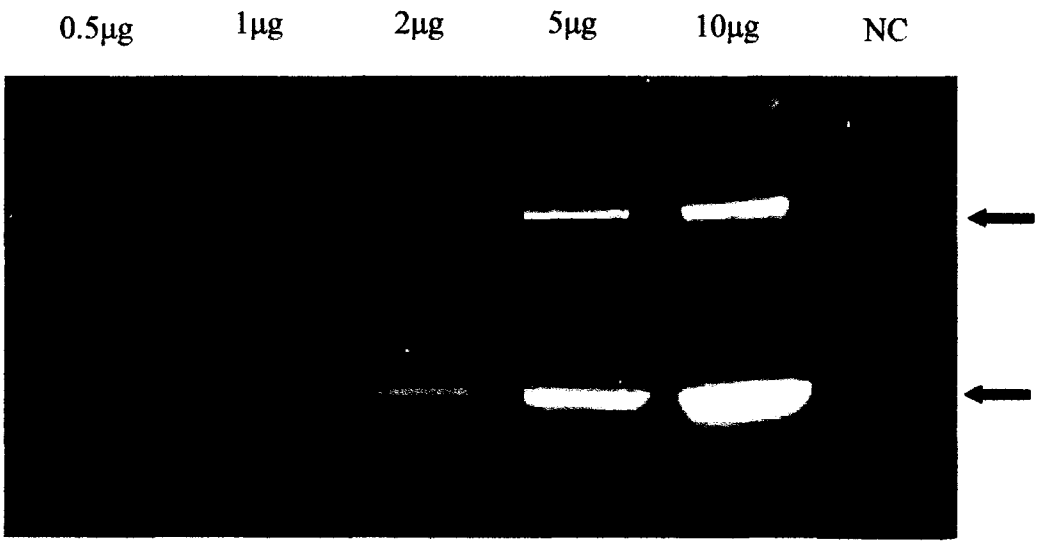

Figure 18. Competition Binding Assay

In the competition binding assay, 10μg of affinity-purified rhHBP (●) was pre-incubated with increasing concentrations of ligand prior to binding a heme affinity column (▮—✦). A: When pre-incubating with a ligand able to bind rhHBP (▮), they interact leaving no protein able to bind the heme agarose; therefore, producing no protein band on SDS-PAGE gel.
B: When pre-incubating with a ligand unable to bind rhHBP (▲), the protein is still able to bind the heme agarose; therefore, rhHBP will be eluted from the heme agarose resulting in a protein band on a SDS-PAGE gel.

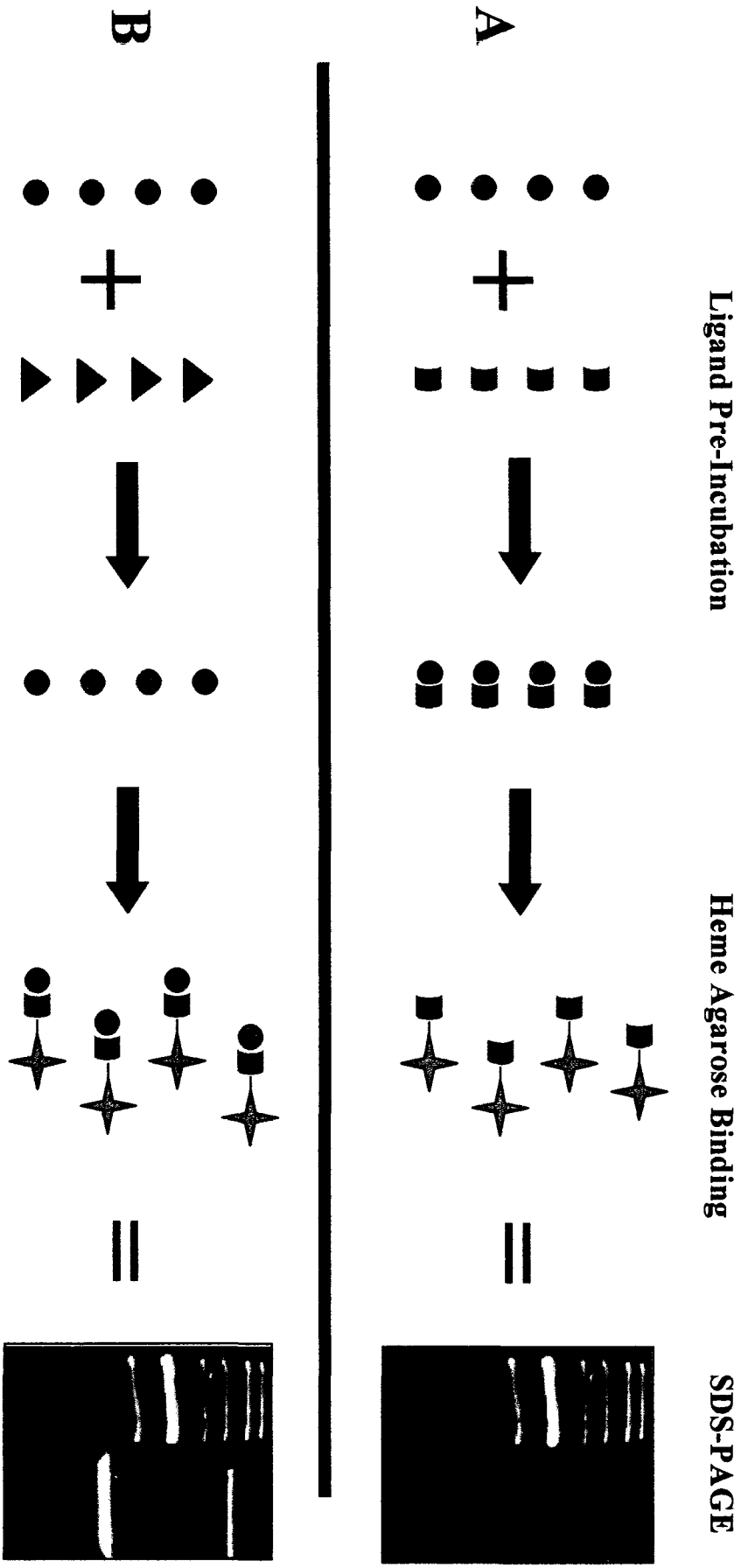

3.7.2.1 Heme Competition Binding Assays

The interaction of rhHBP with the immobilized heme was specific as retention of rhHBP was diminished in a concentration dependent fashion (Figure 19). Experiments were performed in triplicate.

As histidine residues serve as axial ligands in heme binding, the possibility existed that the heme binding observed with rhHBP was mediated by the presence of the histidine residues present in the uncleaved N-terminal fusion tag [143]. To address this likelihood, an ~31kDa recombinant 5' 6xHis-tagged outer membrane lipoprotein from *Leptospira*, rLipL32, was examined for its ability to bind heme in a competition binding assay (Figure 20A). rLipL32 did not bind heme in concentration dependent inhibitory fashion (Figure 20B) as was seen in a heme competition binding assay with rhHBP (Figure 20C). However, the lipoprotein did show some inhibition at heme agarose binding at heme concentrations above 400μM, although, certainly not in a concentration dependent manner. Therefore, the histidine residues present in the fusion tag of rhHBP do not mediate the binding of rhHBP to heme.

3.7.2.2 Protoporphyrin IX Competition Binding Assay

As heme is composed of a porphyrin ring with an iron-chelated iron molecule, recognition of heme as a legitimate ligand by rhHBP may require the presence of iron within the tetrapyrrole ring. Therefore, competitive binding assays were conducted using protoporphyrin IX, the immediate precursor of heme in the heme biosynthetic pathway [215]. Concentrations of protoporphyrin IX (PPIX) above 100μM markedly reduced absorption of rhHBP to the affinity gel (Figure 21). The persistent binding of rhHBP to the heme agarose seen at PPIX concentrations from 600uM to 1mM may derive from the pronounced tendency of porphyrins to aggregate at high concentrations in aqueous solutions [216]. This

Figure 19. Competition binding assay pre-incubating affinity-purified rhHBP with increasing concentrations of heme.

Ten micrograms ($2.7 \times 10^{-7}\mu M$) of affinity-purified rhHBP was pre-incubated with heme in concentrations ranging from 300μM to 1mM. The mixtures were then incubated with heme agarose for one hour and bound proteins were eluted with 2x sample loading buffer. Forty microlitres of each boiled sample was separated by a 12% SDS-PAGE gel and SYPRO Ruby stained. NC represents the negative control where no protein was incubated with the heme agarose. Filled arrows indicate the (~37kDa) rhHBP monomer and (~75kDa) homodimer.

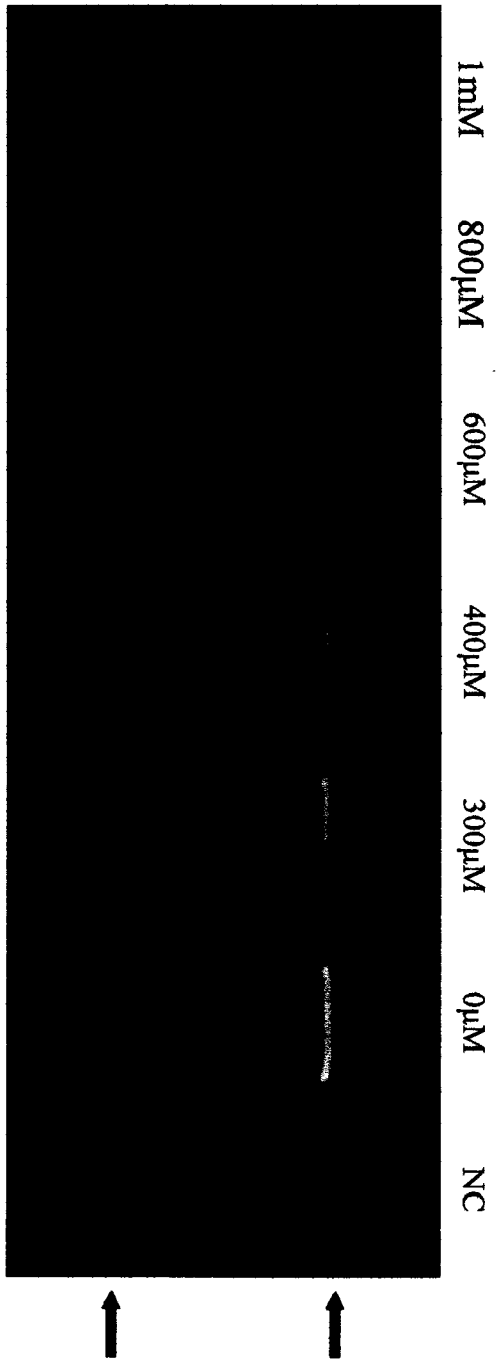

Figure 20. Competition binding assay pre-incubating rLipL32, a recombinant outer membrane lipoprotein from *Leptospira*, with increasing concentrations of heme.

A: The amino acid sequence of the recombinant N-terminal six-histidine tagged outer membrane lipoprotein from *Leptospira*, rLipL32. The fusion tag is indicated in green.
B&C: Ten micrograms (3.2 x 10^{-7}μM) of rLipL32 was pre-incubated with heme in concentrations ranging from 300μM to 1mM **(B)**. In tandem, a competition binding assay using rhHBP as described in figure 19 was performed **(C)**. Mixtures were subsequently incubated with heme agarose for one hour and bound proteins were eluted with 2x sample loading buffer. Forty microlitres of each boiled sample was separated by a 12% SDS-PAGE gel and SYPRO Ruby stained. NC represents the negative control where no protein was incubated with the heme agarose. Filled arrows indicate the (~37kDa) rhHBP monomer and (~75kDa) homodimer; the open arrow indicates the (~31kDa) rLipL32 monomer.

A

rLipL32 Protein Sequence:

Gene length: 283aa ; Protein size: 31 kDa

MHHHHHHG MKKLSILAISAALFASITACGAFGGLPSLKSS
FVLSESTVPGTNETVKTFLPYGSVINYYGYVKPGQAPDGL
VDGNKKAYYLYVWIPAVIAEMGVRMISPTGEIGEPGDGD
LVSDAFKAATPEEKSMPHWFDTWIRVERMSVIMPDQIAK
AAKAKPVQKLNDDDDGDDTYKEERHNKYNSLTRIKIPNP
PKSFDDLKNIDTKKLLVRGLYRISFTTYKPGEVKGSFVAS
VGLLFPPGIPGVSPLIHSNPEELQKQAIAAEESLKKLSILLL
TRLS

B

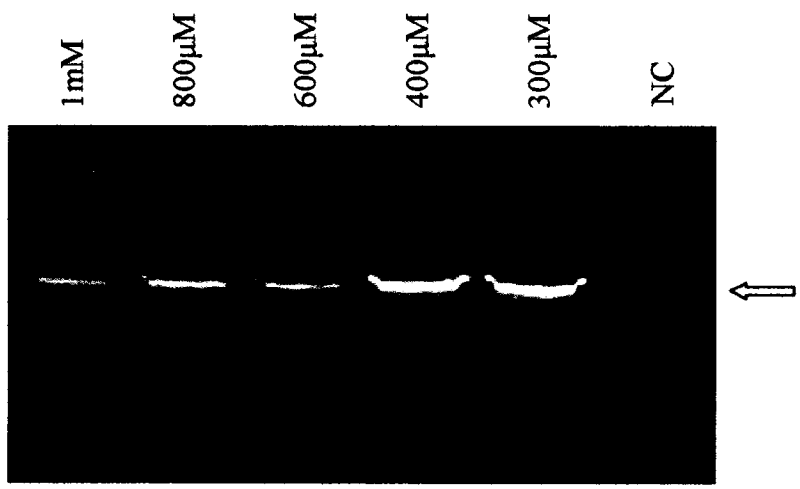

C

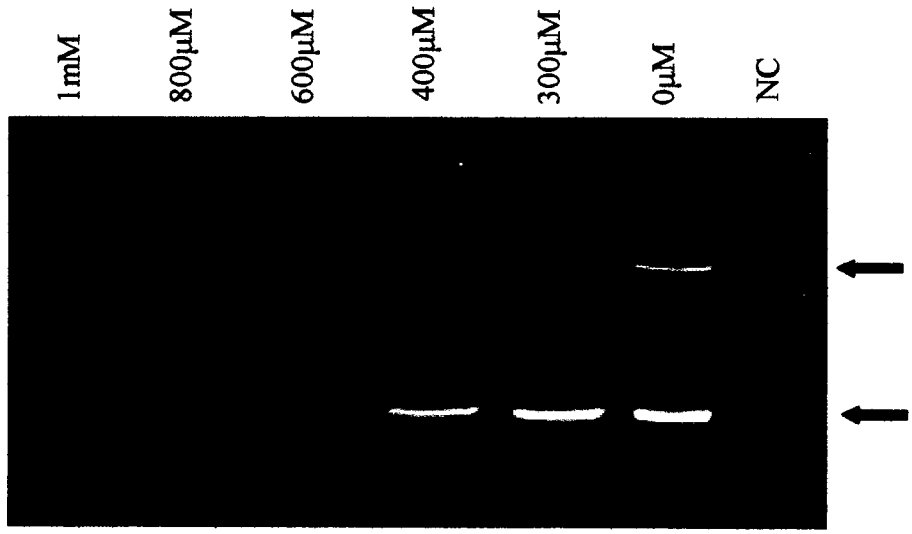

Figure 21. Competition binding assay pre-incubating affinity-purified rhHBP with increasing concentrations of protoporphyrin IX.

Ten micrograms of affinity-purified rhHBP was pre-incubated with protoporphyrin IX in concentrations ranging from 50μM to 1mM. Mixtures were subsequently incubated with heme agarose for one hour and bound proteins were eluted with 2x sample loading buffer. Forty microlitres of each boiled sample was separated by a 12% SDS-PAGE gel and SYPRO Ruby stained. NC represents the negative control where no protein was incubated with the heme agarose. Filled arrows indicate the (~37kDa) rhHBP monomer and (~75kDa) homodimer.

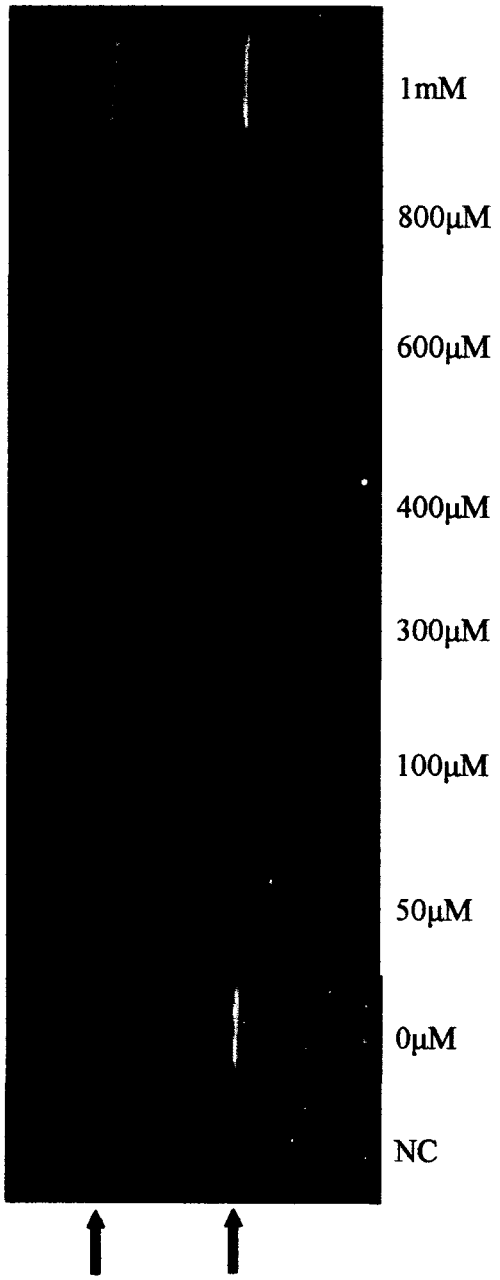

propensity may have reduced the effective concentration of PPIX available for competition or may have interfered with binding of PPIX to rhHBP by steric hindrance. This result indicated that rhHBP recognized the porphyrin ring of the heme molecule. Experiments were performed in duplicate.

3.7.2.3 Iron Competition Binding Assays

As hHBP exhibits homology to other bacterial periplasmic binding proteins involved in iron transport (Figure 10), experiments were performed using either ferric chloride or ferric nitrate as the competing ligand. Neither iron compound demonstrated concentration dependent inhibition of rhHBP to the heme agarose (Figure 22A and 22B). No concentration dependent inhibition was seen in competition binding assays pre-incubating with 0μM to 100μM of ferric chloride or 300μM to 1mM of ferric nitrate (data not shown).

In addition, competition binding assays pre-incubating with concentrations of heme ranging from 300μM to 1mM with the addition of 2,2'-dipyridyl (1.25mM/1mM heme) resulted in a concentration dependent inhibition pattern similar to results seen when pre-incubating with heme alone (Figure 23). These results were obtained in duplicate and indicate that iron dissociated from heme in solution was not responsible for the concentration dependent inhibitory effects demonstrated when pre-incubating with heme alone.

3.7.2.4 Zinc Protoporphyrin IX Competition Binding Assay

Zinc protoporphyrin IX (Zn-PPIX), a substituted non-iron metalloporphyrin, has been shown to exert significant antibacterial activity against *H. ducreyi* [196]. Metalloporphyrins exploit the heme uptake pathway to enter bacterial cells although the precise mechanisms of this antibacterial action and the components of heme acquisition pathway that are co-opted remain incompletely characterized [195,196]. Therefore, to determine whether hHBP was engaged in the transport of Zn-PPIX into *H. ducreyi*, competitive binding assays were

Figure 22. Competition binding assay pre-incubating affinity-purified rhHBP with increasing concentrations of ferric chloride or ferric nitrate.

Ten micrograms of affinity-purified rhHBP was pre-incubated with ferric chloride **(A)** or ferric nitrate **(B)** in concentrations as indicated above each lane. The mixtures were then incubated with heme agarose for one hour and bound proteins were eluted with 2x sample loading buffer. Forty microlitres of each boiled sample was separated by a 12% SDS-PAGE gel and SYPRO Ruby stained. NC represents the negative control where no protein was incubated with the heme agarose. Filled arrows indicate the (~37kDa) rhHBP monomer and (~75kDa) homodimer.

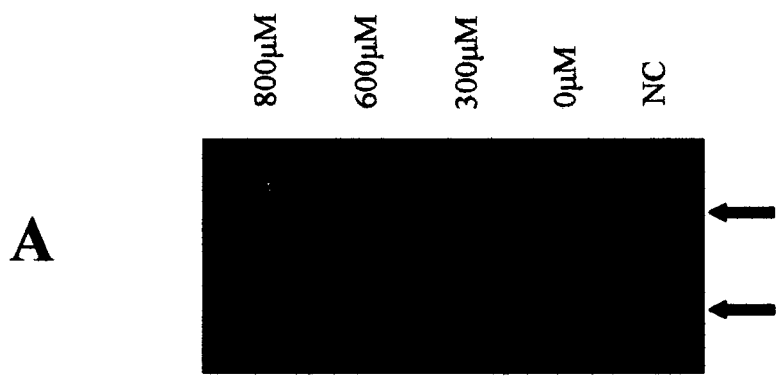

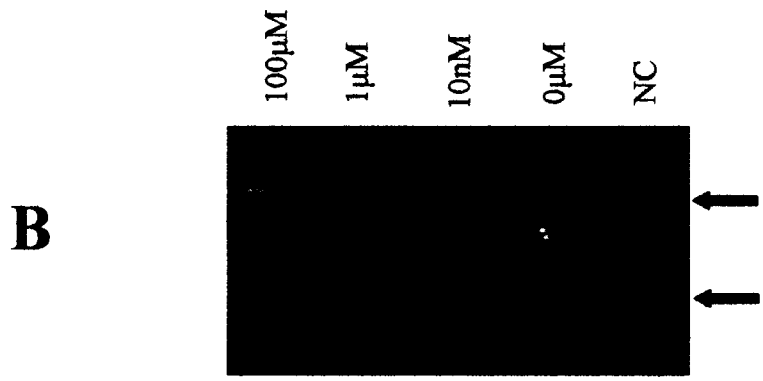

Figure 23. Competition binding assay pre-incubating affinity-purified rhHBP with increasing concentrations of heme with the addition of an iron chelator.

Ten micrograms of affinity-purified rhHBP was pre-incubated with heme in concentrations ranging from 300μM to 1mM with the addition of a fixed concentration of an iron chelator (1.25mM/1mM heme) – 2,2'-dipyridyl. Mixtures were then incubated with heme agarose for one hour and bound proteins were eluted with 2x sample loading buffer. Forty microlitres of each boiled sample was separated by a 12% SDS-PAGE gel and SYPRO Ruby stained. NC represents the negative control where no protein was incubated with the heme agarose. Filled arrows indicate the (~37kDa) rhHBP monomer and (~75kDa) homodimer.

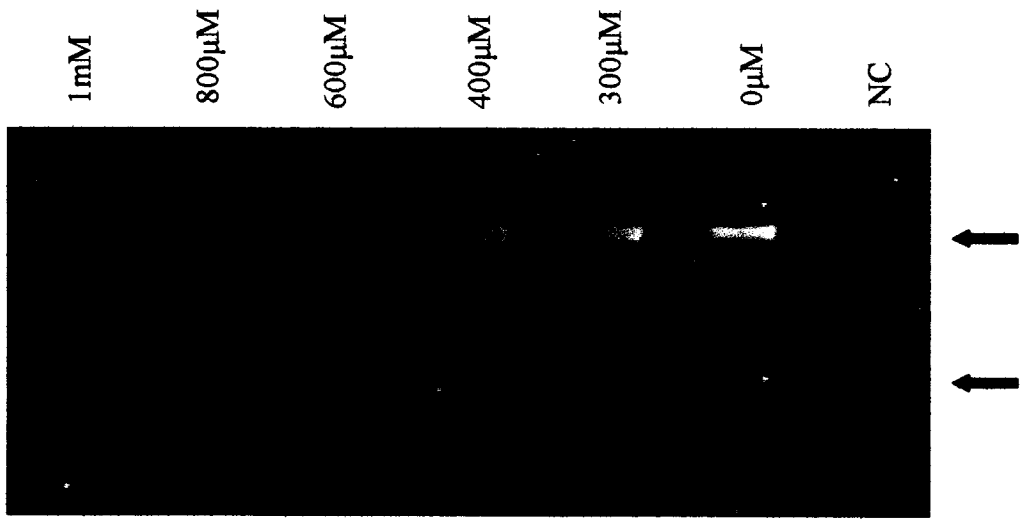

performed using this substituted metalloporphyrin. Concentration dependent inhibition was demonstrated; although, 10-fold higher concentrations of Zn-PPIX compared to heme were required for complete inhibition (Figure 24). This result indicated that the entry of Zn-PPIX into *H. ducreyi* is likely mediated by the binding to the heme periplasmic binding protein, hHBP.

3.8 Heme Regulation of hHBP Expression

The 2D gel analysis of *H. ducreyi* 35 000 grown under heme-limiting and heme-replete conditions included 50μM desferoxamine which eliminated excess iron present in the media or glassware. Although this concentration of desferoxamine would be in excess of the total amount of free iron present in the heme-limiting conditions, this concentration of iron chelator would not account for the possible total dissociation of iron from heme in the heme-replete media where 154μM desferoxamine would be needed. This led to the possibility that the enhanced hHBP expression arose from iron-limitation rather than heme restriction. Therefore, 2D gels of periplasmic protein profiles of *H. ducreyi* 35 000 were prepared from cells grown under heme-replete conditions (GC agar supplemented with 100μg/ml heme) to which increasing concentrations of desferoxamine (10μM to 200μM) was added. 2D gel protein profiles were compared qualitatively by inspection and quantitatively by densitometry (Figure 25, Appendix II). If the expression of hHBP was regulated by iron, enhanced expression would be expected under iron-limited growth, i.e., in the presence of higher concentrations of desferoxamine. However, there was a decrease in hHBP protein spot net intensity at higher desferoxamine concentrations (Figure 25, Appendix II). 2D gel pairwise comparisons were performed in duplicate.

To provide additional evidence that the expression of hHBP was heme-regulated and not governed by iron, the periplasmic extracts were reacted with the anti-hHBP polyclonal

Figure 24. Competition binding assay pre-incubating affinity-purified rhHBP with increasing concentrations of a metalloporphyrin.

Ten micrograms of affinity-purified rhHBP was pre-incubated with zinc-substituted protoporphyrin IX in concentrations ranging from 1mM to 10mM. Mixtures were then incubated with heme agarose for one hour and bound proteins were eluted with 2x sample loading buffer. Forty microlitres of each boiled sample was separated by a 12% SDS-PAGE gel and SYPRO Ruby stained. NC represents the negative control where no protein was incubated with the heme agarose. Filled arrows indicate the (~37kDa) rhHBP monomer and (~75kDa) homodimer.

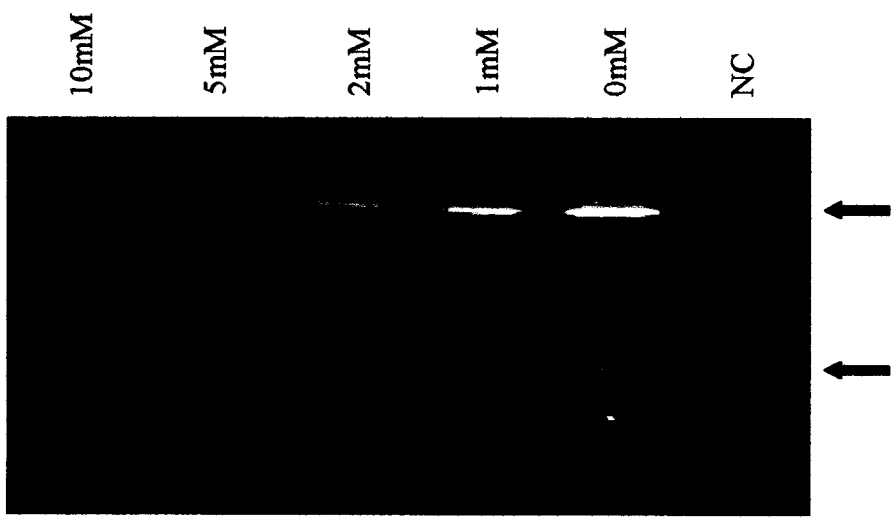

Figure 25. 2D gel analysis determining iron regulation of hHBP.

2D gel comparison of chloroform extracted periplasmic proteins of *H. ducreyi* 35 000 grown under heme-limiting conditions with 100μM **(A),** 10μM **(B),** 200μM **(C),** or 20μM **(D)** desferoxamine. Gels A and B, or C and D were compared for changes in protein expression. Ten micrograms protein sample was rehydrated onto 7cm IPG strips, pH 3-10 and separated in the 1st dimension (pI) for 28 497Vhrs. The 2nd dimension was resolved on a 10% SDS-PAGE gel and stained with SYPRO Ruby. The circled protein spot represents hHBP with the net intensity of each protein spot determined by PDQuest indicated on each gel. Molecular mass standards are indicated in kilodaltons (kDa). Trial 1 experiments were performed on September 9, 2005.

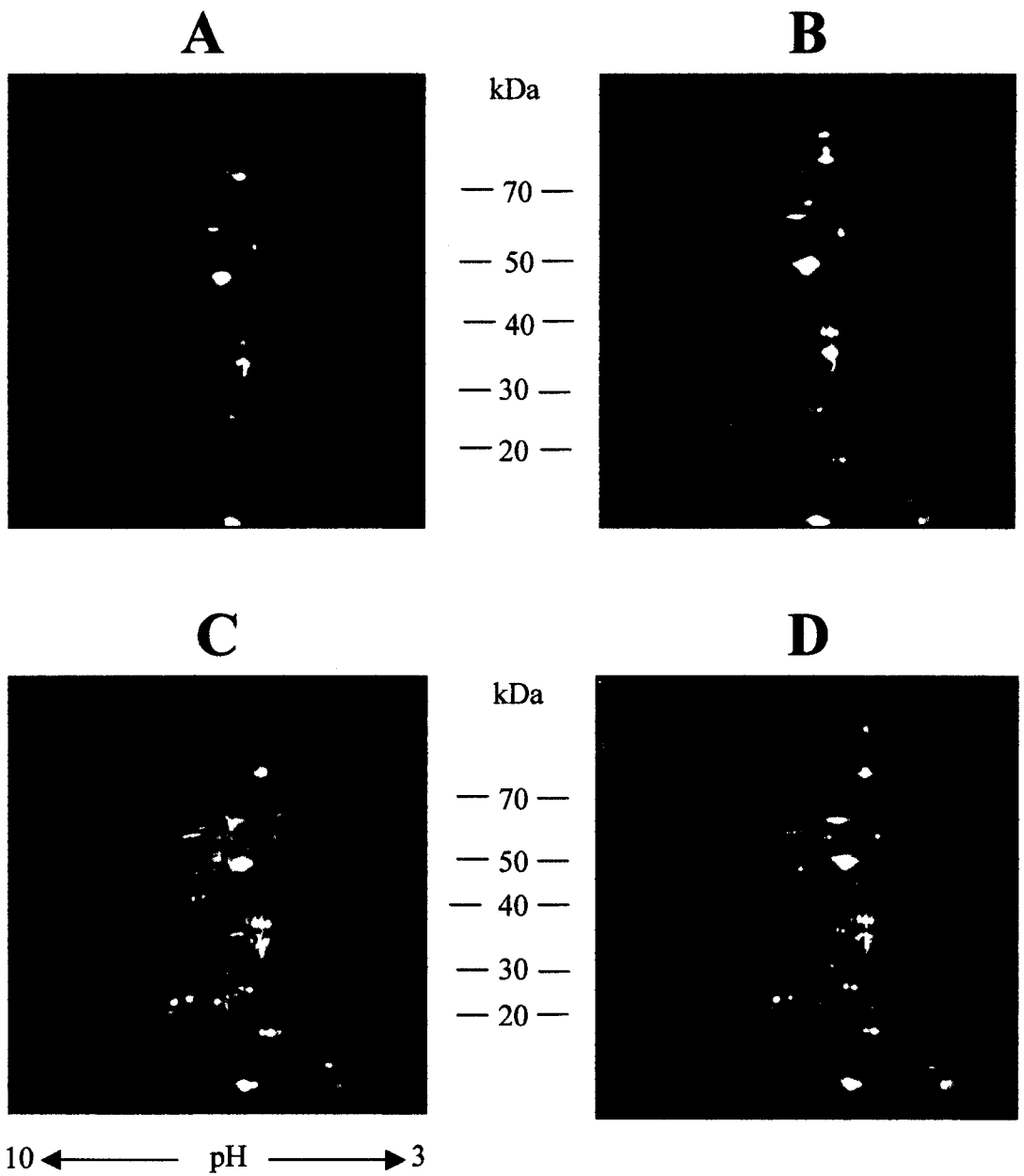

antiserum. An increase in the amount of hHBP was seen in periplasmic extracts derived from cells grown under heme-limiting compared to heme-replete conditions (Figure 26B). In contrast, there was no increase in intensity of the hHBP immunoreactive band in preparations containing desferoxamine compared to extracts without the iron chelator. In addition, increasing the concentration of desferoxamine did not influence the expression of hHBP. These results confirm that the expression of hHBP is enhanced under heme-limiting conditions, and the expression of hHBP is not regulated by iron.

3.9 Distribution of hHBP in Clinical Strains of *H. ducreyi*, *H. influenzae* and *Y. entercolitica*

To determine whether hHBP was present and expressed in other strains of *H. ducreyi* and in *H. influenzae* and *Y. entercolitica*, PCR amplification using hHBP-specific primers and genomic DNA from the above bacteria as well as Western blots of whole cell lysates probed with anti-hHBP polyclonal antiserum were performed. A PCR product of the expected size (940bp) was generated from all geographically diverse and serogroup distinct *H. ducreyi* clinical isolates (Figure 27, Table 1). In contrast, no amplicon was obtained from the *H. influenzae* or *Y. entercolitica* clinical isolates (Figure 27A). Although the iron chelated ABC transporter periplasmic binding protein of *H. influenzae* and hHBP of *H. ducreyi* are 75% homologous in amino acid sequence, the oligonucleotide primers used for PCR amplification of an hHBP-specific band demonstrated only 4-5bp identity to this *H. influenzae* gene. Therefore, an amplicon was not expected for the *H. influenzae* isolates. In Western blots of whole cell lysates from these same clinical isolates, hHBP-specific immunoreactive bands were seen in all *H. ducreyi* and *H. influenzae* isolates (Figure 27C). Although there were several higher molecular weight immunoreactive bands present on the Western blots, these non-specific immunoreactive bands most likely resulted from the

Figure 26. 1D SDS-PAGE gel analysis determining iron regulation of hHBP.

Periplasmic proteins of *H. ducreyi* 35 000 grown under heme-limiting **(H-L)** conditions or heme-replete **(H-R)** conditions with various concentration of desferoxamine (concentrations are indicated above each lane) were extracted using the chloroform method. Four micrograms of each protein sample was separated by a 12% 1D SDS-PAGE gel **(A)**. Molecular mass standards are indicated in kilodaltons (kDa). The Western immunoblot **(B)** was probed with anti-hHBP polyclonal antiserum. Affinity-purified rhHBP (2μg) was used as a positive control for Western blot probing. The filled arrow indicates the mature (~31kDa) hHBP protein bands.

A

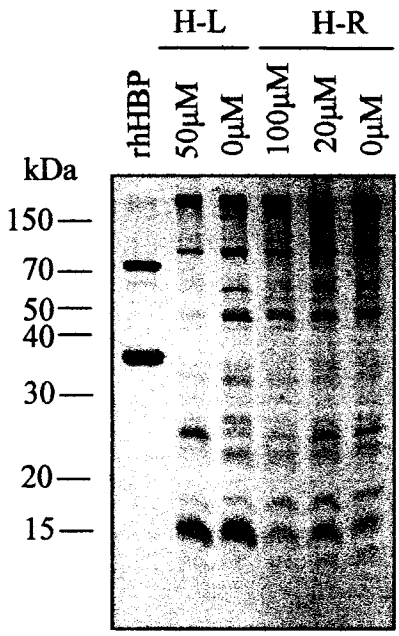

B

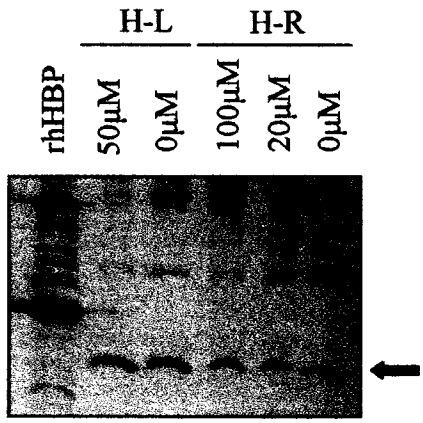

Figure 27. Presence of hHBP in clinical strains of *H. ducreyi*, *H. influenzae* and *Y. entercolitica*.

A: Genomic DNA from clinical strains of *H. ducreyi* **(HD)**, *H. influenzae* **(HI)**, and *Y. entercolitica* **(YE)** was PCR amplified using the hHBP-specific primers used for pET151 vector cloning. PCR reactions were separated on a 1% agarose gel and stained with ethidium bromide. The open arrow indicates the 940bp PCR amplicon. NC represents the negative control where no template DNA was added to the PCR reaction.
B&C: Five micrograms of whole cell lysate from each clinical isolate was separated by a 12% SDS-PAGE gel **(B)** and Western immunoblotted **(C)**. Blots were probed with anti-hHBP polyclonal antiserum with affinity-purified rhHBP (1μg) run as a positive control. Each SDS-PAGE gel has its corresponding Western blot directly below in panel C. Filled arrows indicate hHBP-specific immunoreactive bands representative of the immature (~33kDa) and mature (~31kDa) form of the monomer and a possible degradation product (~28kDa). Molecular mass standards are indicated in kilodaltons (kDa).

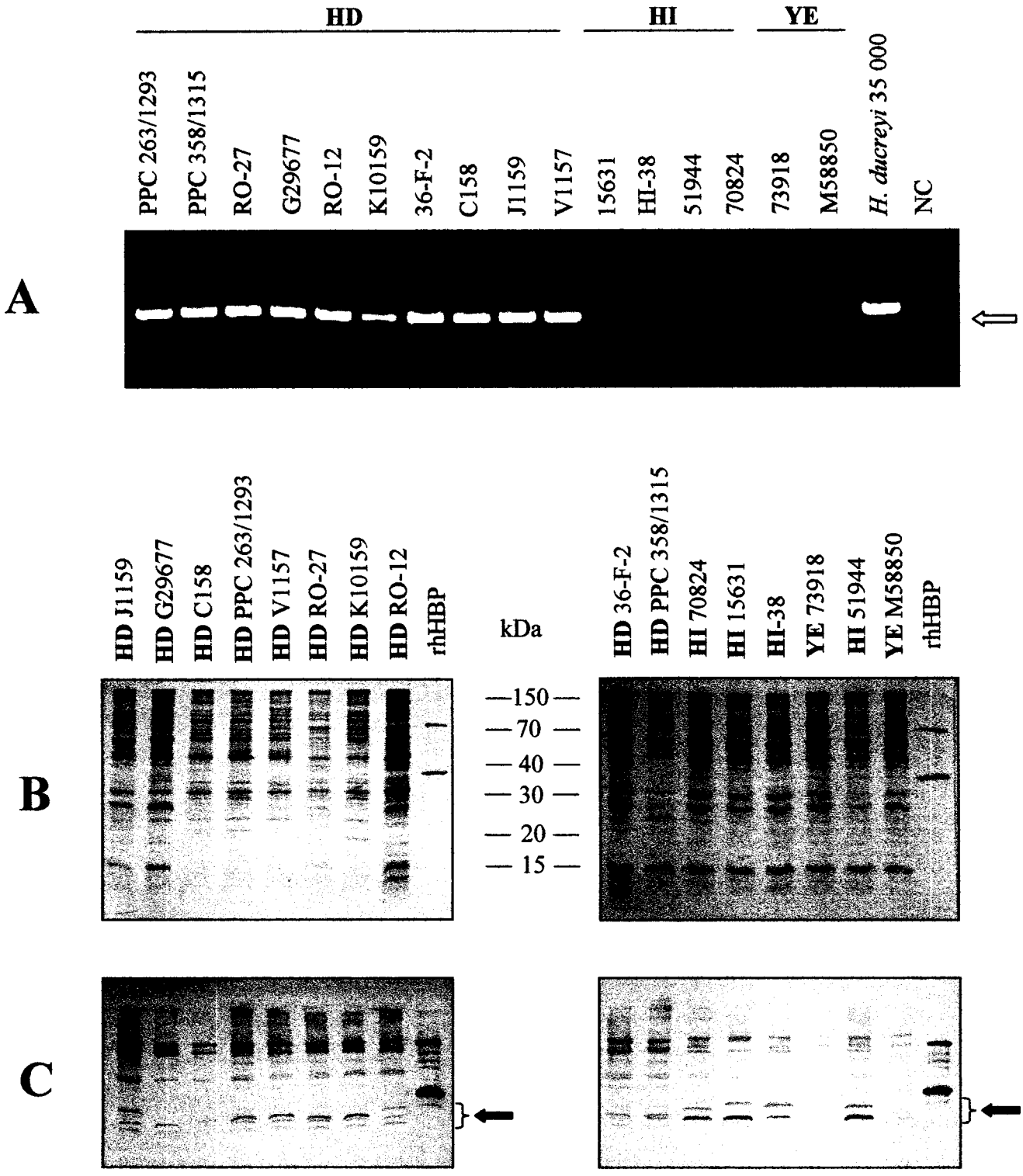

procedure used for anti-hHBP production as previously discussed (see Section 3.6). Two to three hHBP-specific immunoreactive bands were present in all *H. ducreyi* isolates and represent the sizes of both the mature (~31kDa) and immature (~33kDa) forms of the hHBP monomer. The third immunoreactive band was ~28kDa and could represent a degradation product of the monomer or an *H. ducreyi* protein expressing a sequence present in the fusion tag. This ~28kDa bands was also present in all *H. influenzae* isolates. Interestingly, the immunoreactive band ~31kDa corresponding in size to the hHBP monomer was present in the four *H. influenzae* isolates. No hHBP-specific immunoreactive bands were present in both the *Y. entercolitica* clinical isolates tested. These results indicated that hHBP was conserved among *H. ducreyi* strains and also suggests that a similar protein was expressed in *H. influenzae*.

CHAPTER FOUR

DISCUSSION

4.1 Our Experimental Approach

The current study is the first to identify and functionally characterize by biochemical methods a heme-dedicated periplasmic binding protein in *H. ducreyi*. In addition, our approach using proteomics, particularly 2D gel analysis, to determine function prior to identification of the heme regulated protein was unique both to our laboratory and to the literature. With regards to the 2D gel work done on *H. ducreyi*, the only previous study done involves the identification of proteins in whole cell lysates to determine differences in protein profiles among a variety *H. ducreyi* strains [194]. Formerly in our laboratory, both genetic and biochemical approaches were used in order to interrogate the genome of *H. ducreyi* for a putative heme ABC transporter system with little success [203]. For the genetic approach, BLAST and conserved domains searches were used to interrogate ORFs found upstream and downstream of the genes encoding both the heme and hemoglobin outer membrane receptors of *H. ducreyi* to no avail. However, this method had limitations as ABC transporters are not always contiguous to genes encoding their outer membrane counterpart. For the biochemical method, heme affinity chromatography was used to identify the periplasmic heme binding protein from periplasmic extracts. However, the hydrophobic property of heme resulted in the non-specific interaction of proteins to the heme affinity matrix. The most abundant protein isolated using this method was the elongation factor Tu [203]. Elongation factor Tu was also demonstrated as an abundant protein in 2D gel analysis in the present study (Figure 8, Appendix I). What is also evident from 2D gel analysis in this study (Figure 8, Appendix I) and a prior 2D gel analysis of *H. ducreyi* whole cell lysates

[194] is that hHBP is not an abundant protein in the periplasmic space. Therefore, the unsuccessful attempts to isolate hHBP in our laboratory by heme affinity chromatography were due to its low abundance in periplasmic extracts and the excessive binding of non-specific proteins to the heme agarose column.

Little is known about heme transport in both *H. ducreyi* and other bacteria. Most of the research information available about heme transport involves generalizations arising from iron transport or from genetic information based on protein sequence and homology. Comparing 2D gel periplasmic protein profiles of *H. ducreyi* 35 000 grown under heme-limiting and heme-replete conditions allowed for the determination of candidate proteins whose expression was upregulated when heme was restricted. This approach had the selective advantage of narrowing potential candidates to those exhibiting this predicted characteristic of a protein involved in heme transport. This targeted downstream genetics work to genes that had a greater potential of encoding the heme transporter. In addition, the genome of *H. ducreyi* 35 000 has been sequenced, allowing for its interrogation for homologous protein identification by mass spectroscopy. Due to the success of this proteomics technique as an identification tool, it is being applied in our laboratory to determine the identity of heme transporters in *N. meningitidis*.

While 2D gel analysis does have its pitfalls, none have posed significant problems for our analysis. Because of the complexity of protein samples analyzed by 2D gel electrophoresis, the identification of proteins expressed at low levels may be obscured. This potential obstacle was addressed by focusing our analysis on the specific subcellular subset of periplasmic proteins. The use of the highly sensitive stain, SYPRO Ruby, a ruthenium-based fluorescence stain able to detect protein concentrations as low as 1-2ng, assisted in the quantitative determination of differences in proteins expression under the surveyed

conditions [217]. The recognized solubility and restricted pI range of characterized periplasmic proteins are important properties that enhanced their 1st and 2nd dimensional separation and recovery [190]. The majority of proteins in our periplasmic preparations were within the center of the pH separation range with few outliers at the left or right sides of the gel (Figures 8 and 25, Appendices I and II). As the net intensity changes measured by densitometry is user-dependent, gels were analyzed in pairwise comparisons in which photographs and net intensities were assessed at the same exposure. All of the three pairwise comparisons were performed in duplicate to ensure reproducibility.

In our study, we did exploit techniques used by other investigators to determine heme binding specificity of hHBP. Heme affinity chromatography using heme immobilized on agarose beads has been previously used to determine the heme-binding ability of many proteins including the heme receptor, TdhA, in *H. ducreyi* [113]. This methodology has also been used to determine heme binding ability of outer membrane receptors and extracellular heme binding proteins in other pathogenic bacteria [218- 22]. Other investigators have used 6xHis tagged recombinant purified protein to demonstrate heme binding [205,223]. However, because histidine residues often serve as the axial ligands in heme binding [143], the presence of the uncleaved 6xHis tag linked to rhHBP raised the possibility that the binding specificity of rhHBP to heme was mediated by this N-terminal extension. To address this possibility, rLip32, a *Leptospira* outer membrane polyhisidine fusion protein, was pre-incubated with heme in a competition binding assay. No dose-dependent binding was observed (Figure 20) indicating that the histidine tag was not responsible for the interaction of the rhHBP with heme.

4.2 Heme Transport in *H. ducreyi*

Heme transport across the periplasmic space in *H. ducreyi* and other *Haemophilus* species is poorly understood [146]. In *H. ducreyi*, two TonB-dependent outer membrane receptors have been identified and functionally demonstrated to bind heme (TdhA receptor) or hemoglobin (HgbA receptor)[113,179]. Interestingly, a *tdhA/hgbA* double knockout was still able to transport heme across the outer membrane [113]. Therefore, it has been proposed that there is also a separate TonB-independent mechanism for heme acquisition [179]. Because *H. ducreyi* is a heme-obligate bacterium and requires a higher amount of heme as compared to other heme-obligate organisms, it is logical that *H. ducreyi* would have several pathways for heme acquisition. However, once heme is transported across the outer membrane, little is known about its fate. The present study begins to unravel intracellular heme transport once heme is deposited into the periplasmic space of *H. ducreyi* by identifying and functionally characterizing a periplasmic heme-binding protein in this organism. We demonstrated that hHBP was consistently upregulated under heme-limiting conditions; however, its expression was not influenced by the addition of exogenous iron as the amount of hHBP, as demonstrated by 2D gel analysis, did not vary when *H. ducreyi* was grown in the presence of increasing concentrations of the iron chelator desferoxamine (Figure 25, Appendix II). The molecular mass of the immature and mature hHBP is consistent with that of other periplasmic binding proteins found in Gram-negative bacteria, including those involved in heme and iron transport [123,163,165,167,168,205]. The BLAST-P interrogation of the gene encoding the *H. ducreyi* hHBP predicted a gene product with a molecular mass of ~33kDa and PSORT predicted a cleaved N-terminal signal sequence tag allowing for transport to the periplasm [224]. The projected cleavage site was between amino acids 24 and 25, resulting in a predicted mature protein of ~31kDa. N-

terminal sequence analysis of the hHBP protein present in the periplasm of *H. ducreyi* would corroborate the amino acid cleavage site. Our experimental evidence confirmed a mature hHBP protein of approximately 31kDa localized to the periplasm probed with anti-hHBP rabbit polyclonal antiserum (Figure 11). We demonstrated that affinity-purified rhHBP interacted specifically with heme as reflected in the concentration dependent binding to heme agarose (Figures 17). The binding to the matrix bound heme was competitively inhibited by increasing concentrations of free heme (Figures 19). Furthermore, two lines of evidence indicate that the recognition of the tetrapyrrole ring of heme underlies the binding. First, protoporphyrin IX, which comprises a porphyrin ring devoid of the central iron moiety, competitively inhibited binding of rhHBP to the immobilized heme (Figure 21). Second, in similar competitive binding assays, Zn-PPIX, a non-iron metalloporphyrin, was capable of abrogating the interaction of rhHBP to the heme agarose (Figure 24). This demonstrated that substitution of the central chelated metal ion did not alter the binding specificity of rhHBP to heme.

Following our characterization of a heme-dedicated periplasmic binding protein in *H. ducreyi*, the first obvious next step would be the construction of an hHBP isogenic mutant to test its ability to utilize heme sources. However, this may not be achievable as *H. ducreyi* is a heme-obligate organism and knocking out a potentially key component of this uptake pathway could prove lethal. If this is the case, there are several possible ways to deal with this issue. Firstly, growing *H. ducreyi* under anaerobic conditions eliminates its requirement for heme [115,179]. This would allow for selection of hHBP mutants. As well, the heme transport system of *Y. entercolitica* has been well characterized and includes a heme uptake mutant library [225]. Therefore, functional complementation of a *Y. entercolitica* heme-dedicated periplasmic binding protein (*hemT*) mutant with hHBP could prove successful.

4.3 With Respect to Heme Transporters in Other Bacteria

High-affinity periplasmic binding proteins play two particularly significant roles in ligand uptake contributing to ligand specificity and selectivity [205]. These binding proteins also play a critical role in the release of the ligand to the remaining components of the ABC transport system. Several heme-dedicated periplasmic binding proteins have been identified in a variety of Gram-negative bacteria including ShuT, HemT, HmuT, PhuT, ChuT, HutB [146]. However, little functional characterization of these transport proteins has been performed. The proposed heme-binding property has been inferred from mutant analysis and from sequence homology to characterized proteins [226].

The hHBP protein identified in our study was homologous to iron or metal ion transport proteins (Figure 10). The highest homology was to a metal ion transport protein from *A. pleuropneumoniae* and to the iron (chelated) periplasmic binding proteins from *H. influenzae* and *Y. pestis* [224]. The lack of sequence homology to other periplasmic heme binding proteins is not surprising as little homology exists among these transporters [205, 146]. For example, the heme binding protein of *S. dysenteriae*, ShuT, shows no homology to other heme proteins and is most similar to vitamin B_{12} and iron-hydroxamate periplasmic binding proteins. ShuT has been shown to functionally bind heme and play a role in the heme ABC transport system in *S. dysenteriae* [205].

4.4 Putative Heme Transport Operon

Heme is transported across the periplasmic space to the inner membrane by a specific ABC transporter consisting of a periplasmic binding protein, a membrane-spanning permease, and an ATPase for active transport into the cytoplasm [146]. A functional heme-specific ABC transporter is necessary for heme acquisition in Gram-negative bacteria [146].

In our study, we have characterized a heme-dedicated periplasmic binding protein that is a component of a putative heme-specific transport operon in *H. ducreyi* consisting of four genes (Figure 9). A lone putative promoter located immediately upstream of the first gene in the operon and a possible site for a transcriptional termination occurs after the final gene in the proposed operon. While two components of a typical ABC transporter are found in this operon – hHBP and an ATP-binding protein – the remaining genes do not have qualities resembling a prototypical ABC transporter. The protein encoded by ORF-1 is a putative inner membrane protein but does not have any of the classic features of a permease [146]. Although the ATPase component is the most conserved unit of an ABC transporter, the nucleotide sequence of permeases are not as conserved [206]. A conserved motif among permeases, "EAA", located about 100 amino acid residues from the C-terminus is absent in ORF-1 [146]. Despite the absence of nucleotide motifs characteristic of permeases, ORF-1 exhibits several transmembrane spanning domains consistent with membrane proteins. It is interesting to note that the top twenty most homologous proteins as predicted by BLAST-P to this inner membrane protein were immediately followed by a sulfite reductase gamma subunit. This was demonstrated in our proposed operon as ORF-2 displays sequence homology to *dsvC* that encodes a dissimilatory desulfoviridin gamma subunit (DSG) in *Desulphorvibrio vulgaris*. The role of this protein in non-sulfate reducing bacteria remains elusive. The DsvC protein has been proposed to be involved in the assembly, folding or stabilization of sirohaem proteins in bacteria lacking a sulfite reductase such as *H. influenzae* and *E. coli* [211,213]. As *H. ducreyi* also lacks any genes homologous to the sulfite reductase enzyme complex, we speculate that the DSG protein may play a role in stabilizing the hHBP transport protein because *H. ducreyi* is a heme-obligate organism with a high heme requirement. Therefore, an extremely efficient heme transport system would be essential for

heme transport. DSG may possibly stabilize the interaction between the heme molecule and hHBP to meet this demand for high efficiency heme transport.

Genes homologous to ORF-1 and ORF-2 are components of the proposed iron ABC transporter operons in *H. somnus* and *Pasteurella multocida*. In these operons, these two genes were in addition to the genes encoding a periplasmic binding protein, an ATP-binding protein, and two permease proteins. It is interesting that the *H. ducreyi* 35 000 does not have these two permease genes in the operon identified in our study. *H. ducreyi* 35 000 is a laboratory strain and the lack of the permease gene could be a result of excessive *in vitro* passaging in an environment where heme is not limited as seen in the human host.

Many heme transport systems are under the transcriptional regulation of the ferric uptake regulator protein (Fur) [227,151,153] whereby Fur acts as a transcriptional repressor in response to intracellular iron levels. The Fur protein employs Fe^{2+} as a co-repressor and directly binds to highly conserved target palindromic DNA sequences, Fur boxes, in iron-regulated promoters blocking gene transcription [227]. Although *H. ducreyi* possesses a functional Fur system, Fur boxes are not present in the promoter of the proposed heme-specific transport operon [228].

In future work, it would be interesting to investigate the function of each gene in the proposed heme transport operon. In addition, confirmation that the genes are transcribed as a single transcriptional unit can be achieved by real-time reverse transcriptase PCR. Elucidating the role of *dsvC* in the putative heme transport operon via a targeted knockout using the aphA::kan cassette that allows for the construction of a non-polar mutation in *dsvC* would be instructive. It would also be interesting to determine if one or more permease genes are present in the proposed heme transport operon in other strains of *H. ducreyi*.

4.5 hHBP's Expression in Clinical Isolates of *H. ducreyi* and Other Gram-negatives

In a survey of selected *H. ducreyi* clinical isolates, Western immunoblot and PCR amplification experiments indicated that hHBP is likely ubiquitous among *H. ducreyi* strains and that the expressed protein is structurally conserved (Figure 27). This is not surprising because *H. ducreyi* is a heme-obligate organism and heme acquisition systems would be expected to be highly conserved in this organism. In addition, because of the ubiquity of hHBP among *H. ducreyi* isolates, hHBP would represent a potentially powerful target for drug therapy including metalloporphyrins. Our results indicated that hHBP is able to bind to a non-iron metalloporphyrin, Zn-PPIX (Figure 24). Zn-PPIX and Ga-PPIX both possess antibacterial properties against *H. ducreyi* as well as other pathogenic bacteria such as *Y. entercolitica*, *N. gonorrheae* and methicillin-resistant *S. aureus*. Metalloporphyrins enter these bacteria via the heme uptake pathway [195,196] and therefore poses no barrier functions, i.e., bacterial membranes can restrict the function of some antimicrobials. It should be noted that most pathogenic bacteria possess this uptake system at its maximal expression due to the heme-limiting conditions existing in the human host [229].

No amplicon corresponding to the gene encoding hHBP was amplified in *H. influenzae* or *Y. entercolitica* clinical isolates (Figure 27); however, an immunoreactive band corresponding in size to hHBP was identified in all *H. influenzae* on Western immunoblot. This suggested that a structurally related protein was expressed in *H. influenzae.* The discrepancy between the PCR amplification and Western immunoblot data for *H. influenzae* was expected. Although the amino acid sequence of hHBP and the iron chelated ABC transporter periplasmic binding protein of *H. influenzae* are 75% homologous, the oligonucleotide primers used for the PCR amplification contained only 4-5bp of identity to

the *H. influenzae* gene making PCR amplification of an hHBP-specific band unlikely [230]. Thus, it would be of interest to sequence this ~31kDa immunoreactive band present in all *H. influenzae* isolates probed with anti-hHBP polyclonal antiserum and determine its function in relation to heme acquisition in this bacterium.

4.6 Conclusions

In our study, we have identified a heme-dedicated periplasmic binding protein in *H. ducreyi*, hHBP, whose expression is enhanced under heme-limiting conditions. hHBP was able to specifically bind heme in a concentration dependent manner. Although hHBP was shown to recognize the porphyrin ring of the heme molecule, hHBP had no binding specificity for iron. Finally, hHBP was ubiquitous and structurally conserved among *H. ducreyi* clinical isolates.

REFERENCES

1. **Lewis, D.A.** 2000. Chancroid: from clinical practice to basic science. AIDS Patient Care and STDs. **14:**19-36.

2. **Sturm, A.W., and H.C. Zonen.** 1984. Characteristics of *Haemophilus ducreyi* in culture. J. Clin. Microbiol. **19:**672-674.

3. **De Ley, J., W. Mannheim, R. Mutters, K. Peichulla, R. Tytgat, P. Segers, M. Bisgaard, W. Frederiksen, K.-H. Hinz, and M. Vanhoucke.** 1990. Inter- and intrafamilial similarities of rRNA cistrons of the Pasteurellaceae. Int. J. Syst. Bacteriol. **40:**126-137.

4. **Dewhirst, F.E., B.J. Paster, I. Olsen, and G.J. Fraser.** 1992. Phylogeny of 54 representative strains of species in the family Pasteurellaceae as determined by comparison of 16S rRNA sequences. J. Bacteriol. **174:**2002-2013.

5. **Spinola, S.M., M.E. Bauer, and R.S. Munson.** 2002. Immunopathogenesis of *Haemophilus ducreyi* infection (chancroid). Infect. Immun. **70:**1667-1676.

6. **Lagergard, T.** 1995. *Haemophilus ducreyi*: pathogenesis and protective immunity. Trends Microbiol. **3:**87-92

7. **Trees, D.L., and S.A. Morse.** 1995. Chancroid and *Haemophilus ducreyi*: an update. Clin. Microbiol. Rev. **8:**357-375.

8. **Trees, D.L., R.J. Arko, G.D. Hill, and S.A. Morse.** 1992. Laboratory-acquired infection with *Haemophilus ducreyi* type-strain CIP 542. Med. Microbiol. Lett. **1:**330-337.

9. **Elkins, C., K. Yi, B. Olsen, C. Thomas, K. Thomas, and S. Morse.** 2000. Development of a serological test for *Haemophilus ducreyi* for seroprevalence studies. **38:**1520-1526.

10. **Morse, S.A.** 1989. Chancroid and *Haemophilus ducreyi*. Clin. Microbiol. Rev. **2:**137-157.

11. **Lewis, D.A.** 2003. Chancroid: clinical manifestations, diagnosis, and management. Sex. Transm. Infect. **79:**68-71.

12. **Ronald, A.R., and W. Albritton.** 1984. Chancroid and *Haemophilus ducreyi*, p.385-393. *In* K.K. Holmes, P.A. Mardh, P.F. Sparling, and P.J. Weisner (ed.), Sexually transmitted diseases. McGraw-Hill Book Co., New York, NY.

13. **Hammond, G.W.** 1996. A history of the detection of *Haemophilus ducreyi*, 1889-1979. Sex. Transm. Dis. **23:**93-96.

14. **Al-Tawfiq, J.A. and S.M. Spinola.** 2002. *Haemophilus ducreyi*: clinical disease and pathogenesis. Curr. Opin. Infect. Dis. **15:**43-47.

15. Joint United Nations Programme on HIV/AIDS (UNAIDS). Sexually transmitted diseases: policies and principles for prevention and care. New York: World Health Organization. Available at: http://data.unaids.org/Publications/IRC-pub04/una97-6_en.pdf.

16. **Morse, S.A., D.L. Trees, Y. Htun, F. Radebe, K.A. Orle, Y. Dangor, C.M. Beck-Sague, S. Schmid, G. Fehler, J.B. Weiss, and R.C. Ballard.** 1997. Comparison of clinical diagnosis and standard laboratory and molecular methods for the diagnosis of genital ulcer disease in Lesotho: association with human immunodeficiency virus infection. J. Infect. Dis. **175:**583-589.

17. **Risbud, A., K. Chan-Tack, D. Gadkari, R.R. Gangakhedkar, M.E. Shepherd, R. Bollinger, S. Mehendale, C. Gaydos, A. Divekar, A. Rompalo, and T.C. Quinn.** 1999. The etiology of genital ulcer dieses by multiplex polymerase chain reaction and relationship to HIV infection among patients attending sexually transmitted disease clinics in Pune, India. Sex. Transm. Dis. **26:**55-62.

18. **Totten, P.A., J.M. Kuypers, C. Chen, M.J. Alfa, L.M. Parsons, S.M. Dutro, S.A. Morse, and N.B. Kiviat.** 2000. Etiology of Genital Ulcer Disease in Dakar, Senegal, and Comparison of PCR and Serologic Assays for Detection of *Haemophilus ducreyi*. J. Clin. Microbiol. **38:**268-273.

19. **Behets, F.M., A.R. Brathwaite, T. Hylton-Kong, C.Y. Chen, I. Hoffman, J.B. Weiss, S.A. Morse, G. Dallabetta, M.S. Cohen, and J.P. Figueroa.** 1999. Genital ulcers: etiology clinical diagnosis, and associated human immunodeficiency virus infection in Kingston, Jamaica. Clin. Infect. Dis. **28:**1086-1090.

20. **Chen, C.Y., R.C. Ballard, C.M. Beck-Sague, Y. Dangor, F. Radebe, S. Schmid, J.B. Weiss, V. Tshabalala, G. Fehler, Y. Htun, and S.A. Morse.** 2000. Human immunodeficiency virus infection and genital ulcer disease in South Africa: the herpetic connection. Sex. Transm. Dis. **27:**21-29.

21. **Piot, P., and F.A. Plummer.** 1990. Genital ulcer adenopathy syndrome, p. 711-716. *In* K.K. Holmes, P.A. Mardh, P.F. Sparling, P.J. Weisner, W. Cates Jr., S.M. Lemon, and W.E. Stamm (ed.), Sexually Transmitted Diseases, 2nd ed. McGraw-Hill Inc., New York, NY.

22. **Mertz, K., J.B. Weiss, R.M. Webb, W.C. Levine, J.S. Lewis, K.A. Orle, P.A. Totten, J. Overbaugh, S.A. Morse, M.M Currier, M. Fishbein, and M.E. St. Louis**. 1998. An investigation of genital ulcers in Jackson, Mississippi, with use of a multiplex polymerase chain reaction assay: high prevalence of chancroid and human immunodeficiency virus infection. J. Infect. Dis. **178:**1060-1066.

23. **Hammond, G.W., K. Slutchuk, J. Scatliff, E. Sherman, J.C. Wilt, and A.R. Ronald.** 1980. Epidemiologic, clinical, laboratory, and therapeutic features of an urban outbreak of chancroid in North America. Rev. Infect. Dis. **2:**867-879.

24. **Bruisten, S.M, I. Cairo, H. Fennema, A. Pijl, M. Buimer P.G.H. Peerbooms, E. Van Dyck, A. Meijer, J.M. Ossewaarde, and G.J.J. van Doormum.** 2001. Diagnosing genital ulcer disease in a clinic for sexually transmitted diseases in Amsterdam, the Netherlands. J. Clin. Microbiol. **39:**601-605.

25. **Blackmore, C.A., K. Limpakarnjanarat, J.G. Rigau-Perez, W.L. Albritton, and J.R. Greenwood.** 1985. An outbreak of chancroid in Orange County, California: descriptive epidemiology and disease control measures. J. Infect. Dis. **151:**840-844.

26. **Brandt, A.M.** 1987. No magic bullet: a social history of venereal disease in the United States since 1880. Oxford University Press, New York, NY.

27. **Steen, R.** 2001. Eradicating chancroid. Bull. World Health Organ. **79:**818-826.

28. **Brunham, R.C., and A.R. Ronald.** 1991. Epidemiology of sexually transmitted diseases in developing countries, p.61-80. *In* J.N. Wasserheit, S.O. Aral, K.K. Holmes, and P.F. Hitchcock (ed.), Research issues in human behavior and sexually transmitted diseases in the AIDS era, ASM Press, Washington, DC.

29. **Chitwarakorn, A., W. Sittitrai, T. Brown, and D. Mugrditchian.** 1998. Thailand, p. 305-338. *In* T. Brown (ed.), Sexually transmitted diseases in Asia and the Pacific. Venereology Publishing, Armidale, New South Wales, Australia.

30. **Traisupa, A., B. Mokamakkul, and C. Ariyarit.** 1992. Epidemiological treatment of chancroid in female sex-workers in Bangkok. J. Health Science. **1:**363-341.

31. **Dicarlo, R.P., B.S. Armentor, and D.H. Martin.** 1995. Chancroid epidemiology in New Orleans men. J. Infect. Dis. **172:**446-452.

32. **Tyndall, M., M. Malisa, F.A. Plummer, J. Ombetti, J.O. Ndinya-Achola, and A.R. Ronald.** 1993. Ceftriaxone no longer predictably cures chancroid in Kenya. J. Infect. Dis. **167:**469-471.

33. **King, R., S.H. Choudhri, J. Nasio, J. Gough, N.J.D. Nagelkerke, F.A. Plummer, J.O. Ndinya-Achola, and A.R. Ronald.** 1998. Clinical and *in situ* cellular responses to *Haemophilus ducreyi* in the presence or absence of HIV infection. Int. J. STD AIDS **9:**531-536.

34. **Abeck, D., H.C. Korting, M. Kollman, A.P. Johnson, R.C. Ballard, and H. Mensing.** 1992. Lack of immunoglobulin A1 protease production by *Haemophilus ducreyi*. Zentralbl. Bakteriol. **277:**34-38.

35. **Quale, J., E. Teplitz, and M. Augenbraun.** 1990. Atypical presentation of chancroid in a patient infected with the human immunodeficiency virus. Am. J. Med. **88:**43-44.

36. **Chapel, T.A., W.J. Brown, C. Jeffries, and J.A. Stewart.** 1977. How reliable is the morphological diagnosis of penile ulcerations? Sex. Transm. Dis. **4:**150-152.

37. **Dangor, Y., R.C. Ballard, F. da L. Exposto, G. Fehler, S.D. Miller, and H.J. Koornhof.** 1990. Accuracy of clinical diagnosis of genital ulcer disease. Sex. Transm. Dis. **17:**184-189.

38. **Dangor, Y., S.D. Miller, H.J. Knoornhof, and R.C. Ballard.** 1992. A simple medium for the primary isolation of *Haemophilus ducreyi*. Eur. J. Clin. Microbiol. Infect. Dis. **11:**930-934.

39. **Dangor, Y., F. Radebe, and R.C. Ballard.** 1993. Transport media for *Haemophlius ducreyi*. Sex. Transm. Dis. **20:**5-9.

40. **Johnson, S.R., D.H. Martin, C. Cammarata, and S.A. Morse.** 1995. Alterations in sample preparation increase sensitivity of PCR assay for diagnosis of chancroid. J. Clin. Microbiol. **33:**1036-1038.

41. **MacDonald, K., W. Cameron, G. Irungu, L.J. D'Costa, F.A. Plummer, L.A. Slaney, J.O. Ndinya-Achola, and A.R. Ronald**. 1989. Comparison of Sheffield media with standard media for the isolation of *Haemophilus ducreyi*. Sex. Transm. Dis. **16:**88-90.

42. **Lockett, A.E., D.A.B. Dance, D.C.W. Mabey, and B.S. Drasar.** 1991. Serum-free media for the isolation of *Haemophilus ducreyi*. Lancet **338:**326.

43. **Totten, P.A., and W.E. Stamm.** 1994. Clear broth and plate media for culture of *Haemophilus ducreyi*. J. Clin. Microbiol. **32:**2019-2023.

44. **Dziuba, M., P.A. Noble, and W.L. Albritton.** 1993. A study of the nutritional requirements of a selected *Haemophilus ducreyi* strain by impedance and conventional methods. Curr. Microbiol. **27:**109-113.

45. **Pillay, A., A.A. Hoosen, D. Loykissoonlal, C. Glock, B. Odhav, and A.W. Sturm.** 1998. Comparison of culture media for the laboratory diagnosis of chancroid. J. Med Microbiol. **47:**1023-1026.

46. **Jones, C., T. Rosen, J. Clarridge, and S. Collins.** 1990. Chancroid: results form an outbreak in Houston, Texas. South. Med. J. **83:**1384-1389.

47. **Hammond, G.W., C.-J. Lian, J.C. Wilt, and A.R. Ronald.** 1978. Comparison of specimen collection and laboratory techniques for isolation of *Haemophilus ducreyi.* J. Clin. Microbiol. **7:**39-43.

48. **Parsons, L.M., A.L. Waring, J. Otido, and M. Shayegani.** 1995. Laboratory diagnosis of chancroid using species-specific primers from *Haemophilus ducreyi groEL* and the polymerase chain reaction. Diagn. Microbiol. Infect. Dis. **23:**89-98.

49. **Chui L., W. Albritton, B. Paster, I. Maclean, and R. Marusyk.** 1993. Development of the polymerase chain reaction for diagnosis of chancroid. J. Clin. Microbiol. **31:**659-664.

50. **West, B., S.M. Wilson, J. Changalucha, S. Patel, P. Mayaud, R.C. Ballard, and D. Mabey.** 1995. Simplified PCR for detection of *Haemophilus ducreyi* and diagnosis of chancroid. J. Clin. Microbiol. **33:**787-790.

51. **Roesel, D.J., L. Gwanzura, P.R. Mason, M. Joffe, and D.A. Katzenstein.** 1998. Polymerase chain reaction detection of *Haemophilus ducreyi* DNA. Sex. Transm. Infect. **74:** 63-65.

52. **Gu, X.X., R. Rossau, G. Jannes, R. Ballard, M. Laga, and E. Van Dyck.** 1998. The *rrs* (16S)-*rrl* (23S) ribosomal intergenic spacer region as a target for the detection of *Haemophilus ducreyi* by a heminested-PCR assay. Microbiology. **144:**1013-1019.

53. **Johnson, S.R., D.H. Martin, C. Cammarata, and S.A. Morse.** 1994. Development of a polymerase chain reaction assay for the detection of *Haemophilus ducreyi*. Sex. Transm. Dis. **21:**13-23.

54. **Orle, K.A., C.A. Gates, D.H. Martin, B.A. Body, and J.B. Weiss.** 1996. Simultaneous PCR detection of *Haemophilus ducreyi*, *Treponema pallidum* and herpes simplex virus types 1 and 2 from genital ulcers. J. Clin. Microbiol. **34:**49-54.

55. **Karim, Q.N., G. Finn, C.S.F. Easmon, Y. Dangor, D.A.B. Dance, Y.F. Ngeow, and R.C. Ballard.** 1989. Rapid detection of *Haemophilus ducreyi* in clinical and experimental infections using monoclonal antibody: a preliminary evaluation. Genitourin. Med. **65:**361-365.

56. **Ahmed, H.J., S. Borrelli, J. Jonasson, L. Eriksson, S. Hanson, B. Höjer, M. Sunkuntu, E. Musaba, E.L. Roggen, T. Lagergard, and A.A. Lindberg.** 1995. Monoclonal antibodies against *Haemophilus ducreyi* lipooligosaccharide and their diagnostic usefulness. Eur. J. Clin. Microbiol. Infect. Dis. **14:**892-898.

57. **Parsons, L.M., A.L. Waring, M. Shayegani, and L.H. Bopp.** 1989. DNA probes for the identification of *Haemophilus ducreyi*. J. Clin. Microbiol. **27:**1441-1445.

58. **Museyi, K., E. van Dyck, T. Vervoort, D. Taylor, C. Hoge, and P. Piot.** 1988. Use of an enzyme immunoassay to detect serum IgG antibodies to *Haemophilus ducreyi*. J. Infect. Dis. **157:**1039-1043.

59. **Alfa, M.J., N. Olson, P. Degagne, L. Slaney, F. Plummer, W. Namaara, and A.R. Ronald.** 1992. Use of an adsorption enzyme immunoassay to evaluate the *Haemophilus ducreyi* specific and cross-reactive humoral immune response of humans. Sex. Transm. Dis. **19:**309-314.

60. **Alfa, M.J., N. Olson, P. Degagne, F. Plummer, W. Namaara, I.Maclean, and A.R. Ronald.** 1993. Humoral immune response of humans to lipooligosaccharide and outer membrane proteins of *Haemophilus ducreyi*. J. Infect. Dis. **167:**1206-1210.

61. **Desjardins, M., C.E. Thompson, L.G. Filion, J.O. Ndinya-Achola, F.A. Plummer, A.R. Ronald, P. Piot, and D.W. Cameron.** 1992. Standardization of an enzyme immunoassay for human antibody to *Haemophilus ducreyi*. J. Clin. Microbiol. **30:**2019-2024.

62. **Greenblatt, R.M., S.A. Lukehart, F.A. Plummer, T.C. Quinn, C.W. Critchlow, R.L. Ashley, L.J. D'Costa, J.O. Ndinya-Achola, L. Corey, A.R. Ronald, et al.** 1988. Genital ulceration as a risk factor for human immunodeficiency virus infection. AIDS. **2:**47-50.

63. **Jessamine, P.G., and A.R. Ronald.** 1990. Chancroid and the role of genital ulcer disease in the spread of human retroviruses. Med. Clin. North Am. **74:**1417-1431.

64. **Plummer, F.A., J.N. Simonsen, D.W. Cameron, J.O. Ndinya-Achola, J.K. Kreiss, M.N. Gakinya, P. Waiyaki, M. Cheang, P. Piot, A.R. Ronald, and E.N. Ngugi.** 1991. Cofactors in male-female sexual transmission of human immunodeficiency virus type 1. J. Infect. Dis. **163:**233-239.

65. **Nelson, K.E., S. Eiumtrakul, D. Celentano, I. Maclean, A. Ronald, S. Suprasert, D.R. Hoover, S. Kuntolbutra, and J.M. Zenilman.** 1997. The association of herpes simplex virus type 2 (HSV-2), *Haemophilus ducreyi*, and syphilis with HIV infection in young men in northern Thailand. J. Acquir. Immune Defic. Syndr. Hum. Retrovirol. **16:**293-300.

66. **Dada, A.J., A.O. Ajayi, L. Diamondstone, T.C. Quinn, W.A. Blattner, and R.J. Biggar.** 1998. A serosurvey of *Haemophilus ducreyi*, syphilis, and herpes simplex virus 2 and their association with human immunodeficiency virus among female sex workers in Lagos, Nigeria. Sex. Transm. Dis. **25:**237-242.

67. **Kamali, A., A.J. Nunn, D.W. Mulder, E. van Dyck, J.G Dobbins, and J.A.G. Whitworth.** 1999. Seroprevalence and incidence of genital ulcer infections in a rural Ugandan population. Sex. Transm. Dis. **75:**98-102.

68. **Steen, R., and G. Dallabetta.** 2004. Genital ulcer disease control and HIV prevention. J. Clin. Virol. **29:**143-151.

69. **Gadkari, D.A., T.C. Quinn, R.R. Gangakhedkar, S.M. Mehendale, A.D. Divekar, A.R. Risbud, K. Chan-Tack, M. Shepherd, C. Gaydos, and R.C. Bollinger.** 1998. HIV-1 DNA shedding in genital ulcer and its associated risk factors in Pune, India. J. Acquir. Immune Defic. Syndr. Hum. Retrovirol. **18:**227-81.

70. **Kreiss, J.K., R. Coombs, F. Plummer, K.K. Holmes, B. Nikora, W. Cameron, E. Ngugi, J.O. Ndinya-Achola, and L. Corey.** 1989. Isolation of human immunodeficiency virus from genital ulcers in Nairobi prostitutes. J. Infect. Dis. **160:**380-384.

71. **Plummer, F.A., M.A. Wainberg, P. Plourde, P. Jessamine, L.J. D'Costa, I.A. Wamola, and A. R. Ronald.** 1990. Detection of human immunodeficiency virus type 1 (HIV-1) in genital ulcer exudates of HIV-1-infected men by culture and gene amplification. J. Infect. Dis. **161:**810-811. (Letter).

72. **Schacker, T., A.J. Ryncarz, J. Goddard, K. Diem, M. Shaughnessy, and L. Corey.** 1998. Frequent recovery of HIV-1 from genital herpes simplex virus lesions in HIV-1 infected men. JAMA. **280:**61-66.

73. **Humphreys, T.L., C.T. Schnizlein-Bick, B.P. Katz, L. Baldridge, A.F. Hood, R.A. Hromas, and S.M. Spinola.** 2002. Evolution of the cutaneous immune response to experimental *Haemophilus ducreyi* infection and its relevance to HIV-1 acquisition. J. Immunol. **169:**6316-6323.

74. **Behets, F.M.T., G. Liomba, G. Lule, G, Dalabetta, I.F. Hoffman, H.A. Hamilton, S. Moeng, and M.S. Cohen.** 1995. Sexually transmitted diseases and human immunodeficiency virus control in Malawi: a field study of genital ulcer disease. J. Infect. Dis. **171:**451-454.

75. **Ghys, P.D., K. Fransen, M.O. Diallo, V. Ettiegne-Traorev, I.-M. Coulibaly, K.M. Yeboue, M.L. Kalish, C. Maurice, J.P. Whitaker, A.E. Greenberg, and M. Laga.** 1997. The associations between cervicovaginal HIV shedding, sexually transmitted diseases and immunosuppression in female sex workers in Abidjan, Cote d'Ivoire. AIDS **11:**F85-F93.

76. **Dickerson, M.C., J. Johnston, T.E. Delea, A. White, and E. Andrews.** 1996. The causal role for genital ulcer disease as a risk factor for transmission of human immunodeficiency virus: an application of the Bradford Hill criteria. Sex. Transm. Dis. **23:**429-440.

77. **Schmid, G.P.** Treatment of chancroid, 1997. 1999. Clin. Infect. Dis. **28:**S14-S20.

78. **Jessamine, P.G., and R.C. Brunham.** 1990. Rapid control of a chancroid outbreak: implications for Canada. CMAJ. **142:**1082-1085.

79. **Martin, D.H., S.J. Sargent, G.D. Wendel Jr., W.M. McCormack, N.A. Spier, and R.B. Johnson.** 1995. Comparison of azithromycin and ceftriaxone for the treatment of chancroid. Clin. Infect. Dis. **2:**409-414.

80. **MacDonald, K.S., D.W. Cameron, L.J. D'Costa, J.O. Ndinya-Achola, F.A. Plummer, and A.R. Ronald.** 1989. Evaluation of fleroxacin (RO 23-6240) as single-oral-dose therapy of culture-proven chancroid in Nairobi, Kenya. Antimicrob. Agents Chemother. **33:**612-614.

81. **Annan, N.T., and D.A. Lewis.** 2005. Treatment of chancroid in resource-poor countries. Expert Rev. of Anti. Infect. Ther. **3:**295-306. (Summary).

82. **O'Farrell, N.** 1993. Soap and water prophylaxis for limiting genital ulcer disease and HIV-1 infection in men in sub-Saharan Africa. Genitourin Med. **69:**297-300.

83. **Ronald, A.R., and W. Albritton.** 1999. Chancroid and *Haemophilus ducreyi*, p. 515-524. *In* K.K Holmes, P.F. Sparling, P.-A. Mardh, S. Lemon, W. Stamm, P. Piot, and J.N. Wasserheit (ed.), Sexually transmitted diseases, 3rd ed. McGraw-Hill, New York, NY.

84. **Tyndall, M.W., A.R. Ronald, E. Agoki, W. Malisa, J.J. Dwayo, J.O. Ndinya-Achola, S. Moses, and F.A. Plummer.** 1996. Increased risk of infection with human immunodeficiency virus type 1 among uncircumcised men presenting with genital ulcer disease in Kenya. Clin. Infect. Dis. **23:**449-453.

85. **Dowdle, W.R.** 1998. The principles of disease elimination and eradication. Bull. World Health Organ. **75:**22-25.

86. **Bauer, M.E., M.P. Goheen, C.A. Townsend, and S.M. Spinola.** 2001. *Haemophilus ducreyi* associates with phagocytes, collagen, and fibrin and remains extracellular throughout infection of human volunteers. Infect. Immun. **69:**2549-2557.

87. **Gelfanova, V., T.L. Humphreys, and S.M. Spinola.** 2001. Characterization of *Haemophilus ducreyi*-specific T cell lines from lesions of experimentally infected human subjects. Infect. Immun. **69:**4224-4231.

88. **King, R., J. Gough, A. Ronald, J. Nasio, J.O. Ndinya-Achola, F. Plummer, and J.A. Wilkins.** 1996. An immunohistochemical analysis of naturally occurring chancroid. J. Infect. Dis. **174:**427-430.

89. **Palmer, K.L., C.T. Schnizlein-Bick, A. Orazi, K. John, C.Y. Chen, A.F. Hood, and S.M. Spinola.** 1998. The immune response to *Haemophilus ducreyi* resembles a delayed-type hypersensitivity reaction throughout experimental infection of human subjects. J. Infect. Dis. **178:**1688-1697.

90. **Spinola, S.M., L.M. Wild, M.A Apicella, A.A. Gaspari, and A.A. Campagnari.** 1994. Experimental human infection with *Haemophilus ducreyi*. J. Infect. Dis. **169:**1146-1150.

91. **Brown, T.J., R.C. Ballard, and C.A. Ison.** 1995. Specificity of the immune response to *Haemophilus ducreyi*. Microb. Pathog. 19: 31-38.

92. **Bong, C.T., M.E. Bauer, and S.M. Spinola.** 2002. *Haemophilus ducreyi*: clinical features, epidemiology, and prospects for disease control. Microbes Infect. **4:**1141-1148.

93. **Frisk, A., H.J. Ahmed, E. van Dyck, and T. Lagergard.** 1998. Antibodies specific to surface antigens are not effective in complement-mediated killing of *Haemophilus ducreyi*. Microb. Pathog. **25:**67-75.

94. **Lagergard, T.** 1992. The role of *Haemophilus ducreyi* bacteria, cytotoxin, endotoxin and antibodies in animal models for study of chancroid. Microb. Pathog. **13:**203-217.

95. **Lagergard, T., A. Frisk, M. Purven, and L.A. Nilsson.** 1995. Serum bactericidal activity and phagocytosis in host defence against *Haemophilus ducreyi*. Microb. Pathog. **18:**37-51.

96. **Mateo, L.R.S., K.L. Toffer, P.E. Orndorff, and T.H. Kawula.** 1999. Immune cells are required for cutaneous ulceration in a swine model of chancroid. Infect. Immun. **67:**4963-4967.

97. **Chen, C.Y., K.J. Mertz, S.M. Spinola, and S.A. Morse.** 1997. Comparison of enzyme immunoassays for antibodies to *Haemophilus ducreyi* in a community outbreak of chancroid in the United States. J. Infect. Dis. **175:**1390-1395.

98. **Afonina, G., I. Leduc, I. Nepluev, C. Jeter, P. Routh, G. Almond, P.E. Orndorff, M. Hobbs, and C. Elkins.** 2006. Immunization with *Haemophilus ducreyi* hemoglobin receptor HgbA protects against infection in the swine model of chancroid. Infect. Immun. **74:**2224-2232.

99. **Mandell, R.E., J.H. Griffiths, and B.A. Macher.** 1988. Lipooligosaccharides of *Neisseria gonorrhoeae* and *Neisseria meningitidis* have components that are immunochemically similar to precursors of blood group antigens: carbohydrate sequence specificity of the mouse monoclonal antibodies that recognize crossreacting antigens on LOS and human erythrocytes. J. Exp. Med. **168:**107-126.

100. **Gibson, B.W., W. Melaugh, N.J. Phillips, M.A. Apicella, A.A. Campagnari, and J.M. Griffiss.** 1993. Investigation of the structural heterogeneity of lipooligosaccharides form pathogenic *Haemophilus* and *Neisseria* species and of R-type lipopolysaccharides from *Salmonella typhimurium* by electrospray mass spectrometry. J. Bacteriol. **175:**2702-2712.

101. **Mandrell, R.E., J.M. Griffiss, and B.A. Macher.** 1988. Lipooligosaccharides (LOS) of *Neisseria gonorrhoeae* and *Neisseria meningitidis* have components that are immunochemically similar to precursors of human blood group antigens. Carbohydrate sequence specificity of the mouse monoclonal antibodies that recognize crossreacting antigens on LOS and human erythrocytes. J. Exp. Med. **168:**107-126.

102. **Odumeru, J.A., G.A. Wiseman, and A.R. Ronald.** 1985. Role of lipopolysaccharide and complement in susceptibility of *Haemophilus ducreyi* to human serum. Infect. Immun. **50:**495-499.

103. **Melaugh., W., N.J. Phillips, A.A. Campagnari, M.V. Tullius, and B.W. Gibson.** 1994. Structure of the major oligosaccharide from the lipooligosaccharide of *Haemophilus ducreyi* strain 35 000 and evidence for additional glycoforms. Biochemistry **33:**13070-13078.

104. **Gibson, B.W., A.A. Campagnari, W. Melaugh, N.J. Phillips, M.A. Apicella, S. Grass, J. Wang, K.L. Palmer, and R.S. Munson Jr.** 1997. Characterization of a transposon Tn916-generated mutant of *Haemophilus ducreyi* 35 000 defective in lipooligosaccharide biosynthesis. J. Bacteriol. **179:**5062-5071.

105. **Spinola, S.M., A. Castellazzo, M. Shero, and M.A. Apicella.** 1990. Characterization of pili expressed by *Haemophilus ducreyi*. Microb. Pathog. **9:**417-426.

106. **Cortes-Bratti, X., E. Chaves-Oiarte, T. Lagergard, and M. Thelestam.** 2000. Cellular internalization of cytolethal distending toxin from *Haemophilus ducreyi*. Infect. Immun. **68:**6903-6911.

107. **Cope, L.D., S. Lumbley, J.L. Latimer, J. Klesney-Tait, M.K. Stevens, L.S. Johnson, M. Purven, R.S. Munson Jr., T. Lagergard, J.D. Radolf, and E.J. Hansen.** 1997. A diffusible cytotoxin of *Haemophilus ducreyi*. Proc. Natl. Acad. Sci. USA **94:**4056-4061.

108. **Palmer, K.L., and R.S. Munson Jr.** 1995. Cloning and characterization of the genes encoding the haemolysin of *Haemophilus ducreyi*. Mol. Microbiol. **18:**821-830.

109. **Alfa, M.J., P. DeGagne, and P.A. Totten.** 1996. *Haemophilus ducreyi* hemolysin acts as a contact cytotoxin and damages human foreskin fibroblasts in cell culture. Infect. Immun. **64:**2349-2352.

110. **Palmer, K.L., A.C. Thornton, K.R. Fortney, A.F. Hood, R.S. Munson, and S.M. Spinola.** 1998. Evaluation of an isogenic hemolysin-deficient mutant in the human model of *Haemophilus ducreyi* infection. J. Infect. Dis. **178:**191-199.

111. **Wood, G.E., S.M. Dutro, and P.A. Totten.** 1999. Target cell range of *Haemophilus ducreyi* hemolysin and its involvement in invasion of human epithelial cells. Infect. Immun. **67:**3740-3749.

112. **Palmer, K.L., and R.S. Munson.** 1995. Cloning and characterization of the genes encoding the hemolysin of *Haemophilus ducreyi*. Mol. Microbiol. **18:**821-830.

113. **Thomas, C.E., B. Olsen, and C. Elkins.** 1998. Cloning and Characterization of *tdhA*, a locus encoding a TonB-dependent heme receptor for *Haemophilus ducreyi*. Infect. Immun. **66:**4254-4262.

114. **Elkins, C.** 1995. Identification and purification of a conserved heme-regulated hemoglobin-binding outer membrane protein from *Haemophilus ducreyi*. Infect. Immun. **63:**1241-1245.

115. **Stevens, M.K., S. Porcella, J. Klesney-Tait, S. Lumbley, S.E. Thomas, M.V. Norgard, J.D. Radolf, and E.J. Hansen.** 1996. A hemoglobin-binding outer membrane protein is involved in virulence expression by *Haemophilus ducreyi* in an animal model. Infect. Immun. **64:**1724-1735.

116. **Spinola, S.M., G.E. Griffiths, K.L. Shanks, and M.S. Blake.** 1993. The major outer membrane protein of *Haemophilus ducreyi* is a member of the OmpA family of proteins. Infect. Immun. **61:**1346-1351.

117. **Rice, P.A., H.E. Vayo, M.R. Tam, and M.S. Blake.** 1986. Immunoglobulin G antibodies directed against protein III block killing of serum-resistant *Neisseria gonorrhoeae* by immune serum. J. Exp. Med. **164:**1735-1748.

118. **Weiser, J.N. and E.C. Gotschlich.** 1991. Outer membrane protein A (OmpA) contributes to serum resistance and pathogenicity of *Escherichia coli* K-1. Infect. Immun. **59:**2252-2258.

119. **Kroll, J.S., P.R. Langford, K.E. Wilks, and A.D. Keil.** 1995. Bacterial [Cu,Zn]-superoxide dismutase: phylogenetically distinct from the eukaryotic enzyme, and not so rare after all! Microbiology. **141:**2271-2279.

120. **San Mateo, L.R., M.M. Hobbs, and T.H. Kawula.** 1998. Periplasmic copper-zinc superoxide dismutase protects *Haemophilus ducreyi* from exogenous superoxide. Mol. Microbiol. **27:**391-404.

121. **Vallee, B.L., and K.H. Falchuk.** 1993. The biochemical basis of zinc physiology. Physiol. Rev. **1:**79-118.

122. **Coleman, J.E.** 1992. Zinc proteins: Enzymes, storage proteins, transcription factors and replication proteins. Annu. Rev. Biochem. **61:**897-946.

123. **Lewis, D.A., J. Klesney-Tait, S.R. Lumbley, C.K. Ward, J.L. Latimer, C.A. Ison, and E.J. Hansen.** 1999. Identification of the znuA-encoded periplasmic transport protein of *Haemophilus ducreyi*. Infect. Immun. **67:**5060-5068.

124. **Hobbs, M.M., L.R. San Mateo, P.E. Orndorff, G. Almond, and T.H. Kawula.** 1995. Swine model of *Haemophilus ducreyi* infection. Infect. Immun. **63:**3094-3100.

125. **Purcell, B.K., J.A. Richardson, J.D. Radolf, and E.J. Hansen.** 1991. A temperature-dependent rabbit model for production of dermal lesions by *Haemophilus ducreyi*. J. Infect. Dis. **164:**359-367.

126. **Totten, P.A., W.R. Morton, G.H. Knitter, A.M. Clark, N.B. Kiviat, and W.E. Stamm.** 1994. A primate model for chancroid. J. Infect. Dis. **169:**1284-1290.

127. **Genco, C.A., and D.W. Dixon.** 2001. Emerging strategies in microbial haem capture. Mol. Microbiol. **39:**1-11.

128. **Braun, V., and H. Killman.** 1999. Bacterial solutions to the iron-supply problem. Trends Biochem. Sci. **24:**104-109.

129. **Touati, D.** 2000. Iron and oxidative stress in bacteria. Arch. Biochem. Biophys. **373:**1-6.

130. **Bridges, K.R., and P.A. Seligman.** 1995. Disorders of iron metabolism, p. 1433-1472. *In* R.I. Handlin, S.E. Lux, and T.P. Stossel (ed.), Blood, Principles and Practice of Hematology. JB Lippincott Company, London.

131. **Wandersman, C., and I. Stojiljkovic.** 2000. Bacterial heme sources: the role of heme, hemoprotein receptors and hemophores. Curr. Opin. Microbiol. **3:**215-220.

132. **Carson, S.D., P.E. Klebba, S.M. Newton, and P.F. Sparling.** 1999. Ferric enterobactin binding and utilization by *Neisseria gonorrhoeae*. J. Bacteriol. **181:**2895-2901.

133. **Langman L., I.G. Young, G.E. Frost, H. Rosenberg, and F. Gibson.** 1972. Enterochelin system of iron transport in *Escherichia coli*: mutations affecting ferric-enterochelin esterase. J. Bacteriol. **112:** 1142-1149.

134. **Yancey, R.J., S.A. Breeding, and C.E. Lankford.** 1979. Enterochelin (enterobactin): virulence factor for *Salmonella typhimurium*. Infect. Immun. **24:**174-180.

135. **Carniel, E., D. Mazigh, and H.H. Mollaret.** 1987. Expression of iron-regulated proteins in *Yersinia* species and their relation to virulence. Infect. Immun. **55:**277-280.

136. **Fetherston, J.D., P. Schuetze, and R.D. Perry.** 1992. Loss of the pigmentation phenotype in *Yersinia pestis* is due to the spontaneous deletion of 102 kb of chromosomal DNA which is flanked by a repetitive element. Mol. Microbiol. **6:**2693-2704.

137. **Heesemann, J., K. Hantke, T. Vocke, E. Saken, A. Rakin, I. Stojiljkovic, and R. Berner.** 1993. Virulence of *Yersinia enterocolitica* is closely associated with siderophore production, expression of an iron-repressible outer membrane polypeptide of 65,000 Da and pesticin sensitivity. Mol. Microbiol. **8:**397-408

138. **Perry, R.D., and J.D. Fetherston.** 1997. *Yersinia pestis* - etiologic agent of plague. Clin. Microbiol. Rev. **10:**35-66

139. **Wake, A., M. Misawa, and A. Matsui.** 1975. Siderochrome production by *Yersinia pestis* and its relation to virulence. Infect. Immun. **12:**1211-1213

140. **Gobin. J., and M.A. Horwitz.** 1996. Exochelins of *Mycobacterium tuberculosis* remove iron from human iron- binding proteins and donate iron to mycobactins in the *M. tuberculosis* cell wall. J. Exp. Med. **183:**1527-1532.

141. **Loomis, L.D., and K.N. Raymond.** 1991. Solution equilibria of enterobactin and metal-enterobactin complexes. Inorg. Chem. **30:**906-911.

142. **Rouault, T.A.** 2004. Pathogenic bacteria prefer heme. Science. **305:**1577-1578.

143. **Arnoux, P., R. Haser, N. Izadi, A. Lecroisey, M. Delepierre, C. Wandersman, and M. Czjzek.** 1999. The crystal structure of HasA, a hemophore secreted by *Serratia marcescens*. Nat. Struct. Biol. **6:**516-520.

144. **Rossi, M.-S., J.D. Fetherston, S. Létoffé, E. Carniel, R.D. Perry, and J.-M. Ghigo.** 2001. Identification and characterization of the hemophore-dependent heme acquisition system of *Yersinia pestis*. Infect. Immun. **69:**6707-6717.

145. **Ratledge, C., and L.G. Dover.** 2000. Iron metabolism in pathogenic bacteria. Annu. Rev. Microbiol. **54:**881-941.

146. **Stojiljkovic, I., and D. Perkins-Balding.** 2002. Processing of heme and heme-containing proteins by bacteria. DNA and Cell Biol. **21:**281-295.

147. **Rohde, K.H., and D.W. Dyer.** 2003. Mechanisms of iron acquisition by the human pathogens *Neisseria meningitidis* and *Neisseria gonorrhoeae*. Front. Biosci. **8:**1186-1218.

148. **Larson, J.A., H.L. Howie, and M. So.** 2004. *Neisseria meningitidis* accelerates ferritin degradation in host epithelial cells to yield an essential iron sources. Mol. Microbiol. **53:** 807-820.

149. **Lewis, L.A., E. Gray, Y.P. Wang, B.A. Roe, and D.W. Dyer.** 1997. Molecular characterization of *hpuAB*, the haemoglobin-haptoglobin-utilization operon of *Neisseria meningitidis*. Mol. Microbiol. **23:**737-749.

150. **Stojiljkovic, I., J. Larson, V. Hwa, S. Anic, and M. So.** 1996. HmbR outer membrane receptors of pathogenic *Neisseria* spp.: iron-regulated, hemoglobin-binding proteins with a high level of primary structure conservation. J. Bacteriol. **178:**4670-4678.

151. **Thompson, J.M., H.A. Jones, and R.D. Perry.** 1999. Molecular characterization of the hemin uptake locus (*hmu*) from *Yersinia pestis* and analysis of *hmu* mutants for hemin and hemoprotein utilization. Infect. Immun. **67:**3879-3892.

152. **Mills, M., and S.M. Payne.** 1997. Identification of *shuA*, the gene encoding the heme receptor of *Shigella dysenteriae*, and analysis of invasion and intracellular multiplication of a *shuA* mutant. Infect. Immun. **65:**5358-5363.

153. **Oschner, U.A., Z. Johnson, and M.L. Vasil.** 2000. Genetics and regulation of two distinct haem-uptake systems, *phu* and *has*, in *Pseudomonas aeruginosa*. Microbiology. **146:**185-198.

154. **Braun, V.** 1995. Energy-coupled transport and signal transduction through the Gram-negative outer membrane via TonB-ExbB-ExbD-dependent receptor proteins. FEMS Microbiol. Rev. **16:**295-307.

155. **Jarosik, G.P., J.D. Sanders, L.D. Cope, U. Muller-Eberhard, and E.J. Hansen.** 1994. A functional tonB gene is required for both utilization of heme and virulence expression by *Haemophilus influenzae* type B. Infect. Immun. **62:**2470-2477.

156. **Biswas, G.D., J.E. Anderson, and P.F. Sparling.** 1997. Cloning, sequencing and genetic characterization of tonB-exbB-exbD genes of *Neisseria gonorrhoeae*. Mol. Microbiol. **24:**169-179.

157. **Stojiljkovic, I., and N. Srivnisan.** 1997. *Neisseria meningitidis* tonB, exbB, and exbD genes: Ton-dependent utilization of protein-bound iron in neisseriae. J. Bacteriol. **179:**805-812.

158. **Luisa del Rio, M., C.B. Gutiérrez-Martin, J.I. Rodriguez-Barbosa, J. Navas, and E.F. Rodriguez-Ferri.** 2005. Identification and characterization of the TonB region and its role in transferrin-mediated iron acquisition in *Haemophilus parasuis*. FEMS Immunol. Med. Microbiol. **45:**75-86.

159. **Fath, M.J., and R. Kolter.** 1993. ABC transporters: bacterial exporters. Microbiol. Rev. **57:**995-1017.

160. **Anderson, D.S., P. Adhikari, A.J. Nowalk, C.Y. Chen, and T.A. Mietzner.** 2004. The *hFbp*ABC transporter from *Haemophilus influenzae* functions as a binding-

protein-dependent ABC transporter with high specificity and affinity for ferric iron. J. Bacteriol. **186:**6220-6229.

161. **Ames, F.-L.** 1986. Bacterial periplasmic transport systems: structure, mechanism and evolution. Annu. Rev. Biochem. **55:**397-425.

162. **Sanders, J.. L. Cope, and E. Hansen.** 1994. Identification of a locus involved in the utilization of iron by *Haemophilus influenzae*. Infect. Immun. **62:**4515-4525.

163. **Zimmermann, L., Angerer, A., and V. Braun.** 1989. Mechanistically novel iron(III) transport system in *Serratia marcescens*. J. Bacteriol. **171:**238-243.

164. **Adhikari, P., S.A. Berish, A.J. Nowalk, K.L. Veraldi, S.A. Morse, and T.A. Mietzner.** 1996. The *fbp*ABC locus of *Neisseria gonorrhoeae* functions in the periplasm-to-cytosol transport of iron. J. Bacteriol. **178:**2145-2149.

165. **Bearden, S.W., T.M. Staggs, and R.D. Perry.** 1998. An ABC transporter system of *Yersinia pestis* allows utilization of chelated iron by *Escherichia coli* SAB11. J. Bacteriol. **180:**1135-1147.

166. **Wyckoff, E.E., M. Schmitt, A. Wilks, and S.M. Payne.** 2004. *HutZ* is required for efficient heme utilization in *Vibrio cholerae*. J. Bacteriol. **186:**4142-4151.

167. **Adhikari, P., S.D. Kirby, A.J. Nowalk, K.L. Veraldi, A.B. Schryvers, and T.A. Mietzner.** 1995. Biochemical characterization of a *Haemophilus influenzae* periplasmic iron transport operon. J. Biol. Chem. **270:**25142-25149.

168. **Angerer, A., S. Gaisser, and V. Braun.** 1990. Nucleotide sequences of the *sfuA*, *sfuB*, and *sfuC* genes of *Serratia marcescens* suggest a periplasmic-binding-protein-dependent iron transport mechanism. J. Bacteriol. **172**:572-578.

169. **Lafontaine, E.R., and P.A. Sokol.** 1998. Effects of iron and temperatures on expression of the *Pseudomonas aeruginosa tol QRA* genes, role of the ferric uptake regulator. J. Bacteriol. **180:**2836-2841.

170. **Litwin, C.M., S.A. Boyko, and S.B. Calderwood.** 1992. Cloning, sequencing, and transcriptional regulation of the *Vibrio cholerae fur* gene. J. Bacteriol. **174:**1879-1903.

171. **Prince, R.W., C.D. Cox, and M.L. Vasil.** 1993. Coordinate regulation of siderophore and exotoxin production: molecular cloning and sequencing of the *Pseudomonas aeruginosa* fur gene. J. Bacteriol. **175:**2589-2598.

172. **Staggs, T.M., and R.D. Perry.** 1992. Fur regulation in *Yersinia* species. Mol. Microbiol. **6:**2507-2516.

173. **Thomas, C.E., and P.F. Sparling.** 1994. Identification and cloning of a fur homologue from *Neisseria meningitidis*. Mol. Microbiol. **11:**725-737.

174. **Vasil, M.L., and U.A. Ochsner.** 1999. The response of *Pseudomonas aeruginosa* to iron: genetics, biochemistry and virulence. Mol. Microbiol. **34:**399-413.

175. **Coy, M., and J.B. Neilands.** 1991. Structural dynamics and functional domains of the fur protein. Biochemistry. **30:**8201-8210.

176. **Lee, B.C.** 1991. Iron sources for *Haemophilus ducreyi*. J. Med. Microbiol. **34:**317-322.

177. **Hammond, G.W., C.-J. Lian, J.C. Wilt, W.L. Albritton, and A.R. Ronald.** 1978. Determination of the hemin requirement of *Haemophilus ducreyi*: evaluation of the porphyrin test and media used in the satellite growth test. J. Clin. Microbiol. **7:**243-246.

178. **Palmer, K.L., S. Grass, and R.S. Munson Jr.** 1994. Identification of a hemolytic activity elaborated by *Haemophilus ducreyi*. Infect. Immun. **62:**3041-3043.

179. **Elkins, C., P.A. Totten, B. Olsen, and C.E. Thomas.** 1998. Role of the *Haemophilus ducreyi* Ton system in internalization of heme from hemoglobin. Infect Immun. **66:**151-160.

180. **Jungblut, P.R.** 2001. Proteome analysis of bacterial pathogens. Microbes Infect. **3:**831-840.

181. **O'Farrel, P.H.** 1974. High resolution two-dimensional electrophoresis of proteins. J. Biol. Chem. **250:**4007-4021.

182. **Thorén, K., E. Gustafsson, A. Clevnert, T. Larsson, J. Bergström, and C.L. Nilsson.** 2002. Proteomic study of non-typable *Haemophilus influenzae*. J. Chromatogr. B. Analyt. Technol. Biomed. Life Sci. **782:**219-226.

183. **Chambers, G., L. Lawrie, P. Cash, and G.I. Murray.** 2000. Proteomics: a new approach to the study of disease. J. Pathol. **192:**280-288.

184. **Jeffries, J.R.** 2003. 2D Gel electrophoresis for proteomics tutorial. Institute of Biological Sciences, University of Wales at Aberystwyth. Available at: http://www.aber.ac.uk/~mpgwww/Proteome/Tut_2D.html

185. **Langen, H., P. Berndt, D. Roer, N. Cairns, G. Lubec, and M. Fountoulakis.** 1999. Two dimensional map of human brain proteins. Electrophoresis. **20:**907-916.

186. **Arnott, D., K.L. O'Connel, K.L. King, and J.T. Stults.** 1999. An integrated response to proteome analysis: identification of proteins associated with cardiac hypertrophy. Anal. Biochem. **258:**1-18.

187. **O'Connor, C.D., M. Farris, R. Fowler, and S.Y. Qi.** 1997. The proteome of *Salmonella enterica* serovar *typhimurium*: current progress on its determination and some applications. Electrophoresis. **18:**1483-1490.

188. **VanBoglen, R.A., K.Z. Abshire, B. Moldover, E.R. Olsen , and F.C. Neidhart.** 1997. *Escherichia coli* proteome analysis using the gene-proteome database. Electrophoresis. **18:**1243-1251.

189. **Langen, H., B. Takacs, S. Evers, P. Berndt, H. Lahm, B. Wipf, C. Gray, and M. Fountoulakis.** 2000. Two-dimensional map of the proteome of *Haemophilus influenzae*. Electrophoresis. **21:**411-429.

190. **Cordwell, S., A.S. Nouwens, and B.J. Walsh.** 2001. Comparative proteomics of bacterial pathogens. Proteomics. **1:**461-472.

191. **McAtee, C.P., K.E. Fry, and D.E. Berg.** 1998. Identification of potential diagnostic and vaccine candidates of *Helicobacter pylori* by "proteome" technologies. Heliobacter. **3:**163-169.

192. **Cash, P., E. Argo, L. Ford, L. Lawrie, and H. McKenzie.** 1999. A proteomic study of erythromycin resistance in *Streptococcus pneumoniae*. Electrophoresis. **20:**2259-2268.

193. **Jungblut, P.R., U.E. Schaible, H.-J. Mollenkopf, U. Zimny-Arndt, B. Raupach, J. Mattow, P. Halada, S. Lamer, K. Hagens, and S.H.E. Kaufmann.** Comparative proteome analysis of *Mycobacterium tuberculosis* and *Mycobacterium bovis* BCG strains: towards functional genomics of microbial pathogens. Mol. Microbiol. **33:**1103-1117.

194. **Scheffler, N.K., A.M. Falick, S.C. Hall, W.C. Ray, D.M. Post, R.S. Munson, and B.W. Gibson.** 2003. Proteome of *Haemophilus ducreyi* by 2-D SDS-PAGE and Mass Spectrometry: strain variation, virulence, and carbohydrate expression. J. Proteome Res. **2:**523-533.

195. **Stojiljkovic, I., V. Kumar, and N. Srinivasan.** 1999. Non-iron metalloporphyrins: potent antibacterial compounds that exploit haem/Hb uptake systems of pathogenic bacteria. Mol. Microbiol. **31:**429-442.

196. **Bozja, J., K. Yi, W.M. Shafer, and I. Stojiljkovic.** 2004. Porphyrin-based compounds exert antibacterial action against the sexually transmitted pathogens *Neisseria gonorrhoeae* and *Haemophilus ducreyi*. Int. J. Antimicrob. Agents. **24:**578-584.

197. **Martin, H.L., B.A. Richardson, P.M. Nyange, L. Lavreys, S.L. Hillier, B. Chohan, K. Mandaliya, J.O. Ndinya-Achola, J. Bwayo, and J. Kreiss.** 1999. Vaginal lactobacilli, microbial flora, and risk of human immunodeficiency virus type 1 and sexually transmitted disease acquisition. J. Infect. Dis. **180:**1863-1868.

198. **Ames, G.F., C. Prody, and S. Kustu.** 1984. Simple, rapid, and quantitative release of periplasmic proteins by chloroform. J. Bacteriol. **160:**1181-1183.

199. **Leduc, I.** 2001. Ph.D. thesis. Strain typing and vaccine development for chancroid. University of Ottawa, Ontario, Canada.

200. **Ausubel, F.M., R. Brent, R.E. Kingston, D.D. Moore, J.G. Seidman, J.A. Smith, and K Struhl.** 1989. Current Protocols in Molecular Biology. Vol. 2., John Wiley & Sons, New York, NY.

201. **Zhou, D., W.D. Hardt, and J.E. Galan.** 1999. *Salmonella typhimurium* encodes a putative iron transport system within the centisome 63 pathogenicity island. Infect. Immun. **67:**1974-1981.

202. **Forest, K.T., P.R. Langford, J.S. Kroll, and E.D. Getzoff.** 2000. Cu,Zn superoxide dismutase structure from a microbial pathogen establishes a class with a conserved dimer interface. J. Mol. Biol. **296:**145-153.

203. **Negari, S.** 2003. MSc. Thesis. Role of SodC in heme acquisition in *Haemophilus ducreyi*. University of Ottawa, Ontario. Canada.

204. **Huang, X., and W. Miller.** 1991. A time-efficient, linear space local similarity algorithm. Adv. Appl. Math. **12:**337-357. Available at: http://www.ch.embnet.org/software/LALIGN_form.html.

205. **Eakanunkul, S., G.S. Lukat-Rodgers, S. Sumithran, A. Ghosh, K.R. Rodgers, J.H. Dawson, and A. Wilks.** 2005. Characterization of the periplasmic heme-binding protein ShuT from the heme uptake system of *Shigella dysenteriae*. Biochemistry. **44:**13179-13191.

206. The Sexually Transmitted Disease Genome Sequence Database (STDGEN). Los Alamos National Library. Division of Microbiology and Infectious Disease, Bethesda, MD. Available at: http://www.stdgen.lanl.gov/.

207. **Nakai, K., and M. Kanehisa.** 1991. Expert system for predicting protein localization sites in Gram-negative bacteria, Proteins. **11:**95-110. Available at: http://psort.ims.u-tokyo.ac.jp/.

208. FindTerm. Softberry, Inc. Mount Kisco, NY. Available at: http://sun1.softberry.com/berry.phtml?topic=findterm&group=programs&subgroup=gfindb.

209. **Rost, B., and C. Sander.** 1993. Prediction of protein secondary structure at better than 70% accuracy. J. Mol. Biol. **232:**584-599. Available at: http://npsa-pbil.ibcp.fr/cgi-bin/npsa_automat.pl?page=/NPSA/npsa_htm.html.

210. **Pierik, A.J., M.G. Duyvis, J.M.L.M. van Helvoort, R.BG. Wolbert, and W.R. Hagen.** 1992. The third subunit of desulfoviridin-type dissimilatory sulfite reductases. Eur. J. Biochem. **205:**111-115.

211. **Karkhoff-Schweizer, R.R., M. Bruschi, and G. Voordouw.** 1993. Expression of the γ-subunit gene of desulfoviridin-type dissimilatory sulfite reductase and of the α- and β-subunit genes is not coordinately regulated. Eur. J. Biochem. **211:**501-507.

212. **Molitor, M., C. Dahl, I. Molitor, U. Schäfer, N. Speich, R. Huber, R. Deutzmann, and H.G. Trüper.** 1998. A dissimilatory sirohaem-sulfite-reductase-type protein from the hyperthermophilic archaeon *Pyrobaculum islandicum*. Microbiology. **144:**529-541.

213. **Lee, J.P., C.-S. Yi, J. LeGall, and H.D. Peck Jr.** 1973. Isolation of assimilatory- and dissimilatory-type sulfite reductases from *Desulfovibrio vulgaris*. J. Bacteriol. **115:**529-542.

214. **Walker, J.E., M. Saraste, M.J. Runswick, and N.J. Gay.** 1982. Distantly related sequences in the alpha- and beta-subunits of ATP synthase, myosin, kinases and other ATP-requiring enzymes and a common nucleotide binding fold. EMBO J. **1:**945-951.

215. **Frankenberg, N., J. Moser, and D. Jahn.** 2003. Bacterial heme biosynthesis and its biotechnological application. Appl. Microbiol. Biotechnol. **63:**115-127.

216. **Scolaro, L.M., M. Castriciano, A. Romeo, S. Patane, E. Cefali, and M. Allegrini.** 2002. Aggregation behavior of protoporphyrin IX in aqueous solutions: clear evidence of vesicle formation. J. Phys. Chem. **106:**2453-2459.

217. **Berggren, K., E. Chernokalskaya, T.H. Steinberg, C. Kemper, M.F. Lopez, Z. Diwu, P.R. Haugland, and W.F. Patton.** 2000. Background-free, high sensitivity staining of proteins in one- and two-dimensional sodium dodecyl sulfate-polyacrylamide gels using a luminescent ruthenium complex. Electrophoresis. **21:**2509-2521.

218. **Bracken, C.S., M.T. Baer, A. Abdur-Rashid, W. Helms, and I. Stojiljkovic.** 1999. Use of heme-protein complexes by the *Yersinia entercolitica* HemR receptor: residues are essential for receptor function. J. Bacteriol. **181:**6063-6072.

219. **Letoffe, S., J.M. Ghigo, and C. Wandersman.** 1994. Secretion of the *Serratia marcescens* HasA protein by an ABC transporter. J. Bacteriol. **176:**5372-5377.

220. **Battistoni, F., R. Platero, R. Duran, C. Cerveñansky, J. Battistoni, A. Arias, and E. Fabiano.** 2002. Identification of an iron-regulated, hemin-binding outer membrane protein in *Sinorhizobium meliloti*. Appl. Environ. Microbiol. **68:**5877-5881.

221. **Olczak, T., D. White Dixon, and C.A. Genco.** 2001. Binding specificity of the *Porphyromonas gingivalis* heme and hemoglobin receptor HmuR, gingipain K, and gingipain R1 for heme, porphyrins and metalloporphyrins. J. Bacteriol. **183:**5599-5608.

222. **Wyckoff, E.E., D. Duncan, A.G. Torres, M. Mills, K. Maase, and S.M. Payne.** 1998. Structure of the *Shigella dysenteriae* haem transport locus and its phylogenetic distribution in enteric bacteria. Mol. Microbiol. **28:**1139-1152.

223. **Liu, M., and B. Lei.** 2005. Heme transfer from Streptococcal cell surface protein Shp to HtsA of transporter *HtsABC*. Infect. Immun. **73:**5086-5092.

224. **Altschul, S.F., T.L. Madden, A.A. Schäffer, J. Zhang, Z. Zhang, W. Miller, and D.J. Lipman.** 1997. Gapped BLAST and PSI-BLAST: a new generation of protein database search programs. Nucleic Acids Res. **25:**3389-3402. Available at: http://www.ncbi.nlm.nih.gov/BLAST/

225. **Stojiljkovic, I., and K. Hantke.** 1994. Transport of haemin across the cytoplasmic membrane through a haemin-specific periplasmic binding protein-dependent transport system in *Yersinia enterocolitica* Mol. Microbiol. **13:**719-732.

226. **Lansky, I.B., G.S. Lukat-Rodgers, D. Block, K.R. Rodgers, M. Ratliff, and A. Wilks.** 2006. The cytoplasmic heme-binding protein (PhuS) from the heme uptake system of *Pseudomonas aeruginosa* is an intracellular heme-trafficking protein to the δ-regioselective heme oxygenase. J. Biol. Chem. **281:**13652-13662.

227. **Escolar L., J. Pérez-Martin, and V. de Lorenzo.** 1999. Opening the iron box: transcriptional metalloregulation by the fur protein. J. Bacteriol. **181:**6223-6229.

228. **Carson, S.D., C.E. Thomas, and C. Elkins.** 1996. Cloning and sequencing of *Haemophilus ducreyi* fur homolog. Gene. **176:**125-129.

229. **Whitby, P.W., K.E. Sim, D.J. Morton, J.A. Patel, and T.L. Stull.** 1997. Transcription of genes encoding iron and haem acquisition proteins of *Haemophilus influenzae* during acute otitis media. Infect. Immun. **65:**4696-4700.

230. **Gasteiger, E., A. Gattiker, C. Hoogland, I. Ivanyi, R.D. Appel, and A. Bairoch.** 2003. ExPASy: the proteomics server for in-depth protein knowledge and analysis. Nucleic Acids Res. **31:**3784-3788. Available at: http://ca.expasy.org/.

Appendix I. *H. ducreyi* 35 000 periplasmic proteins upregulated under heme-limiting conditions.

2D gel comparison of chloroform extracted periplasmic proteins of *H. ducreyi* 35 000 grown under heme-replete conditions (100μg/ml heme plus 50μM desferoxamine) **(A)** and heme-limiting conditions (15μg/ml heme plus 50μM desferoxamine) **(B)**. Ten micrograms of each protein sample was rehydrated onto 7cm IPG strips, pH 3-10 and separated in the 1st dimension (pI) for 28 903Vhrs. The 2nd dimension was resolved by a 10% SDS-PAGE gel and stained with SYPRO Ruby. Circled protein spots were identified by MALDI tandem mass spectroscopy and MASCOT to be elongation factors G; MW: 77 kDa **(1)**, Tu; MW: 43.4kDa **(2)**, and P; MW: 20.7kDa **(3)** and an iron (chelated) periplasmic binding protein; MW: 33.2kDa **(4)** of *H. ducreyi* 35 000. Changes in net intensity of each protein spot circled determined by PDQuest are listed in the table with (↑) indicating upregulation and (↓) indicating downregulation under heme-limiting conditions. Molecular mass standards are indicated in kilodaltons (kDa). Trial 2 experiments were performed on July 7, 2005.

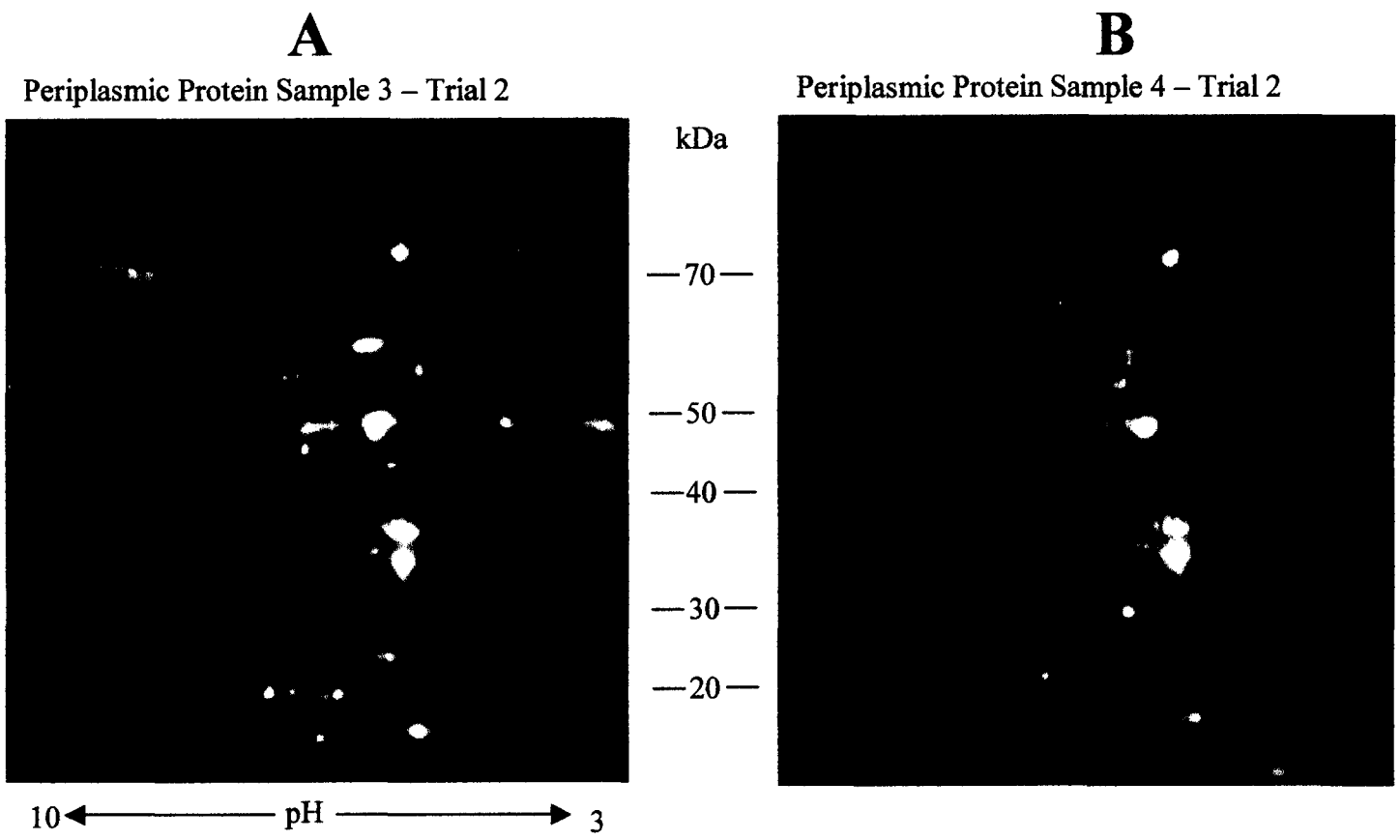

Protein Spot #	Net Intensity		Change in Net Intensity
	Gel A	Gel B	
1	877	1727	↑ 850
2	4581	1341	↓ 3240
3	395	436	↑ 41
4	495	1633	↑ 1138

Appendix I. *H. ducreyi* 35 000 periplasmic proteins upregulated under heme-limiting conditions.

2D gel comparison of chloroform extracted periplasmic proteins of *H. ducreyi* 35 000 grown under heme-replete conditions (100μg/ml heme plus 50μM desferoxamine) **(A)** and heme-limiting conditions (15μg/ml heme plus 50μM desferoxamine) **(B)**. Ten micrograms of each protein sample was rehydrated onto 7cm IPG strips, pH 3-10 and separated in the 1st dimension (pI) for 28 903Vhrs. The 2nd dimension was resolved by a 10% SDS-PAGE gel and stained with SYPRO Ruby. Circled protein spots were identified by MALDI tandem mass spectroscopy and MASCOT to be elongation factors G; MW: 77 kDa **(1)**, Tu; MW: 43.4kDa **(2)**, and P; MW: 20.7kDa **(3)** and an iron (chelated) periplasmic binding protein; MW: 33.2kDa **(4)** of *H. ducreyi* 35 000. Changes in net intensity of each protein spot circled determined by PDQuest are listed in the table with (↑) indicating upregulation and (↓) indicating downregulation under heme-limiting conditions. Molecular mass standards are indicated in kilodaltons (kDa). Trial 2 experiments were performed on July 7, 2005.

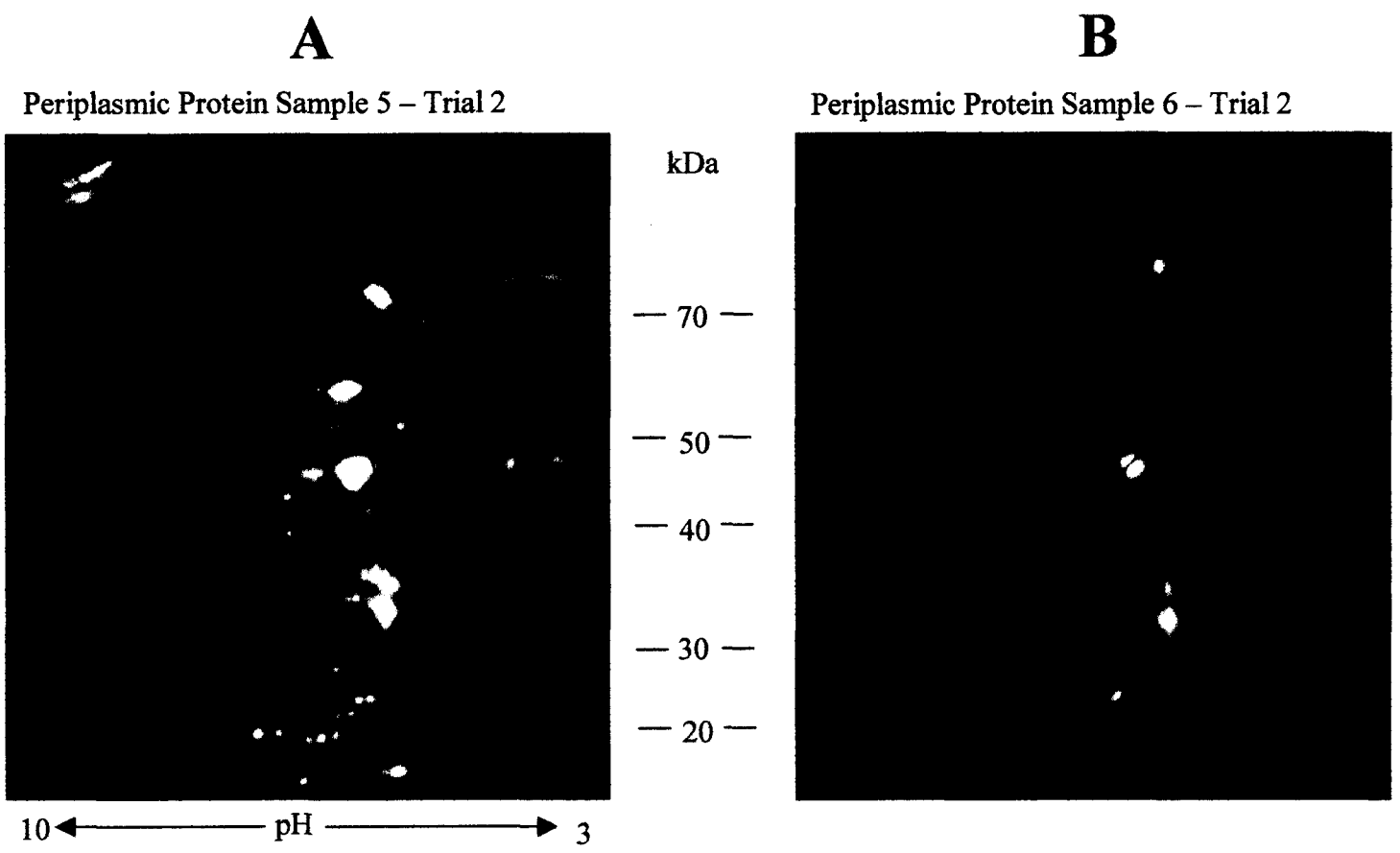

Protein Spot #	Net Intensity		Change in Net Intensity
	Gel A	Gel B	
1	1158	784	↓ 74
2	7883	1591	↓ 6292
3	101	81	↓ 20
4	319	1040	↑ 721

Appendix I. *H. ducreyi* 35 000 periplasmic proteins upregulated under heme-limiting conditions.

2D gel comparison of chloroform extracted periplasmic proteins of *H. ducreyi* 35 000 grown under heme-replete conditions (100μg/ml heme plus 50μM desferoxamine) **(A)** and heme-limiting conditions (15μg/ml heme plus 50μM desferoxamine) **(B)**. Ten micrograms of each protein sample was rehydrated onto 7cm IPG strips, pH 3-10 and separated in the 1st dimension (pI) for 28 902Vhrs. The 2nd dimension was resolved by a 10% SDS-PAGE gel and stained with SYPRO Ruby. Circled protein spots were identified by MALDI tandem mass spectroscopy and MASCOT to be elongation factors G; MW: 77 kDa **(1)**, Tu; MW: 43.4kDa **(2)**, and P; MW: 20.7kDa **(3)** and an iron (chelated) periplasmic binding protein; MW: 33.2kDa **(4)** of *H. ducreyi* 35 000. Changes in net intensity of each protein spot circled determined by PDQuest are listed in the table with (↑) indicating upregulation and (↓) indicating downregulation under heme-limiting conditions. Molecular mass standards are indicated in kilodaltons (kDa). Trial 1 experiments were performed on June 16, 2005.

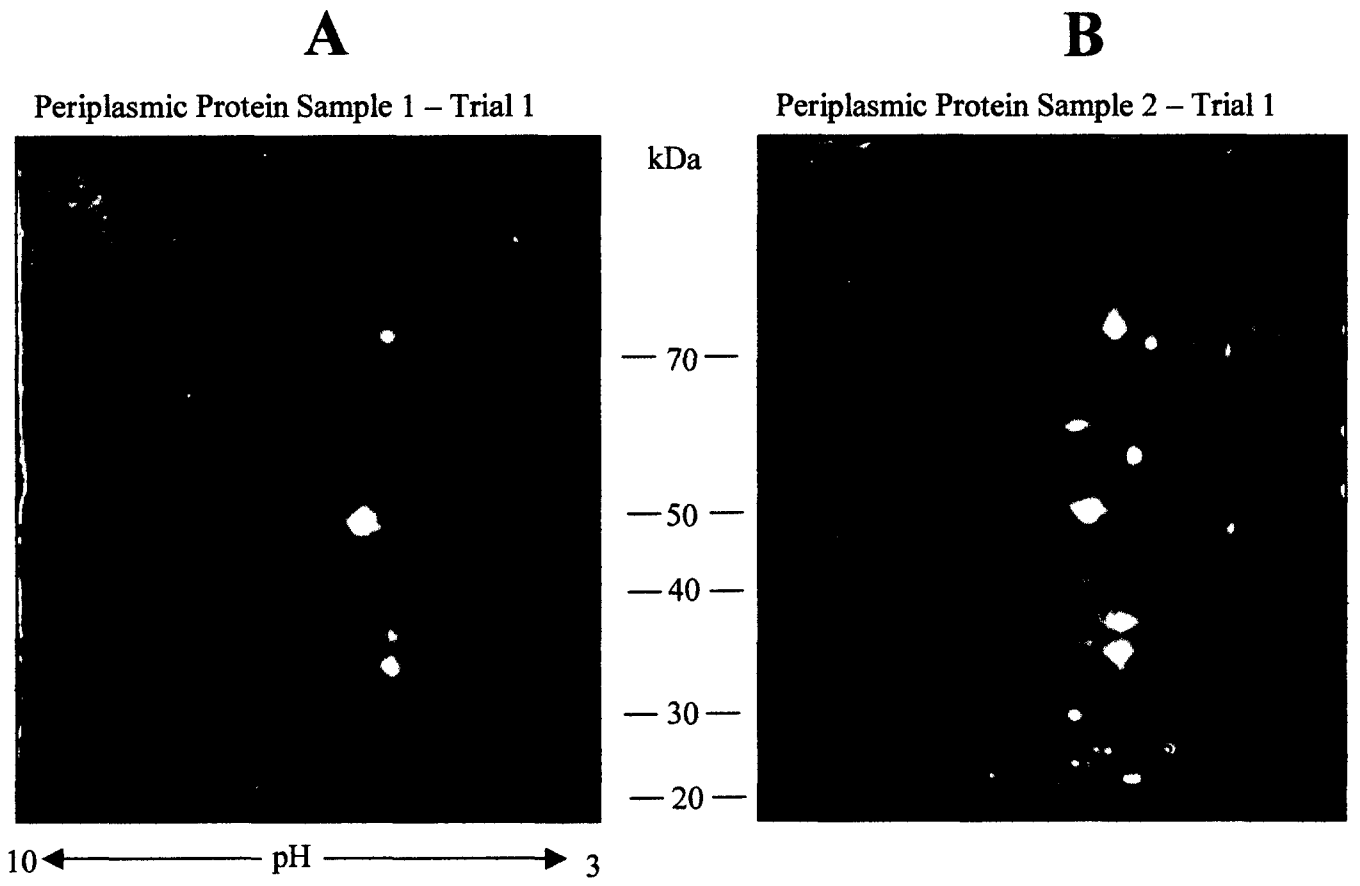

Protein Spot #	Net Intensity		Change in Net Intensity
	Gel A	Gel B	
1	677	2132	↑ 1455
2	1809	2822	↑ 1013
3	107	863	↑ 756
4	348	1836	↑ 1488

Appendix I. *H. ducreyi* 35 000 periplasmic proteins upregulated under heme-limiting conditions.

2D gel comparison of chloroform extracted periplasmic proteins of *H. ducreyi* 35 000 grown under heme-replete conditions (100μg/ml heme plus 50μM desferoxamine) **(A)** and heme-limiting conditions (15μg/ml heme plus 50μM desferoxamine) **(B)**. Ten micrograms of each protein sample was rehydrated onto 7cm IPG strips, pH 3-10 and separated in the 1st dimension (pI) for 28 902Vhrs. The 2nd dimension was resolved by a 10% SDS-PAGE gel and stained with SYPRO Ruby. Circled protein spots were identified by MALDI tandem mass spectroscopy and MASCOT to be elongation factors G; MW: 77 kDa **(1)**, Tu; MW: 43.4kDa **(2)**, and P; MW: 20.7kDa **(3)** and an iron (chelated) periplasmic binding protein; MW: 33.2kDa **(4)** of *H. ducreyi* 35 000. Changes in net intensity of each protein spot circled determined by PDQuest are listed in the table with (↑) indicating upregulation under heme-limiting conditions. Molecular mass standards are indicated in kilodaltons (kDa). Trial 1 experiments were performed on June 16, 2005.

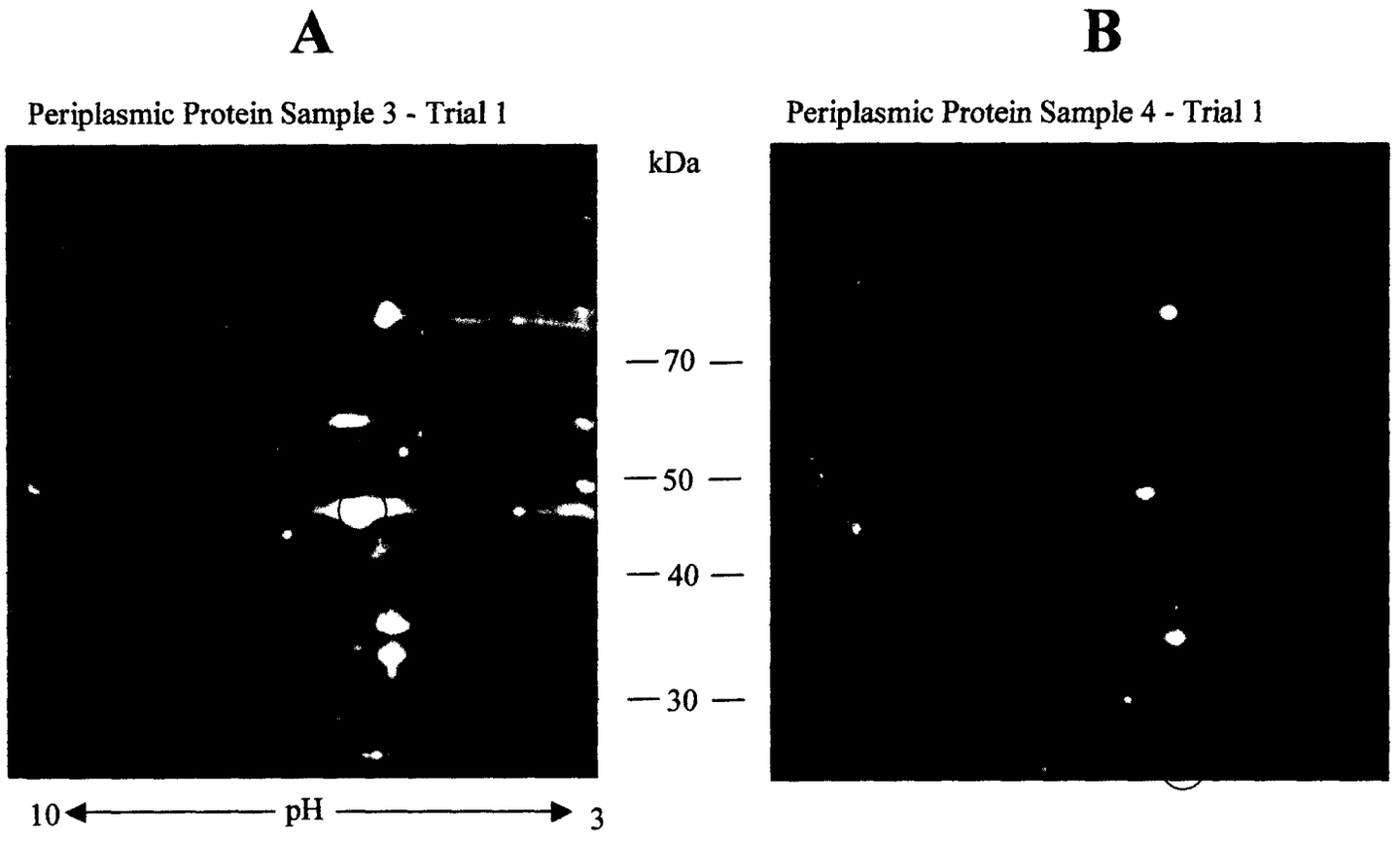

Protein Spot #	Net Intensity		Change in Net Intensity
	Gel A	Gel B	
1	765	1037	↑ 272
2	4290	352	↓ 3938
3	--	259	--
4	404	476	↑ 72

Appendix I. *H. ducreyi* 35 000 periplasmic proteins upregulated under heme-limiting conditions.

2D gel comparison of chloroform extracted periplasmic proteins of *H. ducreyi* 35 000 grown under heme-replete conditions (100μg/ml heme plus 50μM desferoxamine) **(A)** and heme-limiting conditions (15μg/ml heme plus 50μM desferoxamine) **(B)**. Ten micrograms of each protein sample was rehydrated onto 7cm IPG strips, pH 3-10 and separated in the 1st dimension (pI) for 28 902Vhrs. The 2nd dimension was resolved by a 10% SDS-PAGE gel and stained with SYPRO Ruby. Circled protein spots were identified by MALDI tandem mass spectroscopy and MASCOT to be elongation factors G; MW: 77 kDa **(1)**, Tu; MW: 43.4kDa **(2)**, and P; MW: 20.7kDa **(3)** and an iron (chelated) periplasmic binding protein; MW: 33.2kDa **(4)** of *H. ducreyi* 35 000. Changes in net intensity of each protein spot circled determined by PDQuest are listed in the table with (↑) indicating upregulation and (↓) indicating downregulation under heme-limiting conditions. Molecular mass standards are indicated in kilodaltons (kDa). Trial 1 experiments were performed on June 16, 2005.

A

Periplasmic Protein Sample 5 – Trial 1

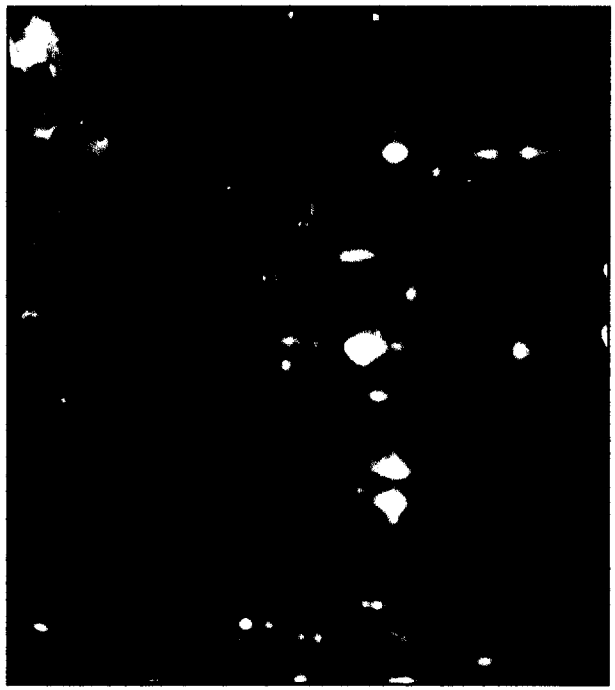

kDa

— 70 —

— 50 —

— 40 —

— 30 —

— 20 —

10 ◄——— pH ———► 3

B

Periplasmic Protein Sample 6 – Trial 1

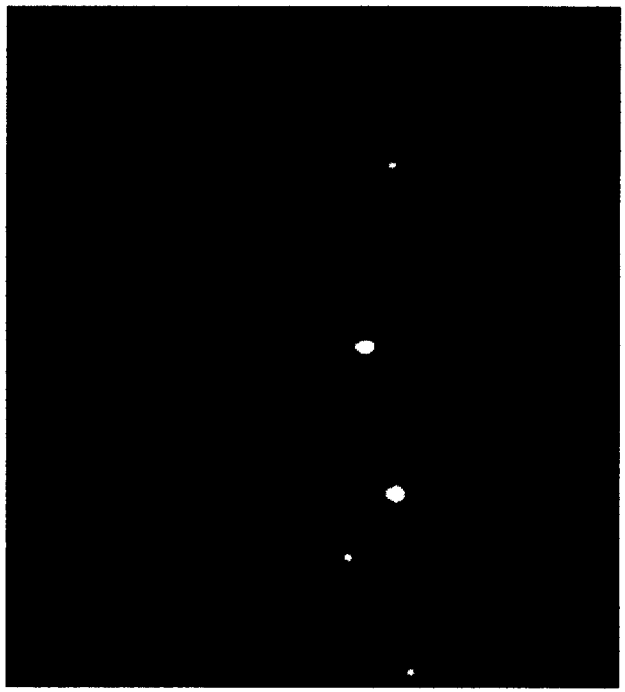

Protein Spot #	Net Intensity		Change in Net Intensity
	Gel A	Gel B	
1	724	721	same
2	3178	1230	↓ 1948
3	305	203	↓ 102
4	147	767	↑ 602

Appendix II. 2D gel analysis determining iron regulation of hHBP.

2D gel comparison of chloroform extracted periplasmic proteins of *H. ducreyi* 35 000 grown under heme-limiting conditions with 100μM **(A),** 10μM **(B),** 200μM **(C),** or 20μM **(D)** desferoxamine. Gels A and B, or C and D were compared for changes in protein expression. Ten micrograms protein sample was rehydrated onto 7cm IPG strips, pH 3-10 and separated in the 1st dimension (pI) for 28 302Vhrs. The 2nd dimension was resolved on a 10% SDS-PAGE gel and stained with SYPRO Ruby. The circled protein spot represents hHBP with the net intensity of each protein spot determined by PDQuest indicated on each gel. Molecular mass standards are indicated in kilodaltons (kDa). Trial 2 experiments were performed on October 5, 2005.

Trial 2

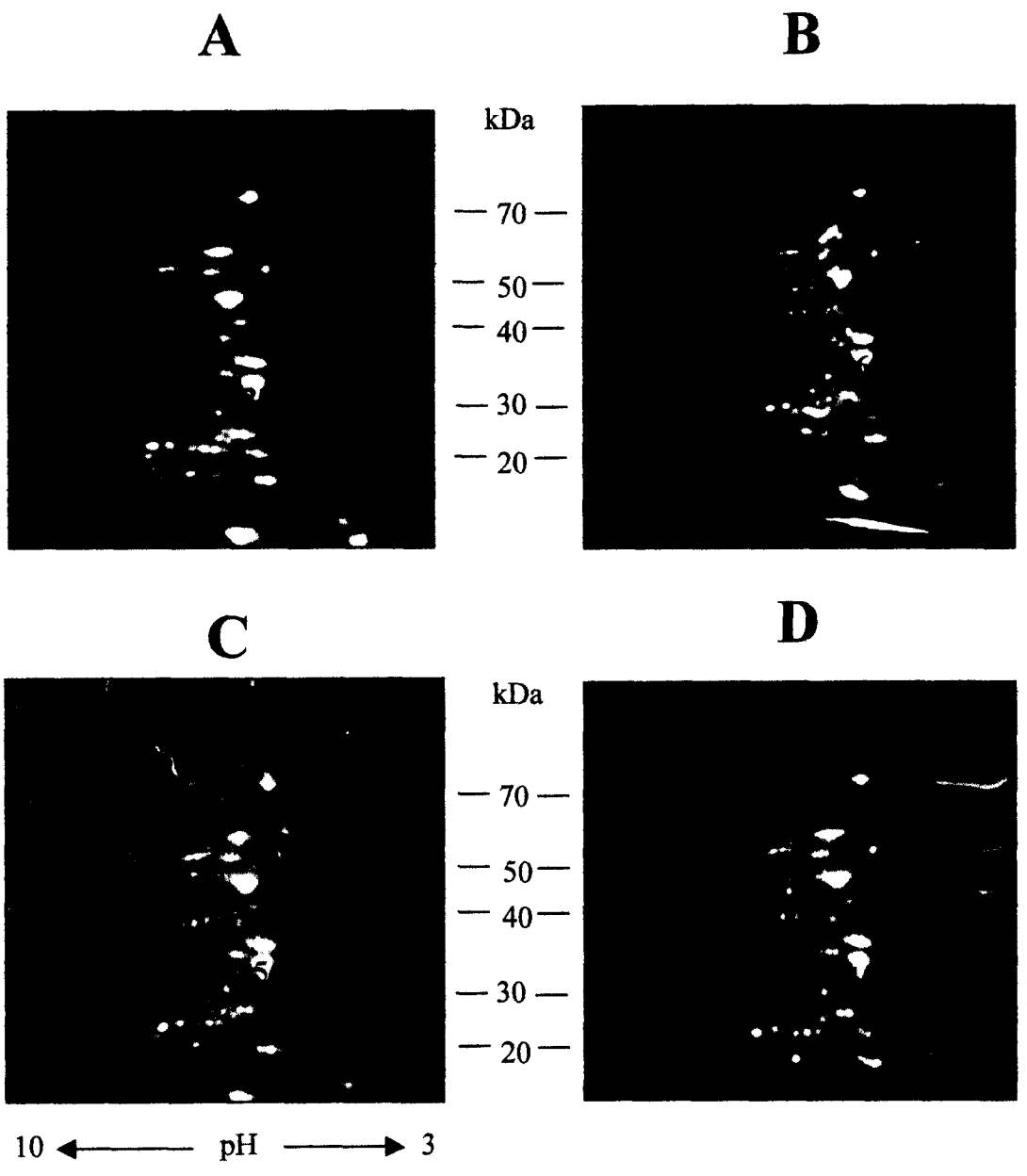

MELISSA ST. DENIS

Home Address:
Apt. 310-1500 Walkley Road
Ottawa, Ontario
K1V 0H8
(613) 521-0735
melissast_denis@hotmail.com

Citizenship: Canadian

RESEARCH OBJECTIVE

I am planning on pursuing a career in the research industry and look forward to applying the experience and knowledge gained upon achieving a Masters of Science degree in Microbiology and Immunology.

ACADEMIC QUALIFICATIONS

2006 — Masters of Science Degree Candidate (granted permission to write Sept. 2006)
Microbiology and Immunology
University of Ottawa, Ottawa, Ontario

2002 — Bachelor of Science, High Honours
Majors in Biology and Biotechnology
Carleton University, Ottawa, Ontario

ACADEMIC AWARDS

Carleton University Dean's Honour List 2002
Carleton University President's Scholarship, $8000
Carleton University's Faculty of Science Award, $500

EMPLOYMENT HISTORY

2002 - present — **Research Assistant**
Department of Special Microbiology and MCBT Laboratory
Children's Hospital of Eastern Ontario, Ottawa, Ontario
Responsibilities:

- provide an ongoing clinical service, Multiple Combination Bactericidal Testing (MCBT), for a wide-range of highly-resistant Gram-negative bacteria mainly isolated from Cystic Fibrosis patients' lungs
- responsible for reporting MCBT results to physicians

- pulsed field gel electrophoresis of *Pseudomonas aeruginosa* and *Burkholderia cepacia* clinical isolates
- implemented recA gene PCR for genomovar determination of *Burkholderia cepacia* clinical isolates
- biofilm research involving MCBT of Staphylococcus species (implant associated infection) and non-typeable *Haemophilus influenzae* (otitis media) clinical isolates
- able to differentiate Pseudomonas species, *Burkholderia cepacia*, and Staphylococcus colonies in sputum cultures collected from CF patients
- carried out susceptibility testing using disc diffusion as well as MIC and/or MBC determination by E-test or microtitre broth dilution
- assisted in directing both Ontario and Canada-wide clinical trials by performing microbiology work-up on Cystic Fibrosis patients' sputum samples
- prepared manuscripts for publication in peer-reviewed journals
- supervised research projects of summer students

2002 **Teaching Assistant**
Biology Department
Carleton University, Ottawa, Ontario
Responsibilities:
- assisted in laboratory setup and answered any questions students posed for a 1st year introductory biology course
- corrected assignments and formal laboratory reports

2001 - 2002 **Information Officer**
Information Carleton
Carleton University, Ottawa, Ontario
Responsibilities:
- supplied campus information through our call centre and also through in-person interactions

1997-2000 **Part-time Sales Clerk/Dispensary Assistant**
Seaway Valley Pharmacy, Chesterville, Ontario
Responsibilities:
- part-time cashier
- assisted in the dispensary with prescription submission, pill counting, and nursing home bi-monthly drug orders
- office management including deposits, skims, purchase orders, and client account database maintenance

M.Sc. THESIS ABSTRACT

Thesis: Identification and Functional Characterization of a Periplasmic Heme Binding Protein in *Haemophilus ducreyi*
Supervisor: Dr. Craig Lee

Department of Biochemistry, Microbiology and Immunology, University of Ottawa, Ottawa, Ontario

Haemophilus ducreyi, a gram-negative and heme-dependent bacterium, is the causative agent of chancroid, a genital ulcer sexually transmitted infection. More prevalent in developing countries, chancroid facilitates the transmission of HIV-1. Although the precise molecular mechanism for heme acquisition is unclear, heme uptake likely proceeds via a receptor mediated process. The initial event involves binding to either of two outer membrane receptors, TdhA and HgbA. Once heme is deposited into the periplasmic space, we hypothesize that a periplasmic heme binding protein (PHBP) is responsible for transporting heme across the periplasmic space to the inner membrane. To identify the PHBP, periplasmic extracts were generated from *H. ducreyi* 35000 grown under high and low heme conditions. The periplasmic preparations were subjected to proteome mapping using **two-dimensional gel electrophoresis**. Peptide sequences of upregulated proteins grown under heme-restrictive conditions were determined by mass spectroscopic analysis allowing for the identification of candidate PHBPs. Matching the peptide mass fingerprint against the sequenced genome of *H. ducreyi* permitted **cloning of the responsible gene** into a pET expression vector. This enabled **purification of the candidate protein** for functional heme-binding characterization. A candidate PHBP was identified with homology to YfeA of *Yersinia pestis*. The gene encoding for this protein is organized in a typical ABC transporter operon. Under iron limiting conditions, no increase in the expression of theYfeA homolog was observed. Using **heme-affinity chromatography**, competition binding experiments demonstrated that the interaction of the purified YfeA homolog with heme was inhibited in a concentration-dependent manner. We conclude that *H. ducreyi* shuttles heme across the periplasmic space using a PHBP homolog of YfeA. Delineating the heme uptake pathway in *H. ducreyi* will serve as a template in the understanding of bacterial heme transport and will ultimately assist in the discovery of new therapeutic strategies.

B.Sc. THESIS ABSTRACT

Thesis: Effects of self-pollination and isolation on *Vincetoxicum rossicum*
Supervisor: Dr. Naomi Cappuccino

Biology Department, Carleton University, Ottawa, Ontario

Vincetoxicum rossicum (Asclepiadaceae), commonly known as pale swallow-wort or dog-strangling vine, is an invasive alien vine found in Ottawa and other localities throughout Southern Ontario and Northeastern United States. In this study, pollination and the effects of isolation on *Vincetoxicum rossicum* were observed. A pollinator-exclusion experiment, in which I bagged nodes with unopened buds, was performed to test whether *V. rossicum* is able to self-pollinate. Excluding pollinators did not have a statistically significant effect on seed production; thus, *V. rossicum* is capable of self-pollination. Observations were made on pollinator visitation rates to plants growing either in large, dense patches or as isolated individuals. Plants in isolation received significantly more visits by pollinators. Observations were also made on the visitation rates to potted plants in three treatments:

dense patch, small patch, and isolated plants. Visitation did have a statistically significant effect on seed pod maturation. Of the mature seed pods collected, a higher percentage of seeds were produced from visited flowers as compared to non-visited flowers for both the isolated individuals, 57%, and the small patch treatments, 53%. The dense patch treatments produced less seeds from visited flowers, 45%, as compared to non-visited flowers. Visitation also had a significant negative effect on the germination of the seeds. About 28% of the seeds produced from visited flowers germinated whereas 39% of the seeds produced from non-visited flowers germinated.

PUBLICATIONS

Slinger, R., Chan, F., Ferris, W., Yeung, S, **St. Denis, M.**, Gaboury, I., and S. Aaron. Multiple combination antibiotic susceptibility testing of non-typeable *Haemophilus influenzae* biofilms. *Diagn Microbiol Infect Dis.* 2006; 56(3): 247-253.

Saginur, R., **St. Denis, M.**, Ferris, W., Aaron, S., Chan, F., Lee, C., and K. Ramotar. Multiple combination bactericidal testing of staphylococcal biofilms from implant-associated infections. *Antimicrob Agents Chemother.* 2006; 50: 55-61.

Aaron, S., Ramotar, K., Ferris, W., Vandemheen, K., Saginur, R., Tullis, E., Haase, D., Kottachchi, D., **St. Denis, M.**, and F. Chan. Adult cystic fibrosis exacerbations and new strains of *Pseudomonas aeruginosa*. *Am J Respir Crit Care Med.* 2004; 169: 811-815.

Aaron, S., Kottachchi, D., Ferris, W., Vandemheen, K., **St. Denis, M.**, Plouffe, A., Doucette, S., Saginur, R., Ramotar, K., and F. Chan. Sputum versus bronchoscopy for diagnosis of *Pseudomonas aeruginosa* biofilms in Cystic Fibrosis. *Eur Respir J.* 2004; 24: 631-637.

St. Denis, M. and N. Cappuccino. Reproductive biology of *Vincetoxicum rossicum* (Kleo.) Barb. (Asclepiadaceae), an invasive alien in Ontario. *J Torrey Bot Soc.* 2004; 131: 8-15.

PAPER ACCEPTED FOR PUBLICATION

St. Denis, M., Ramotar, K., Ferris, W., Vandemheen, K., Chan, F., Tullis, E., Haase, D., Wilcox, P., and S. Aaron. Infection with *Burkholderia cepacia* complex bacteria and pulmonary exacerbations of cystic fibrosis. *Chest.*

ORAL ABSTRACT PRESENTATION

"Identification and Functional Characterization of a Periplasmic Heme Binding Protein in *Haemophilus ducreyi*" presented at the Infection Disease Society of America Conference: 44th Annual Meeting Oct. 12-15, 2006; Toronto, Ontario, Canada.

POSTER ABSTRACTS

Slinger, R., Yan, L., Myers, R., Ramotar, K, **St. Denis, M.**, and S. Aaron. Pyrosequencing™ of a recA gene variable region for *Burkholderia cepacia* complex genomovar identification. American Society for Microbiology Conference: 106th General Meeting May 21-25, 2006; Orlando, FL, USA.

St. Denis, M., Ramotar, K., Ferris, W., Vandemheen, K., Chan, F., Tullis, E., Haase, D., Wilcox, P., and S. Aaron. New strain acquisition is not associated with pulmonary exacerbation in adult cystic fibrosis patients chronically infected with *Burkholderia cepacia* complex. North American Cystic Fibrosis Conference Nov. 9-12, 2005; Baltimore, MD, USA.

Saginur, R., **St. Denis, M.**, Aaron, S., Chan, F., Ferris, W., Lee, C., and K. Ramotar. Multiple combination bactericidal testing (MCBT) of staphylococcal biofilms. American Society for Microbiology Conference: Biofilms Nov. 1-6, 2003; Victoria, British Columbia, Canada.

POSTER ABSTRACT SUBMISSION

Chan, F., Ferris, W., Ramotar, K., **St. Denis, M.**, Wilson, R., Langill K., Yeung, S-W., Slinger, R., Vandemheen, K., and S. Aaron. To Sputolysin Or Not to Sputolysin - That Is the Question for Effective Isolation of *Pseudomonas aeruginosa* from Cystic Fibrosis Patients' Sputa. American Society for Microbiology Conference: 107th General Meeting May 21-25, 2007; Toronto, ON, Canada.

CURRENT MEMBERSHIP

American Society for Microbiology (since 2003)

HOBBIES & OTHER INTERESTS

Swimming, hiking, yoga, crocheting, sewing, and knitting